WORLD METEOROLOGICAL ORGANIZATION

OPERATIONAL HYDROLOGY REPORT No. 46

PRECIPITATION ESTIMATION AND FORECASTING

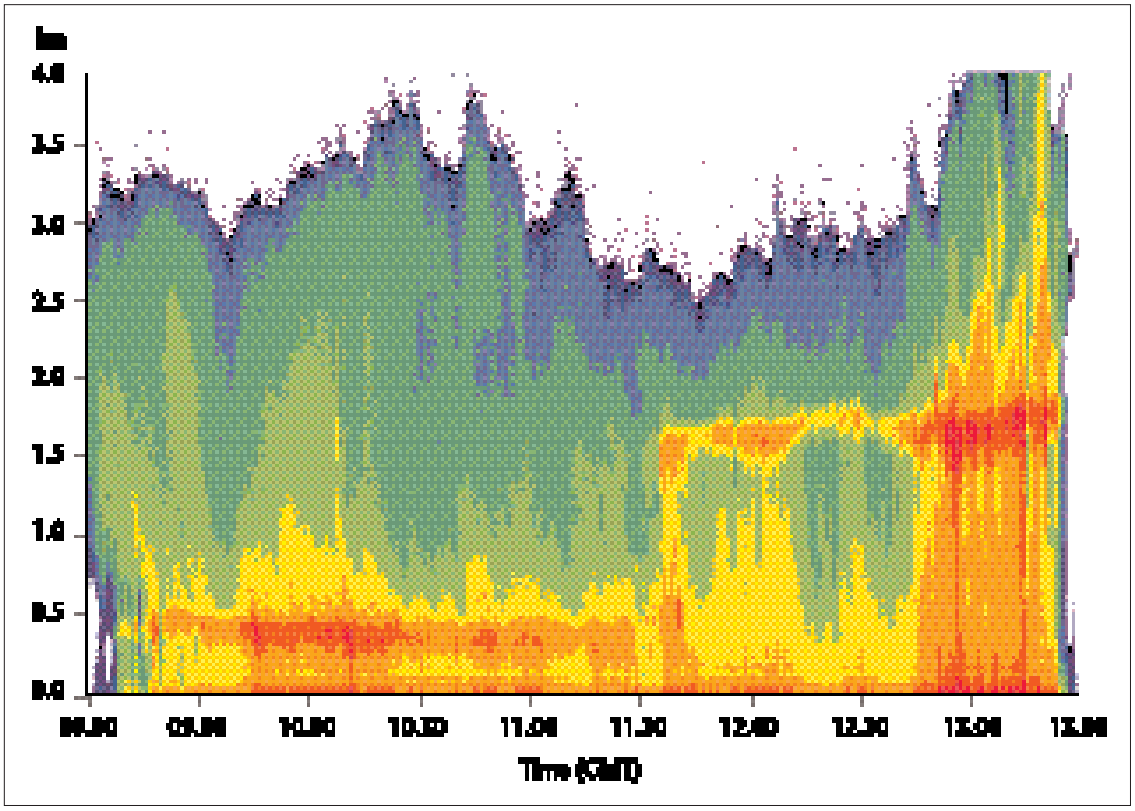

By C. G. Collier

WMO–No. 887

Secretariat of the World Meteorological Organization – Geneva – Switzerland

THE WORLD METEOROLOGICAL ORGANIZATION

The World Meteorological Organization (WMO), of which 185* States and Territories are Members, is a specialized agency of the United Nations. The purposes of the Organization are:

(*a*) To facilitate worldwide cooperation in the establishment of networks of stations for the making of meteorological observations as well as hydrological and other geophysical observations related to meteorology, and to promote the establishment and maintenance of centres charged with the provision of meteorological and related services;

(*b*) To promote the establishment and maintenance of systems for the rapid exchange of meteorological and related information;

(*c*) To promote standardization of meteorological and related observations and to ensure the uniform publication of observations and statistics;

(*d*) To further the application of meteorology to aviation, shipping, water problems, agriculture and other human activities;

(*e*) To promote activities in operational hydrology and to further close cooperation between Meteorological and Hydrological Services; and

(*f*) To encourage research and training in meteorology and, as appropriate, in related fields and to assist in coordinating the international aspects of such research and training.

(Convention of the World Meteorological Organization, Article 2)

The Organization consists of the following:

The World Meteorological Congress, the supreme body of the Organization, brings together the delegates of Members once every four years to determine general policies for the fulfilment of the purposes of the Organization, to approve long-term plans, to authorize maximum expenditures for the following financial period, to adopt Technical Regulations relating to international meteorological and operational hydrological practice, to elect the President and Vice-Presidents of the Organization and members of the Executive Council and to appoint the Secretary-General;

The Executive Council, composed of 36 directors of national Meteorological or Hydrometeorological Services, meets at least once a year to review the activities of the Organization and to implement the programmes approved by Congress;

The six regional associations (Africa, Asia, South America, North and Central America, South-West Pacific and Europe), composed of Members, coordinate meteorological and related activities within their respective Regions;

The eight technical commissions, composed of experts designated by Members, study matters within their specific areas of competence (technical commissions have been established for basic systems, instruments and methods of observation, atmospheric sciences, aeronautical meteorology, agricultural meteorology, marine meteorology, hydrology, and climatology);

The Secretariat, headed by the Secretary-General, serves as the administrative, documentation and information centre of the Organization. It prepares, edits, produces and distributes the publications of the Organization, carries out the duties specified in the Convention and other Basic Documents and provides secretariat support to the work of the constituent bodies of WMO described above.

---

* On 31 December 1999.

WORLD METEOROLOGICAL ORGANIZATION

OPERATIONAL HYDROLOGY REPORT No. 46

PRECIPITATION ESTIMATION AND FORECASTING

By C. G. Collier

WMO–No. 887

Secretariat of the World Meteorological Organization – Geneva – Switzerland
2000

ACKNOWLEDGEMENTS

The author has drawn freely on a wide range of literature and acknowledges the contributions of the authors of many papers, the results and analysis from which have been referenced only via specialist reviews. He has also used material he has published elsewhere, but has drawn together and edited for this review. A particular source is Collier, C. G., 1996: *Applications of Weather Radar Systems: A Guide to Uses of Radar Data in Meteorology and Hydrology*, Second edition, Praxis Ltd., Chichester and John Wiley.

Cover photo: Dr Kevin Tilford
University of Salford

ISBN: 92-63-10887-0

NOTE

The designations employed and the presentation of material in this publication do not imply the expression of any opinion whatsoever on the part of the Secretariat of the World Meteorological Organization concerning the legal status of any country, territory, city or area, or of its authorities, or concerning the delimitation of its frontiers or boundaries.

CONTENTS

Page

Page

FOREWORD

There is an abundance of water on planet Earth, but only a very small proportion is available for use as freshwater. An even smaller proportion resides at any one time in the atmosphere. It has a major influence on the weather and is the source of precipitation that provides moisture to the soil, feeds our rivers and lakes and sustains our aquifers. All hydrological studies rely heavily on the estimation of precipitation over a given area and yet the measurement of this most basic of all hydrological elements is a challenge for the hydrological community.

For this reason, the Commission for Hydrology (CHy) of the World Meteorological Organization, at its ninth session in 1993, appointed Mr C. G. Collier (United Kingdom) as Rapporteur on Precipitation Estimation and Forecasting and assigned him the task of preparing a report on precipitation estimation and forecasting. In 1996, the report was approved for publication by the tenth session of CHy.

This report discusses a wide range of techniques which have been developed worldwide for measuring and forecasting precipitation. However, all the techniques are complementary. Often one technique is used to calibrate or adjust another. It is the purpose of this report to place the sometimes quite different performance characteristics of different methods into perspective. Likewise, forecasting techniques are wide-ranging and aim to generate forecasts from a few hours ahead to days and even a month ahead.

I should like to place on record the gratitude of the World Meteorological Organization to Mr C. G. Collier for the time and effort he has devoted to the preparation of this valuable report.

(G.O.P. Obasi)
Secretary-General

SUMMARY

Over 97 per cent of the water in our world resides in the oceans, and only 0.001 per cent resides in the atmosphere. Indeed, only about 0.005 per cent of the total world water supply is in motion at any one time. However, this very small amount of water is associated with all weather and river flow, and has a profound impact upon the activities of mankind. The measurement of precipitation (rain, snow, hail, etc.) is of primary importance for hydrological calculations.

In this report, a wide range of techniques which have been developed worldwide for measuring and forecasting precipitation are discussed. Measurement techniques range from point gauge measurements to methods based upon the interpretation of, sometimes, very indirect data obtained from space-based instrumentation. However, all the techniques are complementary. Often one technique is used to calibrate or adjust another, and it is the purpose of this report to place the sometimes quite different performance characteristics of different methods into perspective. Likewise, forecasting techniques are wide-ranging, and aim to generate forecasts from a few hours ahead to days and even a month ahead. Mention is also made of prospects for seasonal forecasting.

The approach adopted in this report is to discuss measurement techniques from a technological point of view, reviewing levels of performance achieved, and, where possible, major limitations. While some techniques can be intercompared, for example the use of weather radar and satellite-based procedures, it is stressed that no one technique offers the optimum solution to precipitation measurement. Indeed, some techniques are used with others to achieve a level of improved performance. It is often not possible to recommend particular approaches, as any such recommendations will depend upon the specific applications to which the measurements are put.

The first half of this report outlines point measurements of precipitation using collectors, weighing devices and hailpads. Areal measurements of precipitation using interpolated point values, radar and satellite techniques and combinations of different approaches are discussed. The degree to which current technology and algorithms can satisfy the hydrological requirements for precipitation is considered briefly.

The second half of this report deals with precipitation forecasting over temporal scales from minutes to seasons. Such a wide range of forecast lead times makes it necessary to consider the use of simple extrapolation, artificial intelligence, simple to complex numerical modelling and statistical-dynamical procedures.

Finally, input to hydrological models of both measurements and forecasts of precipitation is not necessarily straightforward. The specific error characteristics of each type of measurement and forecast have different implications for the range of hydrological model types used. An outline description of these model types is followed by consideration of the impact of particular types of input data on the flow forecasts so-generated. The development of real-time error correction procedures is noted, and the importance of further work to understand the inter-relationship between input data quality and model output is considered.

RÉSUMÉ

L'eau de notre planète se trouve à plus de 97% dans les océans, et à 0,001% seulement dans l'atmosphère. Quant à la quantité en mouvement à quelque moment que ce soit, elle ne représente qu'environ 0,005%. Toutefois, cette très petite quantité d'eau correspond à l'ensemble des conditions météorologiques et des écoulements fluviaux et influe très profondément sur les activités humaines. La mesure des précipitations (pluie, neige, grêle, etc.) revêt une importance capitale pour les hydrologues.

Dans le présent rapport sont examinées toute une gamme de techniques mises au point un peu partout dans le monde pour la mesure et la prévision des précipitations. Les techniques de mesure vont de l'utilisation de la pointe limnimétrique à l'application de méthodes fondées sur l'interprétation de données parfois très indirectes provenant de l'observation spatiale. Elles sont cependant toutes complémentaires. Souvent, l'une d'elles est utilisé à des fins d'étalonnage ou d'ajustement. Le rapport vise à faire le point sur les caractéristiques parfois très différentes que présentent diverses méthodes du point de vue de leur efficacité. De même, toute une gamme de technique permettent d'établir des prévisions à des échéances de quelques heures à plusieurs jours, voire un mois entier. Des perspectives de prévisions saisonnières sont également signalées.

La solution adoptée dans le présent rapport consiste à examiner les techniques de mesure d'un point de vue technologique, en analysant leur efficacité et, lorsque cela est possible, les principales lacunes qu'elles présentent. Pour certaines techniques, l'on peut certes procéder à des comparaisons, par exemple lorsqu'il s'agit de méthode faisant appel aux radars météorologiques ou aux satellites, mais on insiste sur le fait qu'aucune technique n'offre de solution optimale pour la mesure des précipitations. En effet, des techniques sont parfois combinées afin d'obtenir une plus grande efficacité. Souvent, il n'est pas possible de recommander une solution plutôt qu'une autre, car tout dépendra des applications particulières des mesures effectuées.

La première moitié du rapport donne des indications sur la mesure ponctuelle des précipitations à l'aide de collecteurs, de dispositifs de pesée et de coussins à grêlons. Il y est question de la mesure des précipitations de zone à partir de valeurs ponctuelles interpolées ou à l'aide de techniques faisant appel aux

radars et aux satellites ou encore de combinaisons de différentes méthodes. L'on y indique brièvement dans quelle mesure les techniques et algorithmes disponibles aujourd'hui permettent d'obtenir les données pluviométriques dont les hydrologues ont besoin.

La seconde moitié du rapport traite de la prévision des précipitations à des échéances allant de quelques minutes à plusieurs saisons. Face à une telle gamme d'échéances, il y a lieu de prendre en considération le recours à de simples extrapolations, à l'intelligence artificielle, à des modèles allant du plus simple au plus complexe et à des méthodes statistiques et stochastiques.

Enfin, il n'est pas toujours simple d'introduire dans les modèles hydrologiques à la fois des mesures et des prévisions des précipitations. Les caractéristiques que présentent les erreurs particulières à chaque type de mesure et de prévision ont des répercussions différentes sur le type de modèle hydrologique utilisé. Après une brève description des types de modèles en question est examinée l'incidence de tel ou tel type de données d'entrée sur les prévisions d'écoulement établies. Il est fait état de l'élaboration de méthodes de correction des erreurs en temps réel, et l'on insiste sur la nécessité de poursuivre les travaux visant à mieux comprendre la corrélation entre la qualité des données d'entrée et les résultats fournis par les modèles.

РЕЗЮМЕ

Более 97 % воды в мире находится в океанах и только 0,001 % — в атмосфере. При этом в любой момент времени в движении находится только около 0,005 % общих запасов воды в мире. Однако это очень небольшое количество воды ассоциируется со всеми погодными явлениями и речным стоком и оказывает глубокое воздействие на деятельность человека. Измерения осадков (дождь, снег, град и т.д.) имеют первоочередную важность для гидрологических расчетов.

В настоящем отчете описывается широкий спектр разработанных в мире методов для измерения и прогнозирования осадков. Методы измерения простираются от измерений в точках на водосборе и до интерпретации подчас весьма косвенных данных, полученных с приборов, установленных на спутниках. Однако все эти методы взаимодополняют друг друга. Один метод часто используется для калибровки или корректировки другого, и цель настоящего отчета состоит в том, чтобы нарисовать перспективу использования некоторых подчас весьма различных по своим показателям методов. Аналогично этому, методы прогноза также весьма разнообразны и имеют целью выпуск прогнозов с заблаговременностью от нескольких часов до нескольких дней и даже месяца. Упоминается также о перспективах сезонных прогнозов.

В отчете применяется подход, основанный на описании методов измерения с технологической точки зрения, рассмотрении достигнутых уровней показателей и, по мере возможности, описании основных ограничений. При том, что некоторые методы можно взаимно сравнить, например использование метеорологического радиолокатора и спутниковые измерения, тем не менее подчеркивается, что ни один метод не дает оптимального решения проблемы измерения осадков. На практике одни методы используются в совокупности с другими для достижения определенного улучшенного уровня показателей. Часто невозможно рекомендовать тот или иной подход, поскольку любая такая рекомендация будет зависеть от конкретных применений, для которых будут использоваться данные измерения.

В первой части отчета описываются измерения осадков в точке с использованием коллекторов, взвешивающих устройств и градовых плит. Описываются измерения осадков по площади, использующие интерполяцию значений в точках, радиолокационные и спутниковые методы и сочетания различных подходов. Кратко рассматривается степень удовлетворения гидрологических потребностей в данных об осадках с помощью существующей технологии и алгоритмов.

Вторая часть отчета посвящена прогнозированию осадков во временных масштабах от минут до сезонов. Такой широкий диапазон сроков прогнозов ведет к необходимости рассмотреть использование простой экстраполяции, искусственного интеллекта, численных моделей от простых до сложных и статистико-динамических процедур.

Наконец, введение в гидрологические модели как данных измерений, так и прогнозов осадков, не всегда является простым. Конкретные характеристики ошибок для каждого типа измерений и прогнозов имеют различное значение для используемых разнообразных типов гидрологических моделей. За общим описанием этих типов моделей следует рассмотрение влияния различных типов входных данных на выпускаемый такими моделями прогноз стока. Сообщается о разработке оперативных процедур исправления ошибок, и отмечается важность дальнейшей работы по углублению понимания взаимосвязи между качеством входных данных и выходной продукции моделей.

RESUMEN

El presente informe trata de la modelización zonal utilizando las técnicas más recientes en materia de teledetección y Sistemas de Información Geográfica (SIG).

Los procesos de los ciclos hidrológicos varían espacial y temporalmente. Habitualmente, en la modelización de esos procesos, las variaciones espaciales y temporales de las variables hidrológicas se han considerado como un todo espacial con procesos de variación temporal.

Sin embargo, los adelantos en la tecnología referente a teledetección han permitido la adquisición de datos distribuidos espacialmente sobre condiciones de superficie tales como la vegetación, el uso de la tierra, las propiedades geológicas, y datos hidrológicos como las precipitaciones y la humedad del suelo. Asimismo, se ha preparado de modo electrónico en todo el mundo información topográfica y datos distribuidos en el espacio con diferentes parámetros estadísticos. El material y programa informáticos, diseñados para analizar esa información espacial de múltiples dimensiones, se han reunido para crear un Sistema de Información Geográfica y se han utilizado operativamente o para estudios sobre el terreno en el ámbito de la hidrología y los recursos hídricos.

El informe consta de cinco capítulos. En el Capítulo 1 se explica brevemente el contenido del informe y se clasifican los modelos hidrológicos para la modelización zonal.

El Capítulo 2 abarca un análisis del estado y los problemas actuales de los modelos distribuidos espacialmente y contiene información sobre modelos físicos y distribuidos. Incluye los parámetros de modelos físicos por unidades zonales, así como ejemplos de modelos distribuidos típicos con tablas para las necesidades de datos y los problemas de los modelos de distribución.

En el Capítulo 3 se hace un estudio de las aplicaciones de los datos de teledetección en la hidrología y su limitación práctica y se trata la teledetección para la modelización y la observación de variables hidrológicas.

El Capítulo 4 contiene una descripción de la modelización espacial utilizando el SIG y aplicaciones a la modelización hidrológica, con referencia particular a la creación de modelos con el Modelo Digital de Terreno (MDT). Aborda el análisis de las características topográficas de las cuencas utilizando el MDT.

El Capítulo 5 se refiere a los perspectivas futuras de la modelización zonal utilizando la teledetección y el SIG. Contiene una lista de los nuevos satélites que llevan a bordo múltiples sensores de teledetección diseñados para observar las características físicas y biológicas de la Tierra, cuyo lanzamiento está previsto para el año 2000. Aborda asimismo una nueva tendencia hacia sistemas de información geocientíficos.

CHAPTER 1

INTRODUCTION

1.1 BACKGROUND

At the ninth session of WMO's Commission for Hydrology (January 1993) it was agreed that the author should act as Rapporteur on Precipitation Estimation and Forecasting during the following inter-sessional period.

Over 97 per cent of the water in our world resides in the oceans, and only 0.001 per cent resides in the atmosphere. Indeed, only about 0.005 per cent of the total world water supply is in motion at any one time. However, this very small amount of water is associated with all weather and river flow, and has a profound impact upon the activities of mankind. The measurement of precipitation (rain, snow, hail, etc.) is of primary importance for hydrological calculations.

In this report we discuss a wide range of techniques which have been developed worldwide for measuring and forecasting precipitation. Measurement techniques range from point gauge measurements to methods based upon the interpretation of, sometimes, very indirect data obtained from space-based instrumentation. However, all the techniques are complementary. Often one technique is used to calibrate or adjust another, and it is the purpose of this report to place the sometimes quite different performance characteristics of different methods in perspective. Likewise, forecasting techniques are wide-ranging, and aim to generate forecasts from a few hours ahead to days and even a month ahead. Mention is also made of prospects for seasonal forecasting.

1.2 STRUCTURE OF THE DOCUMENT

The approach adopted in this report is to discuss measurement techniques from a technological point of view, reviewing levels of performance achieved, and, where possible, major limitations. While some techniques can be intercompared, for example the use of weather radar and satellite-based procedures, it is stressed that no one technique offers the optimum solution to precipitation measurement. Indeed, some techniques are used with others to achieve a level of improved performance. It is often not possible to recommend particular approaches, as any such recommendations will depend upon the specific applications to which the measurements are put.

The first half of this report outlines point measurements of precipitation using collectors, weighing devices and hailpads. Areal measurements of precipitation using interpolated point values, radar and satellite techniques and combinations of different approaches are discussed. The degree to which current technology and algorithms can satisfy the hydrological requirements for precipitation is considered briefly.

The second half of this report deals with precipitation forecasting over temporal scales from minutes to seasons. Such a wide range of forecast lead times makes it necessary to consider the use of simple extrapolation, artificial intelligence, simple to complex numerical modelling and statistical-dynamical procedures.

Finally, input to hydrological models of both measurements and forecasts of precipitation is not necessarily straightforward. The specific error characteristics of each type of measurement and forecast have different implications for the range of hydrological model types used. An outline description of these model types is followed by consideration of the impact of particular types of input data on the flow forecasts so-generated. The development of real-time error correction procedures is noted, and the importance of further work to understand the inter-relationship between input data quality and model output is considered.

CHAPTER 2

MEASUREMENTS

2.1 POINT AND AREAL MEASUREMENTS OF PRECIPITATION

Most variables in the hydrological cycle show large and frequent spatial variations and often exhibit rapid temporal variations. Of particular importance is precipitation, and it is often necessary in many hydrological process studies and applications to monitor precipitation continuously at as many points as possible. Barrett, *et al*. (1986) were able to write only 10 years ago that "the feasibility of observations and measurements is limited and practically all hydrological measurements are point measurements (with the exception of stream flow measurements) with the result that considerable interpolation between isolated point measurements is needed in order to determine spatial patterns. This is particularly the case with respect to rainfall, snow measurement ...". This may well continue to be the situation for some years to come, but a range of new techniques are, as we shall see, now available for areal measurements.

Point measurements are insufficiently representative of sub-catchment scales, and hence it is difficult to understand and model hydrological processes using such data. The basic measurement requirement of hydrology is for areal measurements albeit over sometimes very small, as well as very large, areas. Both ground-based and satellite-borne instrumentation now offer these measurements. However, the wide range of error characteristics associated with these measurements ensure that point measurements will remain of central importance. Nevertheless, as techniques improve reliance on dense networks of point measurements will undoubtedly diminish. It is, though, not expected that the need for extensive point measurements will vanish altogether in the foreseeable future.

The best measurement of point rainfall is that achieved using a raingauge, but, as pointed out by Bellon and Austin (1986), the use of satellite-based techniques to measure areal rainfall in mid-latitudes becomes better than the use of interpolated raingauge measurements when the raingauge spacing is greater than about 40 km. Similarly, in highly variable convective precipitation, the use of radar offers the only practical approach to measuring rainfall over areas from 0.5 km^2 to 5 km^2 over periods of one minute to 15 minutes (Collier, 1990).

2.2 HYDROLOGICAL REQUIREMENTS FOR MEASUREMENT: RESOLUTION, PRECISION AND ACCURACY

The hydrological requirements for measurements of precipitation are shown in Table 2.1, where the maximum, minimum and most usual values for resolution, frequency of observation and accuracy are given. Clearly which requirement value is appropriate will depend upon the application to which the measurements are put.

The precision with which measurements should be made refers to their reproducibility in space, time and quantity. Precision is expressed quantitatively as the standard deviation of results from repeated trials under identical conditions. Hence a measurement may be quantitatively accurate, but imprecise and vice versa as shown in Figure 2.1. The reasons for this depend upon the inter-relationship between resolution, frequency and numerical accuracy.

A measurement from a raingauge is spatially precise, but may be imprecise in time and quantity. Hence in Table 2.1 we have added requirements for precision where this quantity is taken as the standard deviation about the mean requirements for resolution, frequency and accuracy. It is therefore a tolerance within which the requirement stated must be met.

Table 2.1 — Hydrological requirements for measurements of precipitation giving maximum, minimum and most usual requirements. Resolution requirements for point measurements refer to the area around the point around which the measurement is considered to be representative

	Resolution (km)			*Frequency*			*Accuracy (per cent)*			*Precision*		
Rainfall												
(*a*) Point	0.1	5	1	5 min	1 month	1 hour	2	10	5	0.1	1	3
(*b*) Area												
- rural (>20 km^2)	0.5	5	2	5 min	1 month	1 hour	10	30	10	2	5	5
- urban/very small	0.25	2	1	1 min	5 min	2 min	5	20	20	0.2	0.5	3
- rural (<20 km^2)												
Snowfall												
(*a*) depth	0.03	10	0.2	1 hour	1 month	24 hours	2 cm	10 cm	5 cm	0.1	30	4 cm
(*b*) water equivalent	0.03	10	1	1 hour	1 month	24 hours	1 mm	100 cm	10 mm	0.2	30	4 cm

NOTE: The requirement for snowfall measurement refers to both point (max) and areal (min) values.

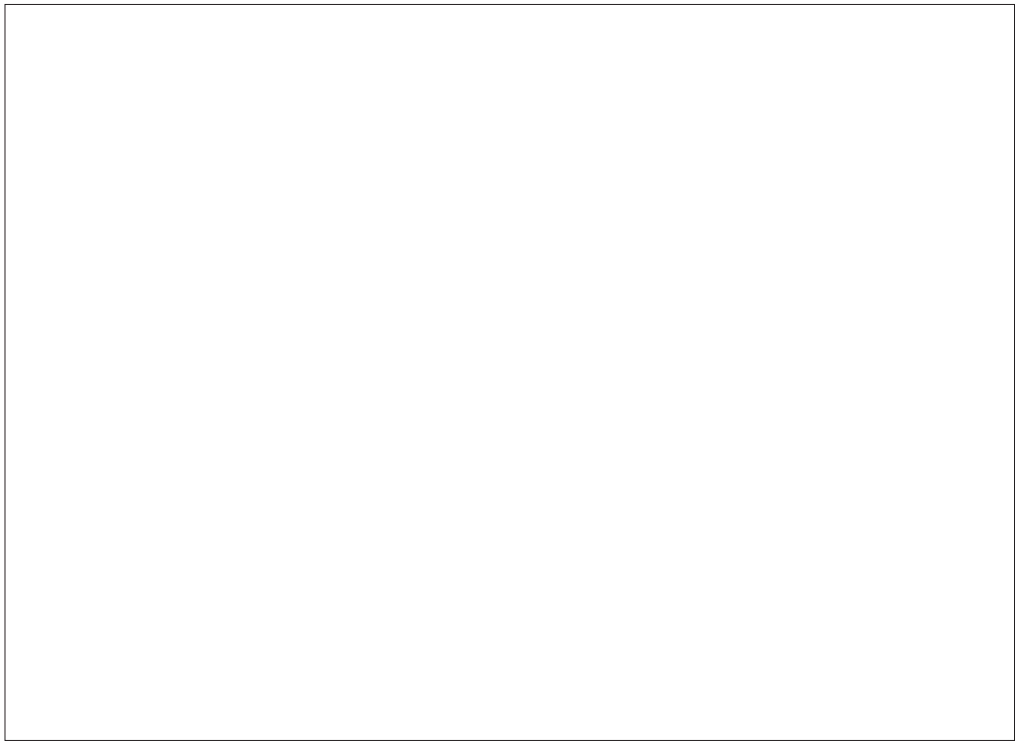

Figure 2.1 — Precision and accuracy, (*a*) accurate and precise; (*b*) not accurate but precise; (*c*) accurate but not precise; (*d*) not accurate, not precise (from Chatfield, 1983).

CHAPTER 3

POINT MEASUREMENTS USING GAUGES

3.1 SITING

Ideally the catch of a raingauge would represent the precipitation falling on the surrounding area, but this is difficult to attain in practice as the effect of the wind has a significant impact upon the amount of precipitation measured. Wind effects are of two types: the effects on the gauge itself, which generally reduce the amount of water collected, and the effects of the site on the wind trajectories, which are frequently more important and can give rise to either an excess or a deficiency in measured precipitation.

The disturbance created by an obstacle depends on the ratio of the obstacle's linear dimensions to the falling speed of precipitation. This effect is reduced, if not entirely overcome, by choosing the site so that the wind speed at the level of the gauge orifice is as small as possible. All gauges in any area should have comparable exposures and the same siting criteria should be applied to all.

The WMO *Guide to Hydrological Practices* (WMO, 1994) states that the gauge should be exposed with its orifice being horizontal over ground level. Where possible, the gauge site should be protected from wind movement in all directions by objects (trees, shrubs, etc.) of as nearly uniform height as possible. The height of these objects above the orifice of the gauge should be at least half the distance from the gauge to the objects, but should not exceed the distance from the gauge to the objects (to avoid interception of precipitation that should reach the gauge). The ideal situation is to have the angle from the top of the gauge to the top of the encircling objects between 30° and 45° to the horizontal.

In very exposed places, where natural shelter is not available, it has been found that better results can be obtained for liquid precipitation if the gauge is installed in a pit, so that the gauge rim is at ground level. A strong plastic or metal anti-splash grid should span the pit with a central opening for the gauge funnel. An alternative installation, which is not quite so effective, is to install the gauge in the middle of a circular turf wall.

Precipitation in the form of snow is much more subject to adverse wind effects than is rainfall. In exceptionally windy locations, the catch in a gauge, with or without a windshield, may be less than half the actual snowfall. Sites selected for measurement of snowfall and/or snow cover should, as far as possible, be in areas sheltered from the wind.

3.2 RAINGAUGE TYPES

Raingauge types are considered in two categories:

Non-recording gauges

The non-recording gauges used by most Hydrological and Meteorological Services for official measurements generally consist of open receptacles with vertical sides, usually in the form of right cylinders. Various sizes of orifice and height are used in different countries and, therefore, measurements are not strictly comparable. The depth of precipitation caught in a gauge is measured by means of a graduated flask or dipstick.

Recording gauges

Three types of precipitation recorders are in general use: the weighing type, the tipping-bucket type, and the float type. The only satisfactory instrument for measuring all kinds of precipitation utilizes the weight principle. The use of the other two types is primarily limited to the measurement of rainfall.

Weighing type: The weight of a receiving can plus the precipitation accumulating in it is recorded continuously.

Float type: The rainfall is fed into a float chamber containing a light float. As the level of the water rises, the vertical movement of the float is transmitted into the movement of a pen on a chart.

Tipping-bucket type: A light metal container is divided into two compartments and is balanced in unstable equilibrium above a horizontal axis. The rain is led from a conventional collecting funnel into the uppermost compartment and, after a predetermined amount of rain has fallen, the bucket tips over operating a relay contact to produce a record of the number of tips. Each tip is usually either 0.2 mm, 0.5 mm or 1 mm.

Some special purpose rainfall-intensity recorders are available using either electronic or optical mechanisms (see for example Norbury, 1974; Norbury and White, 1975).

3.3 ERRORS IN MEASUREMENT

The commonly accepted standard method of rainfall measurement is the use of a can-type raingauge. However, such raingauges exposed above ground-level are subject to appreciable systematic error (–3 to –30 per cent or even more) (WMO, 1982). This error is due to wind-field deformation above the gauge rim, to wetting, evaporation, splashing of raindrops and blowing of snow. The components of the systematic error are related to the meteorological and instrumental factors listed in Table 3.1 and can be statistically analysed. The general model for corrections takes the following form:

$$P_K = kP_C = k(P_g + \Delta P_1 + \Delta P_2 + \Delta P_3 + \Delta P_4 - \Delta P_5) + P_r \quad (3.1)$$

where:
P_K = corrected amount of precipitation;
P_g = gauge catch = gauge measured precipitation;
k = conversion factor due to wind-field deformation;
P_C = the amount of precipitation caught by the gauge;
ΔP_1- ΔP_5 = corrections for various components of systematic error according to Table 3.1;
P_r = random observational and instrumental errors.

Table 3.1 — Main components of the systematic error if *n* precipitation measurement and their meteorological and instrumental factors listed in order of general importance (after WMO, 1982)

Symbol	*Component of error*	*Magnitude*	*Meterological Factors*	*Instrumental factors*
k	Loss due to wind-field deformation above the gauge orifice	2–10 per cent 10–50 per cent	Wind speed at the gauge rim during precipitation and the structure of precipitation	The shape, orifice area and depth of both the gauge rim and the collector
ΔP_1+ ΔP_2	Losses from wetting on internal walls of the collector and in the container when it is emptied	2–10 per cent	Frequency, type, and amount of, precipitation, the drying time of the gauge and the frequency of emptying the container	The same as above and, in addition, the material colour and age of both the gauge collector and container
ΔP_3	Loss due to the evaporation from the container	0–4 per cent	Type of precipitation, saturation deficit and wind speed at the level of the gauge rim during the interval between the end of precipitation and its measurements	The orifice area and the isolation of the container, the colour and, in some cases, the age of the collector, or the type of funnel (rigid or removal)
ΔP_4	Splash-out and splash- in	1 per cent	Rainfall intensity and wind speed	The shape and depth of the gauge collector and the kind of gauge installation
ΔP_5	Blowing and drifting snow		Intensity and duration of snow-storm, wind speed and the state of snow cover	The shape, orifice area and depth of both the gauge rim and collector

*Snow

The conversion factor k, as well as the corrections $\Delta P_{1–5}$ for a particular gauge, can be estimated experimentally by field comparisons or by laboratory tests. The meteorological factors needed can be estimated using standard meteorological observations at the gauge site or in its vicinity.

As the components of systematic error vary with the instrument and meteorological factors from very small to significant values, not all of them must be taken into consideration for certain gauge types, seasons and regions. For example, the use of pit gauges prevents loss from wind-field deformation. Evaporation losses can be reduced by placing oil in the container or by designing the gauge so that only a small part of the water surface is exposed, ventilation is minimal and the inside temperature of the gauge is not allowed to become excessive. Also, the wetting loss can be reduced by making the internal wall of the collector and container as smooth as possible, so that the water does not adhere to it. Splash-in and -out can be reduced by the proper design of the collector, its rim and in the case of the pit gauge, the construction of the non-splash surface.

It can be seen from Table 3.1 that errors due to deformation of the wind field can be very large if gauges are not installed in pits. Therefore considerable effort has been put into the design of aerodynamic raingauges. In the United Kingdom, WMO (1986*a*) used computer models of airflow over gauges to explore possible new shapes for collectors, and Strangeways (1984) reported comparable field experiments. This work led to the development of "champagne-glass" gauges as shown in Figure 3.1; recent field trials reported by Hughes, *et al*. (1993) have demonstrated significant improvements of such gauges over more conventional designs.

Figure 3.1 — Prototype of 'champagne-glass' gauge.

3.4 AREAL MEASUREMENTS OF RAINFALL DERIVED FROM RAINGAUGE NETWORKS

Weisner (1970) summarizes the techniques which have been developed to extrapolate point measurements of rainfall to areal measurements. Empirical formulas have been derived having the form:

$$P = a\text{-}b\,A^{1/2} \tag{3.2}$$

where a and b are constants which represent the maximum rainfall at the focus and the mean rainfall gradient, and A is the

area over which the measurement is requirement. However, such formulas are only applicable if carefully tuned for particular climate and orographic regimes, and it is much more reliable to use a dense raingauge network using one of the following techniques:

$$\text{Arithmetic mean } \overline{P} = \sum_{i}^{n} \frac{P_n}{n}$$

$$\text{Areal weighting or Thiessen polygons, where } \overline{P} = \sum_{i}^{n} \frac{W_n P_n}{100}$$

W_n is the percentage weighting factor derived from the areas of polygens formed by the gauge locations. In addition, raingauge values may be interpolated using triangulation; an isohyetal procedure using linear interpolation; an isohyetal procedure using a subjective approach to interpolation; and weighting individual gauge values based upon the isohyetal pattern or other independent data such as orography.

Clearly all these techniques depend upon the density of the raingauge network being employed. Considerable work over many years has been carried out to investigate the effect of raingauge network density upon areal measurement of rainfall. A recently reported example is that shown in Figure 3.2 from Seed and Austin (1990*a*, *b*) derived for networks in Florida and South Africa. Krstonovic and Singh (1992*a*, *b*) describe an approach based upon an evaluation of entropy for gauge networks in Louisiana, and showed that for larger sampling intervals (greater than one day) the number of necessary raingauges to produce acceptable areal measurements could be reduced significantly. Nevertheless care is needed when areal measurements are used to estimate stream flow. Duncan, *et al*. (1993) shows that gauge density has a very strong effect on the estimation accuracy of hydrograph parameters, with the standard error generally falling off as a power law with increasing gauge density.

3.5 GLOBAL PRECIPITATION CLIMATOLOGY CENTRE (GPCC)

The GPCC was initiated by WMO in October 1988, and is a central element of the Global Precipitation Climatology Project, which was established by the World Climate Research Programme (WCRP) to provide global monthly precipitation totals on a grid of 2.5° latitude and longitude (see section 6.1). The GPCC is operated by the Deutscher Wetterdienst (German Weather Service) and is a contribution of the Federal Republic of Germany to the WCRP. The tasks of the GPCC are defined in WMO, 1990.

At the GPCC, monthly precipitation totals based on conventional measurements are available from climate reports or can be calculated from synoptic reports disseminated via the World Weather Watch Global Telecommunication System (GTS) for about 4 000 stations worldwide. However, the resulting station density over many parts of the continents is insufficient for a reliable calculation of the areal mean monthly precipitation.

Several countries (including Australia, Ghana, Great Britain, the Netherlands, New Zealand, Russia, and the United States) have supplied additional monthly precipitation data, partly from very dense networks. Some of those additional data have been included in the global dataset being used for preliminary studies and results described in this report. Consequently, the number of stations used for the preliminary monthly analyses of the year 1987 has been increased to approximately 6 600 stations.

An objective interpolation method is being used for the operational spatial analysis on the basis of the gauge-measured precipitation data. The interpolation method is based on the distance and angular weighting scheme of Shepard (1968), which is valid on a plane, and has been transformed to spherical coordinates by Willmott, *et al*. (1985).

Intercomparisons between the monthly gauge measurements overland; space-based estimates and precipitation estimated from the European Centre for Medium-range Weather Forecasts (ECMWF) have been carried out. It has

Figure 3.2 — Errors in the estimation of mean areal daily rainfall over 45 000 km^2 using distance-weighting interpolation: Florida and Nelspruit (Seed and Austin, 1990*a*, *b*).

become clear that a sufficient number of conventionally-measured data are essential to obtain reliable areal precipitation totals overland. The products of the GPCC are available including gridded monthly precipitation maps and anomalies.

CHAPTER 4

POINT MEASUREMENTS OF SNOWFALL AND HAIL

4.1 TECHNIQUES

4.1.1 Snowfall

Snowfall is the amount of fresh snow deposited over a limited period. Measurements are made of depth and water equivalent. Direct measurements of fresh snow on open ground are made with a graduated ruler or scale. A mean of several vertical measurements should be made in places where there is considered to be an absence of drifting snow. Special precautions should be taken so as not to measure any old snow.

The depth of snow may also be measured in a fixed container of uniform cross-section after the snow has been levelled without compressing. The container should be well above the average snow level and not exposed to drifting snow. The receiver should be sufficiently deep to protect the catch from being blown out or else be fitted with a snow cross (i.e., two vertical partitions at right angles, subdividing it into quadrants) (WMO, 1995*a*).

Ordinary unshielded receivers are unreliable when the wind is strong because of the wind eddies around the mouth of the receiver. Their catch is usually much less than that of a shielded gauge. On the other hand, large errors may be caused, in spite of the use of a shield, by drifting snow being caught. Heated tipping-bucket precipitation gauges may be used, but Hanson, *et al*. (1983) noted that this type of gauge recorded between 30 and 50 per cent less precipitation that weighing recording gauges. The temperature of tipping-bucket

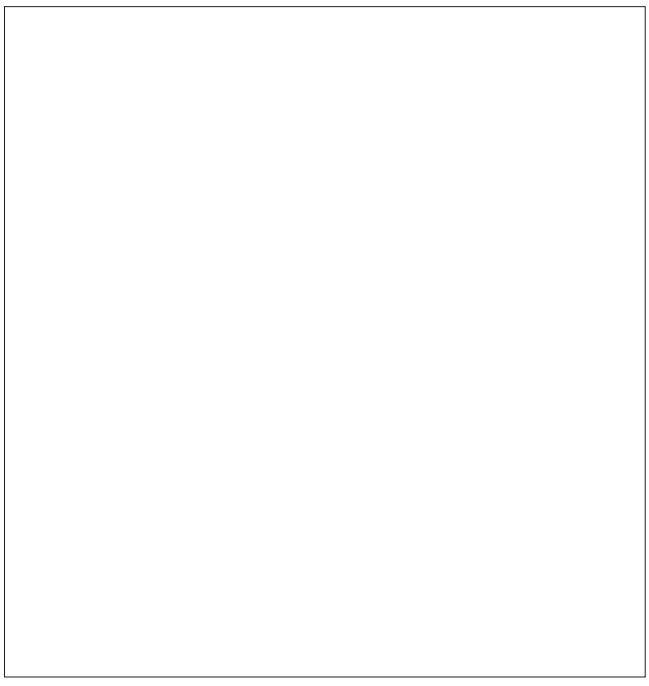

Figure 4.1 — Central Illinois, United States hail-rain network operated during 1968 (from Changnon, 1970).

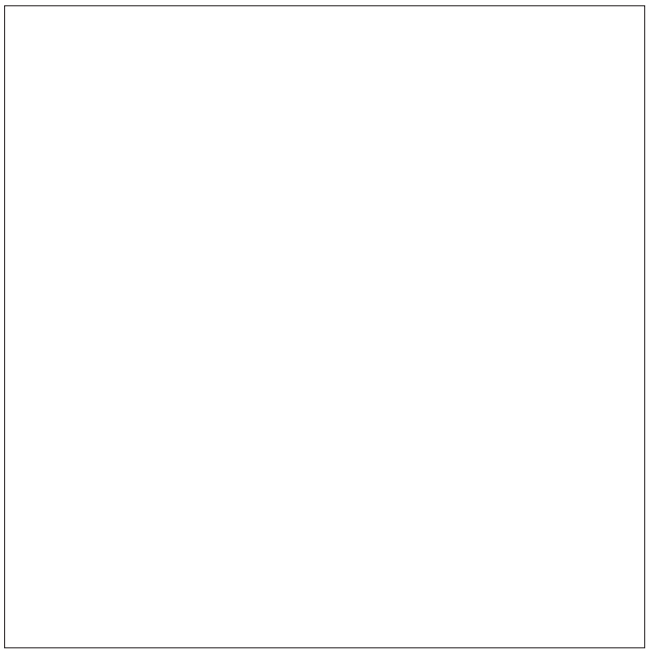

Figure 4.2 — Precipitation catch deficit and the correction factor in relation to wind speed according to the data of the United States Army Corps of Engineers (1956).

gauges should be maintained as low as possible to minimize the undercatch.

The water equivalent of a snowfall is the amount of liquid precipitation contained in that snowfall. It should be determined by one of the following techniques:

(*a*) Weighing or melting — Cylindrical samples of fresh snow are taken with a suitable snow sampler and either weighed or melted;

(*b*) Using raingauges — Snow collected in a non-recording raingauge should be melted immediately and measured by means of an ordinary measuring cylinder graduated for rainfall. The weighing-type recording gauge may also be used to determine the water content of snowfall. During snowfall periods, the funnels of the gauges should be removed so that any precipitation can fall directly into the receiver;

(*c*) Radioisotope gauges — Radioactive gamma sources are used to measure the water equivalent of snow. Attenuation of the gamma radiation signal is proportional to snow depth and the water equivalent of the snow.

It is important to take representative samples. In some areas, a snow course is used that is a permanently

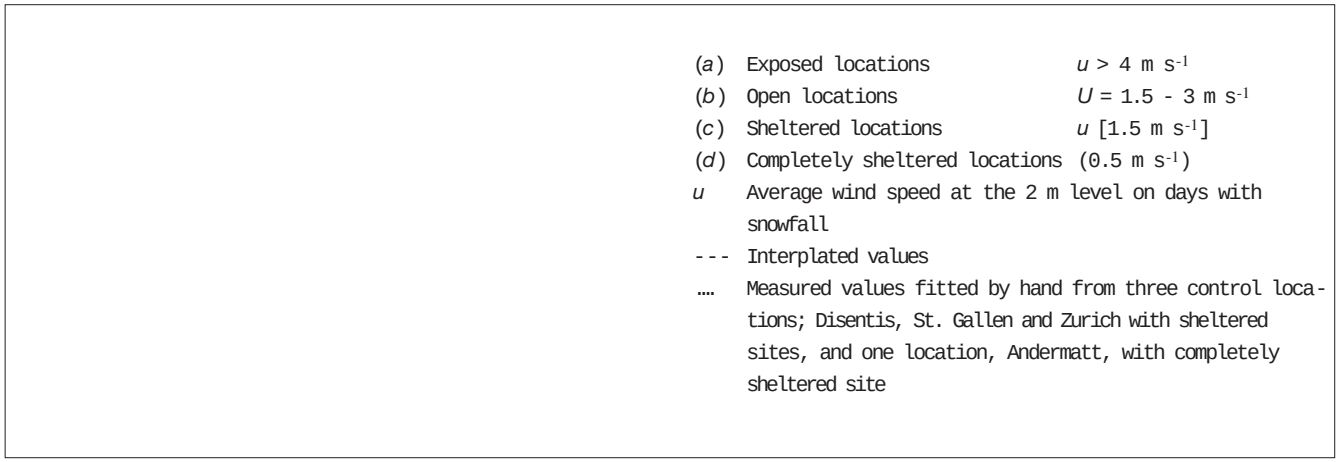

Figure 4.3 — Nomogram for the assessment of snowfall density (ρ) in Switzerland (from Sevruk, 1986) — average values.

marked line where snow surveys are taken each year. The comparative performance of a range of instruments has been discussed in WMO (1989).

4.1.2 Hail

Hail can only be measured directly by observers recording their observations on hail report cards or from the indentations made on hail pads. Hailpads are made from styrofoam (or similar material) one inch thick by 0.5 m × 0.5 m (say). The material is wrapped in aluminium foil and mounted on a supporting platform. Hail size is correlated with the foil indentations. It is necessary to use a very dense network of hailpads to provide reliable estimates of the hail swath. An example of an experimental network used in central Illinois, United States is shown in Figure 4.1. The dense network had 96 hailpads in an area of 100 square miles (about 259 km^2).

4.2 DIFFICULTIES AND ERRORS

As for raingauges (Chapter 3), the most important error in snow measurement is that due to precipitation catchment deficit. Empirical relationships between the wind speed and the correction factors for rain and snow, as shown in Figure 4.2, indicate that this is a particularly important problem for snow.

Snowfall density, on average, decreases with decreasing temperature, although the density also decreases with decreasing wind speed as shown in Figure 4.3. At open locations in Switzerland the snowfall density varies from 0.09 to 0.120 gm cm^{-1} depending on the local wind speed (Sevruk, 1986).

The measurement of hail is more straightforward than that of snow, although these measurements suffer from the imprecision of the hail indentations on the hailpads and melting effects. Such measurements can also be subject to errors in the determination of the precise diameter as hail can occur with a variety of shapes. The water content of hail is also problematic as hail comprises layers of ice of different densities and pockets of air. Hence, simple relationships may be in error and, if the water content is needed, then very careful melting is necessary.

Figure 5.1 — (*a*) The geometry of the radar beam relative to the curvature of the Earth. A radar pulse having length *l* is located at a range *r* from the radar. The height of the base of the beam at range *r* having an angular width of θ is *h*; (*b*) Permanent echoes (PE) and screening caused by hills close to the radar site are also shown (from Browning and Collier, 1989).

CHAPTER 5

GROUND-BASED RADAR MEASUREMENTS

5.1 OUTLINE OF TECHNIQUES

A ground-based radar offers areal measurements of rainfall from a single location, over large areas in near real time. Techniques are based on four types of measurements: (*a*) the intensity of the backscattered radiation (radar reflectivity); (*b*) the difference in reflectivity between two orthogonal radiation polarizations; (*c*) the attenuation of radar energy; and (*d*) the attenuation and reflectivity determined simultaneously at two wavelengths. Of these measurements, only the first has been used widely and implemented operationally. Hence we confine our discussion to this method, although technically more advanced techniques offer potential for operational development.

As a radar beam rotates about a vertical axis, measurements are made at many ranges out to 100 km or more, and at difference azimuths, of the energy backscattered from precipitation particles in volumes above the ground (Figure 5.1*a*). Given a radar wavelength λ, and considering a spherical raindrop with diameter D, we may define a back scattering cross-section $\sigma_b(D)$ and a total attenuating cross-section $\sigma_a(D)$ which are proportional to D^6/λ^4 assuming Rayleigh scattering. This is the justification for introducing a physical parameter called "radar reflectivity factor", Z, defined as:

$$Z = \int_0^a N(D) D^6 \, dD \tag{5.1}$$

where $N(D)$ is the drop size distribution (DSD) within the resolution cell (Z in $mm^6 \cdot m^{-3}$, D in mm, $N(D)$ in $mm^{-1}\ m^{-3}$). In the absence of attenuation along the radar path, and as long as the Rayleigh theory holds (small drops), the backscattered power from a resolution cell is proportional to Z. However, when the ratio $\pi D/\lambda$ becomes larger than 0.1 that is for large drops and hail, then the Mie theory should be used in place of the Rayleigh theory. To take account of this effect, an "equivalent" radar reflectivity faction Z_e is generally considered. Z_e is the same as Z for light rain (mainly composed of small rain drops) but departs from it as the rainfall rate increases; the departure increases more rapidly as the radar wavelength decreases. It may be shown that if liquid precipitation uniformly fills the pulse volume, then the average power returned from precipitation at range r is proportional to Z/r^2, where Z is the so-called radar reflectivity factor given by the sum of the precipitation particle diameters raised to the sixth power (see section 6.4 for further details). Z is related to the rate of rainfall R by the empirical relationship $Z = AR^B$, where A and B depend on the type of rainfall. Many values have been suggested (Battan, 1973), but values often used for rain are $A = 200$ and $B = 1.6$ (Marshall and Palmer, 1948).

Use of R:Z relationships to measure rain, modifying A and B as appropriate, would appear to be straightforward. There are a number of problems, however, arising from the characteristics of both the radar and the precipitation. The importance of these problems will depend upon the particular radar configuration in use and the meteorology of particular situations. Hence they are not listed in order of importance in what follows.

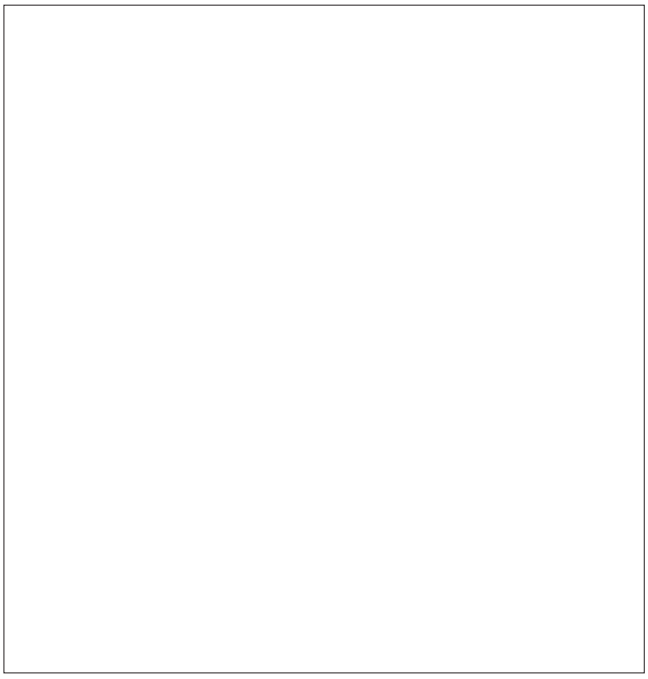

Figure 5.2 — Absolute error (per cent) in 5 min accumulations as a function of the resolution of the reflectivity maps and sampling intervals (from Fabry, *et al*., 1994).

5.2 SINGLE POLARIZATION REFLECTIVITY MEASUREMENTS

5.2.1 Problems arising from the characteristics of the radar and of the radar site

1. *Inadequate radar hardware stability and calibration*
   Maintenance of a stable system is extremely important. Joss and Waldvogel (1990) state that by using up-to-date solid state electronics, it is possible to keep the cumulative error of transmitted power, antenna parameters, noise figure, amplification in the receiver chain, and analogue to digital conversion well within 2 dB. This corresponds to a 36 per cent error in precipitation rate.
2. *Ground clutter and occultation*
   Many aspects of a radar site affect the quality of radar measurements. In general, to obtain good estimates of surface precipitation, a low (less than 0.5°) horizon is required to enable the beam to be kept low. Figure 5.1*a* shows an idealized radar beam from a well-sited radar under normal conditions of atmospheric propagation. However, Figure 5.1*b*, which is for less ideal situations, shows that the main radar beam (or subsidiary beams outside the main beam, known as side lobes which contain much less, but still significant, amounts of microwave power), may encounter ground targets, causing strong persistent echoes (ground clutter) which may be misinterpreted as rainfall. Interception of the beam by the ground also causes occultation or screening of part of the beam, such that only a fraction of the power illuminates the rain at longer ranges. These problems may be partially overcome by using a clutter map collected over a few dry days, to remove pixels contaminated by clutter, in conjunction with a look-up table of correction factors to allow for occultation effects (see for example Harrold, *et al*. 1974). Anomalous refraction of the radar beam,

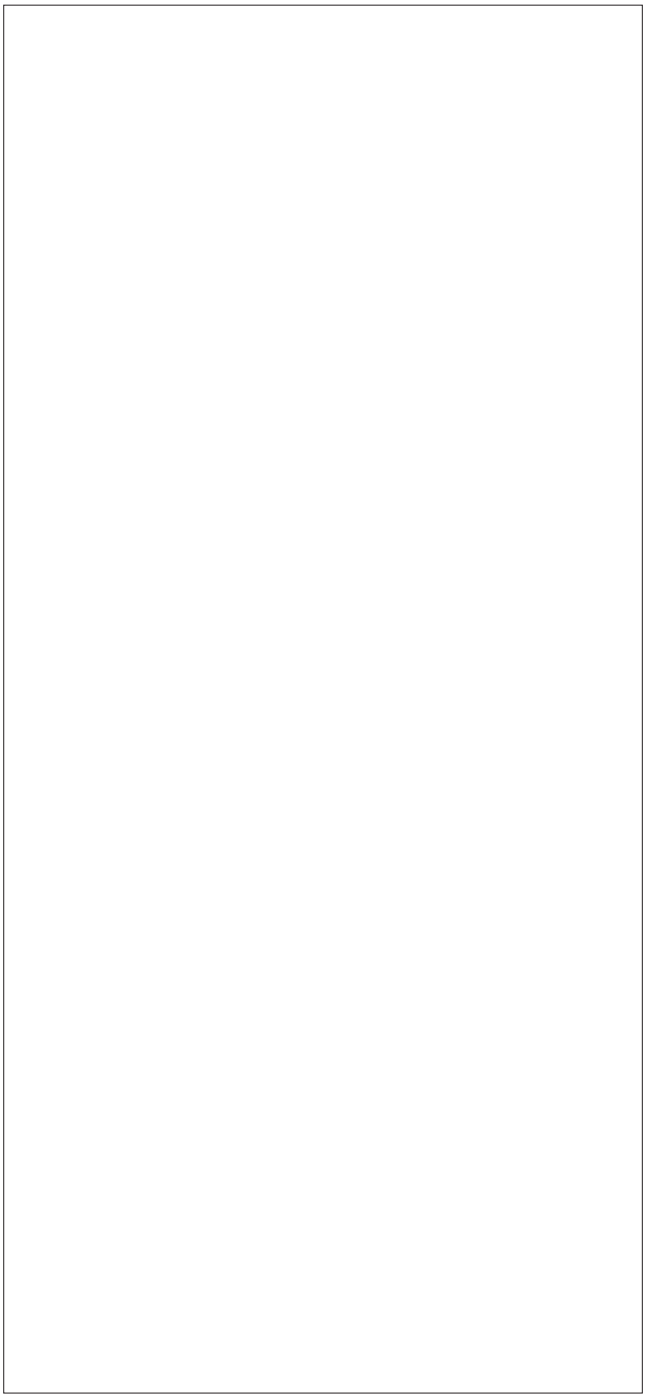

Figure 5.3 — Vertical profiles seen by the radar at various ranges in convective and widespread rain, in low-level rain or snow, and in orographic rain. The numbers in each figure give the percentage (referred to the true melted water value which would be measured at ground level using a raingauge) of rain rate deduced from the maximum reflectivity of the profile. A radar with a 1° beam width is assumed, in a flat country. If the radar is lower than nearby obstacles, then much less precipitation can be observed at far ranges. The top and bottom of the main part of a 1° beam elevated at 0.5° are shown as dashed lines labelled 0° and 1° (partly after Joss and Waldvogel (1990) and Browning and Collier (1989)).

caused by warm, dry air overlaying cooler, moister air, may cause additional ground echoes known as anomalous propagation echoes (ANAPROP). Intersection of the lower parts of the radar beam by water surfaces leads to clutter which may vary significantly over time with the direction of movement of waves and wave height.

3. *Attenuation or poor resolution depending on radar wavelength*
   Use of long wavelengths (10 cm or more) avoids errors caused by attenuation due to precipitation. However, for the same antenna size the beam width at 10 cm is twice as large as at 5 cm. This causes reduced spatial resolution at long ranges and leads to more ground clutter (Harrold, 1974). Moreover, Ulaby, *et al*. (1981) point out that precipitation echoes observed at 10 cm are 12 dB weaker than those observed at 5 cm for the same output power, whereas the ground clutter echo strength is almost independent of wavelength. Although a 3-cm radar would be even more effective than a 5-cm radar having the same beam width in reducing clutter, it would suffer unacceptably from attenuation in only moderately heavy rain. In practice, the choice of wavelength is between 5 and 10 cm; it is influenced by cost and the frequency of occurrence of very heavy rain and large hail which cause significant attenuation of a 5-cm radar beam. Operational radars in the United States, including the next generation radar network (NEXRAD) (now known as the WSR-88D) radars, are 10-cm radars, as hail and exceedingly heavy rain are frequent over much of the United States. Attenuation by moderate or heavy rainfall can be corrected for using a 5-cm radar beam, although when the beam intersects the melting level or hail, such corrections are somewhat unreliable.
4. *Radome attenuation*
   The antenna of a radar is often housed in a radome made from rubberized material or fibreglass and either inflated or supported by aluminium strips. Such structures protect the antenna from precipitation and pollutants. By eliminating wind loading, they also allow less powerful drive motors to be used. Unfortunately, precipitation on the radome attenuates the radar beam. The degree of wetting and resulting attenuation depends on the radar wavelength, the nature of the surface, and the size of the radome. Wilson (1978) found that a rainfall rate of 40 mm h^{-1} produced an attenuation of a 5-cm radar of 1 dB. This type of attenuation can be reduced somewhat by the use of Teflon coating on the radome, although regular cleaning is also essential. Snow can produce a much bigger effect, and it is necessary to heat the radome to prevent a build-up of snow and ice.

5.2.2 Problems arising from the characteristics of the precipitation

1. *Errors due to the fluctuating nature of the signal from precipitation averaging over areas of non-uniform precipitation and samples*
   Scattering of microwave radiation from a population of precipitation particles within the radar pulse volume produces a fluctuating signal at the radar receiver. To produce a measurement of precipitation intensity, it is necessary to average the received power over a number of independent samples either in time or in space. Rainfall rate may vary by a factor of 10 within a 10-min period or within a distance of 2 km, so the averaging must be done on smaller scales. If such variations occur within the radar pulse volume (for example, at long ranges where the beam width is several kilometres wide), this may lead to a large error of several decibels (Mueller, 1977; Zawadzki, 1984). These effects are often noted when comparing radar and raingauge measurements of rainfall (for example Joss and Waldvogel, 1990).
   Fabry, *et al*. (1994) investigated the dependence of the accuracy of short-period radar rainfall accumulations on periodic sampling of the rain field. Errors due to sampling can be greater than all the other errors if accumulations are improperly computed. It was found that the best accumulations are obtained with very high time resolution data. For a given time resolution, there is an optimum spatial resolution that minimizes rainfall accumulation errors, as shown in Figure 5.2.
2. *Variability of the R:Z relationship*
   The values of A and B in the $R:Z$ relationship depend upon the nature of the raindrop size distribution which differs greatly between drizzle at one extreme and thunderstorms at the other. Battan (1973) lists over 60 $R:Z$ relationships. The presence of updrafts or downdrafts also affects the $R:Z$ relationship (Lee, 1988). Austin (1987) calculates that in a strong downdraft of 8 m s^{-1}, the reflectivity value for a given rainfall rate would be about 3 dB less than in still air, producing an underestimate of the rainfall rate of 40 per cent.
3. *Variability of reflectivity in the vertical*
   The radar beam at far ranges from the radar site is at a considerable height above the surface of the Earth. For a beam elevation of 0.5°, the axis of the beam is at a height of 2 km at 130 km range and 4 km at a 200 km range. Reflectivity varies in

Equation	*Precipitation Type*	*Reference*
$140\ R^{1.5}$	Drizzle	Joss, *et al*. (1970)
$250R^{1.5}$	Widespread rain	Joss, *et al*. (1970)
$200R^{1.6}$	Stratiform rain	Marshall and Palmer (1948)
$31R^{1.71}$	Orographic rain	Blanchard (1953)
$500R^{1.5}$	Thunderstorm rain	Joss, *et al*. (1970)
$486R^{1.37}$	Thunderstorm rain	Jones (1956)
$2000R^{2.0}$	Aggregate snowflakes	Gunn and Marshall (1958)
$1780R^{2.21}$	Snowflakes	Sekhon and Srivastava (1970)

Table 5.1 — Typical empirical relationships between reflectivity factor Z ($mm^6\ m^{-3}$) and precipitation intensity, R (mm h^{-1}) (after Battan, 1973)**. Discussion of relationships in snow are included here for comparison and are discussed further in this chapter**

the vertical because of growth or evaporation of precipitation, vertical air motion and melting (where melting of snowflakes occurs, there is a layer of enhanced reflectivity known as the bright band).

These factors can lead to large differences between the apparent precipitation intensity measured by radar and the intensity of precipitation reaching the ground (Fabry, *et al*., 1992). Average vertical reflectivity profiles have been derived for different precipitation conditions. The top three profiles in Figure 5.3 are for convective rain (Figure 5.3*a*), widespread rain with bright band (Figure 5.3*b*), and snow or shallow rain (Figure 5.3*c*). Although there may be large deviations from these profiles on particular occasions, it is instructive to use them as an indication of the percentage of the precipitation observed by radar at various ranges allowing for Earth curvature. In particular, the profiles in Figures 5.3*b* and 5.3*c* draw attention to the difficulties of making measurements in the presence of bright band or shallow rain. Another problem in some parts of the world is orographic growth of precipitation at low levels over hills exposed to strong moist maritime air flows. To some extent, orographic low-level growth can be estimated by applying climatological correction factors, but where possible the radar should be sited so that it can observe the low-level precipitation directly. As shown in Figure 5.3*d*, considerable orographic enhancement may occur within $^1/_2$ km of the ground, and so it is observable only at very close ranges.

5.2.3 *Z:R* relationships

Measurements of radar reflectivity (Z) are transformed to measurements of rainfall (R) using the empirical relationship discussed in section 5.1. However, the exact form of this relationship depends upon rainfall type; Battan (1973) lists 69 published relationships all of which have been found to be applicable in particular circumstances. Fortunately, most of the relationships do not differ greatly for the same type of rainfall at rainfall rates between about 20 and 200 mm h^{-1}. The most typical relationships for particular rainfall types are shown in Table 5.1, which also illustrates the variability of the published data for the same type of precipitation. The *Z:R* relationship for orographic rain must be viewed with caution as, since these data were published, an understanding of the growth of orographic rainfall at very low levels has been gained (see for example Browning, 1990). Low-level orographic precipitation enhancement may well account for the relationship given in Table 5.1.

Following work by Zawadzki (1984), Collier (1986*a*), Joss and Waldvogel (1990) and Rosenfeld, *et al*. (1992) it has become clear that uncertainties in the dropsize distribution may not be the largest source of errors in radar-based rainfall measurements. Collier, *et al*. (1983) recognized the need to apply different *Z:R* relationships derived from raingauge data for different rainfall regimes. Hence, stimulated by the work of Doneaud, *et al*. (1984), who found an excellent correlation between integrated convective rainfall volume and

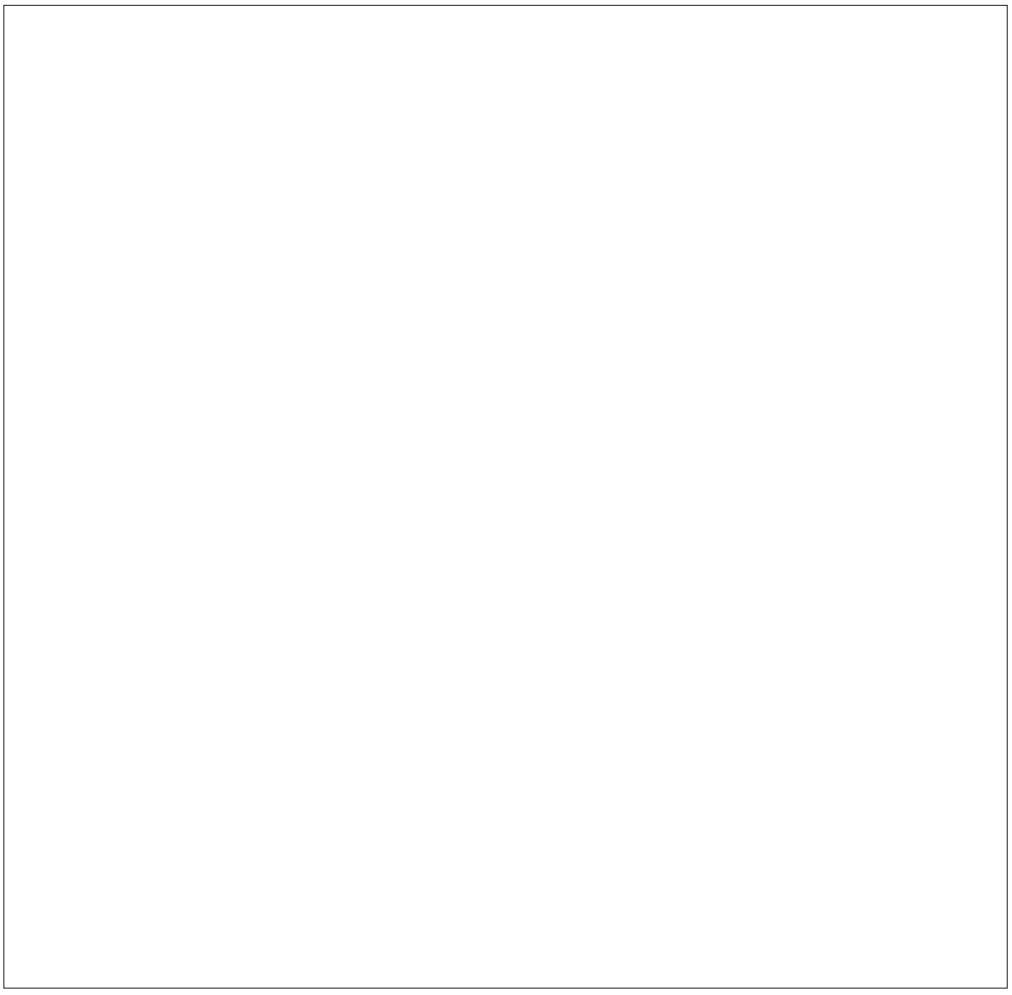

Figure 5.4 — Variation of hourly assessment factor measured over each month during 1982 for four raingauge sites at different ranges from the Hameldon Hill radar site in north-west England (from Collier, 1986*a*).

the area-time integral (ATI) of the area exceeding a given optimum threshold reflectivity value (τ dBz) (see section 6.2.3), recent work (Atlas, *et al.,* 1990; Atlas and Bell, 1992) has sought to use the high correlation between the area average rain intensity, <R>, and the fraction of the domain covered with reflectivity greater than a given threshold (τ), $F(\tau)$.

This work led to the development of the probability matching method (PMM) of deriving the *Z:R* relationship, in which rainfall rate, R, is related to the observed radar reflectivity, Z_e, by matching R and Z_e pairs that have the same cumulative probability (Calheiros and Zawadzki, 1987). The assumption made was that the unconditional probability for any given rainfall intensity was constant everywhere in the radar field, and that this probability was sampled in a representative way by raingauges. The need for this assumption was removed by Rosenfeld, *et al*. (1993) who assumed that the conditional probability density function of rainfall intensity, regardless of the integrated rain depth for any given rainfall regime is the same everywhere. The Z_e:R relationships so derived varied greatly with the rainfall regime and with the radial distance from the radar.

This work has been developed further by Rosenfeld, *et al*. (1994; 1995*a*, *b*). Zawadzki (1975) showed that the spread of the radar beam over an area of A km^2 is analogous to the

Figure 5.5 — Probability (P, per cent) of particular errors (E, millimetres) occurring in measurements of hourly point rainfall for three classes of rainfall amount (G) and for cases (left) with no bright band and (right) with bright band present. Both real-time-adjusted (solid lines) and unadjusted (dashed lines) plots using raingauge data analyses are distinguished. The number of hours in each category (M) is also given. The data are for the Hameldon Hill radar in north-west England during 1982 (after Collier, 1986*a*, *b*).

spread of a raingauge measurement in time T where:

$$T = \frac{1}{3} \times \frac{A^{1/2}}{V} \tag{5.2}$$

and V (km h^{-1}) is the horizontal velocity of the rainfall. Using a fixed value of T, the radar-indicated rainfall intensity over an area becomes independent of T and is minimally affected by the radial distance from the radar (Rosenfeld, *et al.,* 1994). The probability density function of Z_e is taken from radar windows centred over the coordinates of the raingauges typically of size 3° azimuthally by 3 km radially. The probability density function of R is obtained from the three three-minute averaged raingauge intensities centred at the time of the radar scan. The unconditional cumulative probabilities of Z_e and R are matched, and hence the Z_e and R having the same cumulative percentile are related to each other.

This technique is referred to as the window probability matching method (WPMM) and was improved further by Rosenfeld, *et al*. (1995*a*, *b*). Rainfall types are classified using the horizontal radial reflectivity gradients, the cloud depth as scaled by the effective efficiency, the bright band fraction within the radar field window and the height of the freezing level (see section 6.2.3). The results of tests in Australia and Israel are very impressive, and it is felt by the authors that this procedure should result in considerable improvement of both point and areal rainfall measurements with respect to any other method using reflectivity-only radars, If this is so, then the extent to which raingauge adjustment schemes using interpolation of raingauge to radar ratios, discussed in the next section, must be questionable. Also, the WPMM does not require that range effects be removed or that the bright-band be corrected in the radar imagery, but rather that its presence and the fraction of enhanced echoes close to the 0°C level be recognized. This requires only an independent method of defining the 0°C or bright-band altitude. Finally, Rosenfeld, *et al*. (1995*a*) define and test successfully procedures for recognizing windows contaminated by ground clutter or spurious echoes which negate the need for procedures more complex than the use of a simple clutter map. In spite of the great potential of this approach, further extensive testing is required to verify its operational robustness. Also, it must be remembered that a number of, albeit not very many, raingauges are an essential element in this approach.

5.2.4 Raingauge adjustment procedures

Considerable work has been carried out over the past 20 years or so to address all of the problems discussed in sections 5.2.1–5.2.3. This has led to the development of procedures for adjusting radar measurements of precipitation using data from raingauges (heated gauges for snowfall), although the use of heating can introduce large errors, see section 4.1.1. Wilson and Brandes (1979) provide a useful summary for much of the early work. Techniques have ranged from the application of an adjustment factor derived by simple averaging or statistical procedures for the whole area of interest, to the use of a large number of raingauges to define the detailed spatial variations in the adjustment factor.

Many of the reported estimates of the accuracy of rainfall measurements by radar refer to the results of carefully controlled research assessments rather than to operational systems. An exception is the study described by Collier (1986*a*, *b*). This was carried out using an operational system in north-west England for a 12-month period during 1982/1983. A raingauge adjustment procedure (see Collier, *et al.,* 1983) was used consistently throughout the period, and all data were included regardless of their quality. Figure 5.4 shows the variation of the monthly mean adjustment factors (radar/gauge) over the 12-month period for four raingauge sites at different ranges from the radar. Three of these sites were within the area covered by the real-time adjustment system (up to 75 km range); the fourth, Nottingham, is included to illustrate the performance at greater range. During the summer, when deep convective rainfall was common, the radar estimated rainfall well at all ranges. The average performance was not as good during the winter. The record for Nottingham shows the underestimation which can occur at far ranges in winter because of the intensification of reflectivity below the radar beam. The other graphs indicate a tendency to overestimate at near ranges, probably as a result of uncorrected bright-band effects within the radar beam.

At any time of the year the adjustment factors at individual raingauge sites may vary considerably from the mean monthly values. When these variations are examined, the bright-band effect is seen to be very significant. If all observations influenced by bright band are excluded, the average percentage difference between hourly unadjusted radar estimates and raingauge readings in conditions of widespread frontal rainfall is 60 per cent (Collier, 1986*a*).

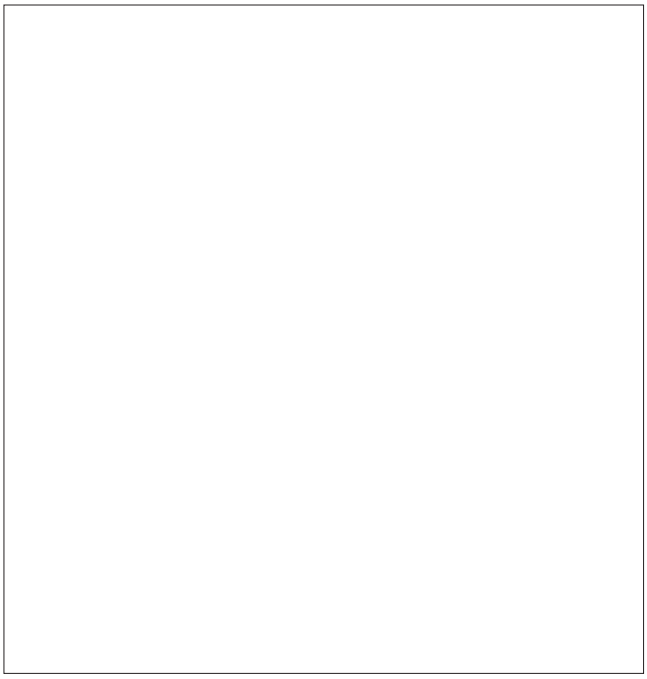

Figure 5.6 — The best estimate of the r.m.s. error in surface precipitation rate derived from the C-band Wardon Hill radar, United Kingdom during seven periods of frontal rainfall. The r.m.s. error is plotted as a function of the mean equivalent precipitation rate in the S-band Chilbolton radar comparison data. The open symbols are for the raw Wardon Hill data and the closed symbols for the corrected data. Some cases were repeated using Wardon Hill data from higher elevation beams which present a more severe test of the correction method (from Kitchen, *et al.,* 1994).

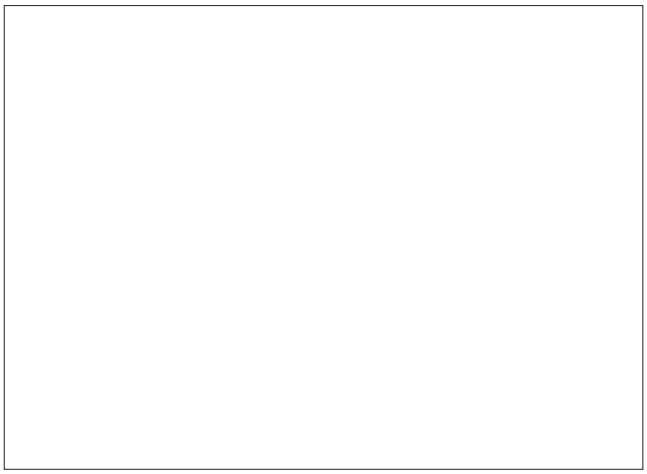

Figure 5.7 — Differential rainfall rate (R_{BB}-R_o) versus surface rainfall rate (R_o) derived for three radar frequencies using a microphysical model of the bright band (BB) (from Hardaker, *et al.,* 1995).

Real-time adjustment reduced this average difference to 45 per cent. In convective rainfall, without bright band, adjustment improves the figures from 37 per cent to 21 per cent. When bright-band effects are present, the average difference is 100 per cent, and adjustment reduced this to 75 per cent. The probability of getting a particular error, and the improvement achieved by using real-time raingauge adjustment, are shown in Figure 5.5 for three categories of rainfall, with and without bright band.

While raingauge adjustment can clearly improve the accuracy of radar measurements of precipitation it should be noted that on any individual case this is not necessarily so. Indeed, in convective precipitation raingauge adjustment can actually decrease accuracy. Kitchen and Blackall (1992) note that much of the difference between point raingauge values and radar measurements is due to gauge sampling problems. They conclude that where precipitation is dominated by orographic effects, raingauge adjustment is useful, but in other areas or on other occasions this is not so. Even techniques using data from a very dense network of raingauges (for example Moore, *et al.,* 1991) suffer from the problem of random and bias errors introduced by representativeness errors in the gauge-radar comparisons. In addition, economic networks cannot completely resolve errors due to the bright band or orographic enhancement. Nevertheless, the advantage of raingauge adjustment is that in relating radar measurements to surface precipitation a range of the errors discussed in sections 5.2.1 and 5.2.2 may be partially dealt with in a single process. Time integrated, G/R values are probably the most appropriate adjustment factors to use. However, point values are not representative of wide area radar measurements and it is important to use schemes involving some type of areal integration.

An alternative approach to deriving the relationship between radar-observed reflectivity, Z_e, and raingauge measured rainfall intensity, R, has been described in section 5.2.3. The observed reflectivity is often very different from the true reflectivity near the surface due to the averaging of the real reflectivity field aloft by the beam attenuation and variations in the drop-size distribution between the pulse volume and the surface. The formulation of the Z_e-R function is constrained such that: (*a*) the radar-retrieved probability density function of R is identical to the raingauge measured probability density function; and (*b*) the fraction of the time that it is raining is identical for both the radar and for simultaneous co-located raingauge measurements. The resultant Z_e-R functions are not necessarily power laws. This approach, discussed in more detail earlier and in section 6.2.3, may prove a more productive approach than that involving interpolation of raingauge-radar ratios.

5.2.5 Range and bright-band corrections

Joss and Waldvogel (1990) concluded that errors in the radar measurement of surface precipitation are dominated by the effect of variations in the vertical profile of reflectivity. Such variations occur on the scale of individual pixels (Kitchen and Jackson, 1993), and therefore it would seem that any correction method would have the greatest potential benefit by providing adjustments on a pixel-by-pixel basis. Kitchen, *et al.* (1994) discuss three approaches to adjusting radar estimates of precipitation for both range and bright-band effects, as follows:

(*a*) Raingauge adjustment: As discussed in section 5.2.4, all gauge adjustment schemes suffer from the problem of random and bias error introduced by representativeness errors in the comparisons;

(*b*) Analytic methods based on using radar data alone: Procedures described by Harrold and Kitchingman (1975), Koistinen (1991), Gray (1991), Andrieu and Creutin (1995) and Andrieu, *et al.* (1995), derive an average reflectivity profile by analysing data from several radar beam elevations at ranges up to a few tens of kilometres from the radar. The average profile is then used to correct data from longer ranges. Assumptions of spatial homogeneity are necessary, both in the derivation of the profile and in its application to data at longer ranges. In effect, a correction domain is employed which encompasses the whole area of coverage of a radar, or at least a sector thereof.

Smith (1986) devised an analytic technique for reducing errors due to the bright band which proved very promising in tests. In routine operation, however, it was found to be susceptible to large errors when significant variations in the freezing level occurred over the area covered by a radar. Such variations are common in frontal precipitation in the United Kingdom and Harrold, *et al.* (1974) described some particularly dramatic examples. More recently, Rosenfeld, *et al.* (1995*a*, *b*) derived a number of radar echo classification criteria which may be employed to recognize the occurrence of bright band effects, partial beam filling and reduction of bias error in data. Further work is needed to assess the operational reliability of this technique;

(*c*) Physically-based methods using independent meteorological data: Austin (1987) (see also Dalezois and Kouwen, 1990; Fabry, *et al.,* 1992)) recommend physically-based techniques. One such has recently been described by Kitchen, *et al.* (1994). An idealized reflectivity factor profile was constructed from analysis of radar data. The heights of significant turning points in the profile are

diagnosed from relevant meteorological data (for example surface temperatures) at each radar pixel. The parametrized profile is weighted by the radar-beam power profile and the surface precipitation rate found by an iterative method in real-time.

Since this technique can exploit a wide range of meteorological information from conventional observations and forecast models to derive the reflectivity factor profile Kitchen, *et al*. (1994) felt that the technique is better than those using analyses of radar data alone. Figure 5.6 shows the r.m.s. error in surface precipitation rate before and after correction during seven periods of frontal rain. This is undoubtedly true, although the strong dependence on other meteorological observations and model data makes the procedure vulnerable to the availability and accuracy of these data sources.

Table 5.2
Example values of R and Z_e for rain and snow
(from Smith, 1984)

	Precipitation rate R *(mm h^{-1})*	
	1	10
Z_e (rain) – dBz	23	39
Z_e (snow) dBz	26	48

A somewhat different approach has been described by Hardaker, *et al*. (1995). A microphysical model is used to calculate the reflectivity profile using as input lapse rate information from either radio-sondes or a mesoscale numerical model. Simple relationships between bright-band intensity and surface rainfall rate were derived (Figure 5.7) which may be useful in the absence, in real-time, of extensive computing facilities or independent meteorological data. This approach enables improvements in the stylized bright band profile to be made, and tests using numerical model temperature profiles as input to a correction procedure showed encouraging results.

The development of approaches to bright band correction seem to be following two distinct routes, namely techniques using independent meteorological data and techniques using solely radar data. There is a need to intercompare these approaches on a routine operational basis. It is likely that work will continue in this area.

5.2.6 Area-average method

Chiu (1988) found a high correlation between the instantaneous area-average rainfall rate and fractional area covered by radar echoes above a predefined rainfall-rate threshold, using data from the Global Atmospheric Research Programme (GARP) Atlantic Tropical Experiment (GATE). Rosenfeld, *et al*. (1990) also found the same high correlation using GATE data and data from South Africa, Texas and Darwin. Further details are given in section 6.2.3 as this type of technique can be used with satellite as well as radar data.

Atlas *et al*. (1990) showed that the relationship depends on the existence of a well-behaved probability density function (pdf) of rainfall rate. A theoretical explanation of the correlation between the instantaneous area-average rainfall rate and fractional area occupied by rain of intensity greater than a set threshold was also provided by Kedem, *et al*. (1990), based on the assumption of a homogeneous pdf. Recently, Cheng and Brown (1993) demonstrated that this technique could be used to estimate instantaneous frontal rainfall over areas of about 105 km^2 with an accuracy of around 14 per cent.

5.2.7 Measurements of snowfall

In section 5.1 the "equivalent" radar reflectivity, Z_e was defined. For spherical drops with small diameters compared to the radar wavelength, Z_e is equal to Z. However, as discussed by Smith (1984) for snowflakes or other ice particles, the fact that the particle shapes are generally far from spherical complicates matters.

According to Marshall and Gunn (1952), for particles small enough to fall in the Rayleigh scattering region (which requirement is reasonably well fulfilled at the usual weather radar wavelengths by snowflakes and small ice particles), the radar cross-section of an irregular particle composed of a weak dielectric like ice is the same as that of a sphere of the same mass. Hence the exact shape of the particle is immaterial.
The radar cross-section of an ice particle is:

$$\nabla = \pi^5 \, |K|_i^2 \, D^6 / \lambda^4 \qquad (5.3)$$

where $|K|^2$ is the dielectric factor being $|(\varepsilon_r - 1) / (\varepsilon_r + 2)|^2$, the relative permitivity. (It is related to the index of refraction n by $\varepsilon_r = n^2$.) The subscript i indicates that a value appropriate for ice should be used. The diameter implied in equation 5.3 is that of a sphere having the same mass as the particle in question.

The radar reflectivity, Z (or radar cross-section per unit volume), of the array of particles in the radar contributing region of volume, V_c, is:

$$Z = \sum_{V_c} \frac{\nabla}{V_c} = \frac{\pi^5 |K|_i^2}{\lambda^4} \cdot \sum_{V_c} \frac{D^6}{V_c} \qquad (5.4)$$

The equivalent radar reflectivity factor, Z_e, is defined as:

Figure 5.8 — The dependence of the mean percentage error, regardless of sign, of estimates of snow depth over areas of 100 km^2 derived from radar data, on the assumed height of the melting level (from Collier and Larke, 1978).

$$Z_e = \frac{\lambda^4 z}{\pi^5 \left|K\right|_w^2} \tag{5.5}$$

where the subscript *w* indicates that the value appropriate for water (approximately 0.93 for the usual meteorological radar wavelengths) is used by convention. That convention is adopted because when radar measurements are made, it is often not certain whether the particles are water or ice. Substituting the value of *Z* from equation 5.4 into equation 5.5, for ice particles:

$$Z_e = \frac{|K|_I^2}{|K|_W^2} \sum_{V_c} \frac{D^6}{V_c} \frac{D^6}{V_c} \tag{5.6}$$

When particle size data are analysed to determine radar variables, the quantity usually calculated is the radar reflectivity factor *Z* and not the equivalent radar reflectivity factor Z_e. The analysis yields values of:

$$\sum_s \frac{D^6}{V_s} = \sum_{V_c} \frac{D^6}{V_c} = Z \tag{5.7}$$

where V_s is some sampling volume, much smaller than V_c.

Figure 5.9 — Time-integrated radar reflectivity for the period 14 GMT/8 Jan to 02 GMT/9 Jan 1982. National Grid (Transverse Mercator) projection. Isopleths are drawn for equivalent snowfall totals in excess of 1 cm (dotted contours), 5, 10 and 20 cm (solid contours with stippled shading). The plotted numbers indicate ground truth estimates of the amount of snow (cm) which fell in the corresponding 12-hour period (from Browning, 1983).

Comparing equations 5.6 and 5.7 it can be seen that, for ice particles:

$$Z_e = \frac{|K|_i^2}{|K|_w^2} Z \tag{5.8}$$

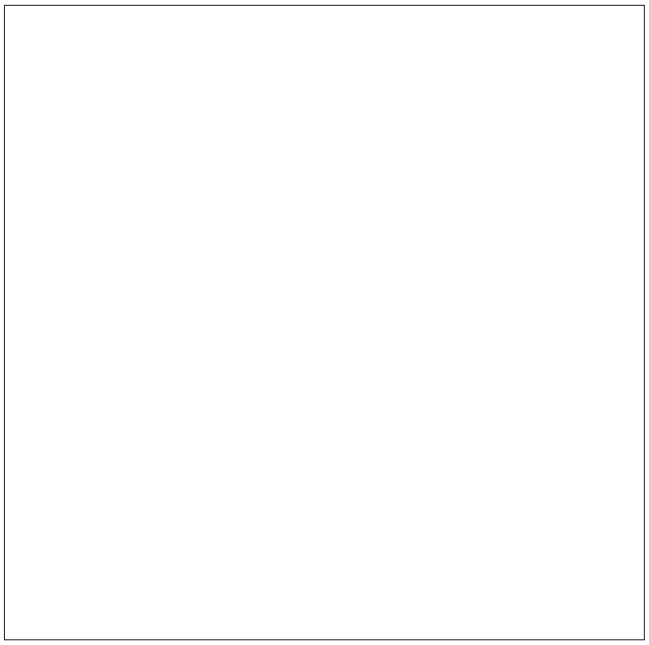

Figure 5.10 — Schematic illustration of the dual-wavelength method of hail detection proposed by Eccles and Atlas (After Carbone, *et al*., 1973; from Browning, 1978).

Smith (1984) discusses the appropriate value of $|K|_i^2$ pointing out that there are two possible "correct" values depending upon how the particle sizes are determined. If the particle sizes used are melted drop diameters, then $|K|_i^2$ is 0.208 and

$$Z_e = 0.224\, Z \tag{5.9}$$

However, if the particle sizes are expressed as equivalent ice sphere diameters, then $|K|_i^2$ is 0.176 and

$$Z_e = 0.189\, Z \tag{5.10}$$

Normally, radars use the "water equivalent" Z_e defined with $|K|_w^2 = 0.93$, and the dielectric factor is not changed when the precipitation form changes from liquid to solid. Table 5.2 compares equivalent radar reflectivity factors calculated for precipitation rates of 1 and 10 mm h^{-1} for rain, using the Marshall-Palmer relationship (section 5.2.3) and for snow, using the Sekhon and Srivastava (1970) relationship (section 5.2.3). At R=1 mm h^{-1}, the Z_e value for snow is 3 dB higher than that for rain. Hence, in general, radar echoes from snow are not weaker than those from rain, although there is a tendency for the precipitation rates to be generally lower in snow than in rain.

Much work has been done on the accuracy of radar measurements of rainfall, but only a limited amount of data on the accuracy of radar measurements of snowfall has been obtained. Jatila (1973), using as a calibration the water equivalent of snow collected in a single raingauge, found that 60 per

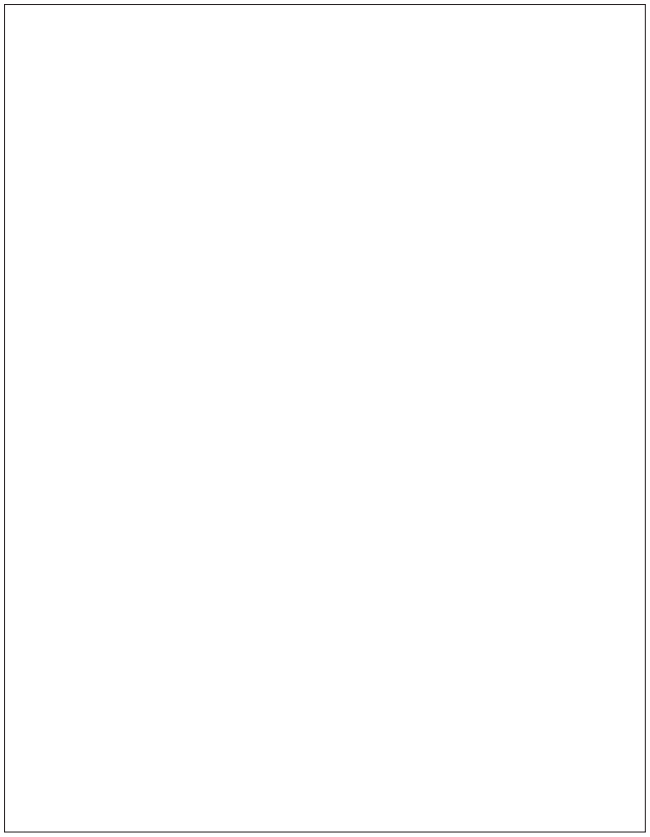

Figure 5.11 — A nomogram for distinguishing between hail and heavy rain in convective precipitation (from Auer, 1984).

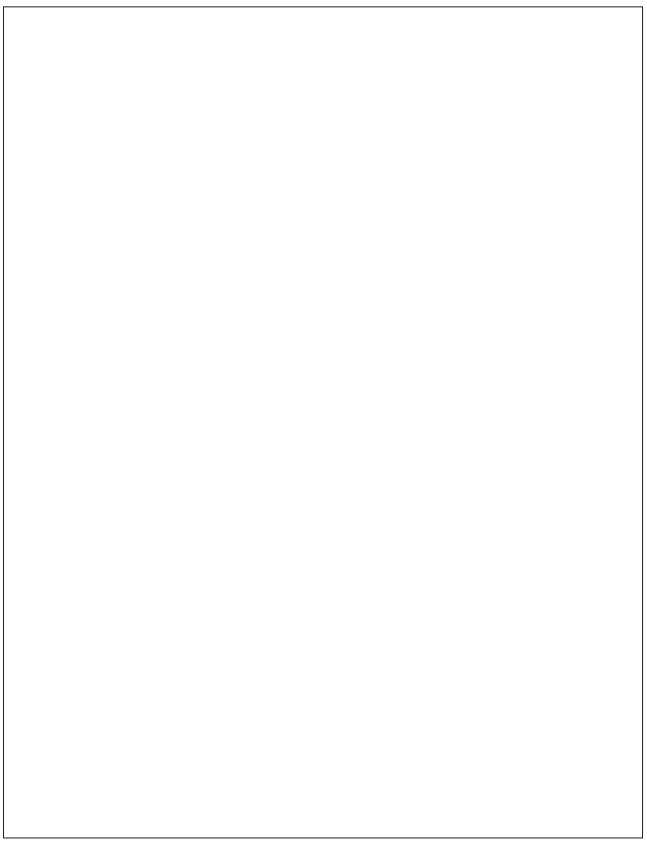

Figure 5.12 — A plot of hail diameter against radar reflectivity, assuming a mono-disperse drop-size distribution (from Hardaker and Auer, 1994).

cent of the snowfall amounts derived from radar measurements within about 50 km of the radar site fell in the interval –24 to + 32 per cent of the daily amounts of snowfall measured by gauges. The most extensive measurements to date have been carried out by Pollock and Wilson (1972). This project used three radars and an extensive gauge network which included 13 weighing-recording precipitation gauges (Peck, *et al*., 1973). The accuracy of radar measurements of snowfall was found to be similar to that reported by Jatila within about 30 km of the radar, but it rapidly decreased as the height of the radar beam increased with increasing distance from the radar. Both of the above studies were made over flat terrain, but Collier and Larke (1978) showed that comparable accuracy can also be achieved in hilly terrain provided the height at which melting occurs is known (Figure 5.8). More recently, Boucher (1981) reported additional measurements confirming the accuracy noted by Jatila and by Pollock and Wilson within 50 km of the radar, although Browning (1983) points out that snowfall development below the radar beam due to orographic effects can lead to significant underestimates of the surface snowfall. This is illustrated in Figure 5.9 where radar estimates over South Wales are about 50 per cent of the values measured at the surface.

5.2.8 Measurements of hail

When a radar observes hail, the backscattered power is no longer proportional to the sixth power of the particle size and Mie scattering (see section 5.1) theory is applicable as the particle diameters are larger than one tenth of the radar wavelength. Battan (1973) proposed a Marshall-Palmer Z_e-R relation, which accounted for Mie scattering. At 5.5 GHz (C-band) and 0°C this relation is:

$$Z_e = 10 \log_{10}(280R^{1.45}) \text{ dBZ} \qquad (5.11)$$

Problems occur in heavy convective rainfall, when reflectivity is often contaminated by hail. This increases reflectivity, because of the large hail diameters compared with the size of the raindrops, and therefore produces an artificially large value of R through the use of a Z_e–R, or Z-R relationship.

Considering hail alone, then a simple relationship between reflectivity and hail diameter, Z–D_H, can be obtained (Hardaker and Auer, 1994). Here, the hail diameter D_H is in millimetres. If it is assumed that the hail conforms to a monodisperse drop-size distribution (Auer and Marwitz, 1972, 1973), that is, the hail in the convective cell is all of similar diameter, then (Auer, 1972):

$$N(D_H) = 561 \times D_H^{-3.4} \qquad (5.12)$$

Assuming Rayleigh scatter in the hail at C-band then:

$$Z_e = 10 \log_{10} (561 \times D_H^{2.6}) \text{ dBZ} \qquad (5.13)$$

There is an overall increase in Z_e with hail size especially at 10 cm wavelength. Hence, the measurement of (Z_e) max provides a method of hail detection (Geotis, 1963; Donaldson, 1965).

A method of hail detection was proposed by Atlas and Ludlam (1961) based upon the strong dependence of Z_e on wavelength in the Mie region, but the lack of wavelength dependence of Z_e in the Rayleigh scattering region. This technique was implemented by Sulakvelidze, *et al*. (1967) in the Russian Federation although their approach is suspect as they made no correction for attenuation in calculating Z_e. Eccles and Atlas (1973) proposed a method using y, the ratio of Z_e values measured at 10 cm and 3 cm. The signature of hail given by the value of dy/dr, where r is the range from the radar, is shown in Figure 5.10. Unfortunately, Jameson (1975) showed that in some circumstances false signatures or no signatures at all may be observed (Srivastava and Jameson, 1975, 1977).

Waldvogel, *et al*. (1979) suggest the following simple criterion:

$$H_{45} > H_0 + 1.4 \text{ km} \qquad (5.14)$$

where H_{45} is the height of the 45 dBZ contour which must exceed the height H_0 of the 0°C level by more than 1.4 km. This algorithm detected all hail cells early in their life but about 30 per cent of the cells identified as dangerous never actually produced hail at the ground. Joss and Waldvogel (1990) report that similar relationships have been used in South Africa (Mather, *et al*., 1976) and in north-east Colorado (Foote and Knight, 1979).

To measure hail quantitatively, Waldvogel, *et al*. (1978*a*, *b*), using a 10-cm radar, established a relationship

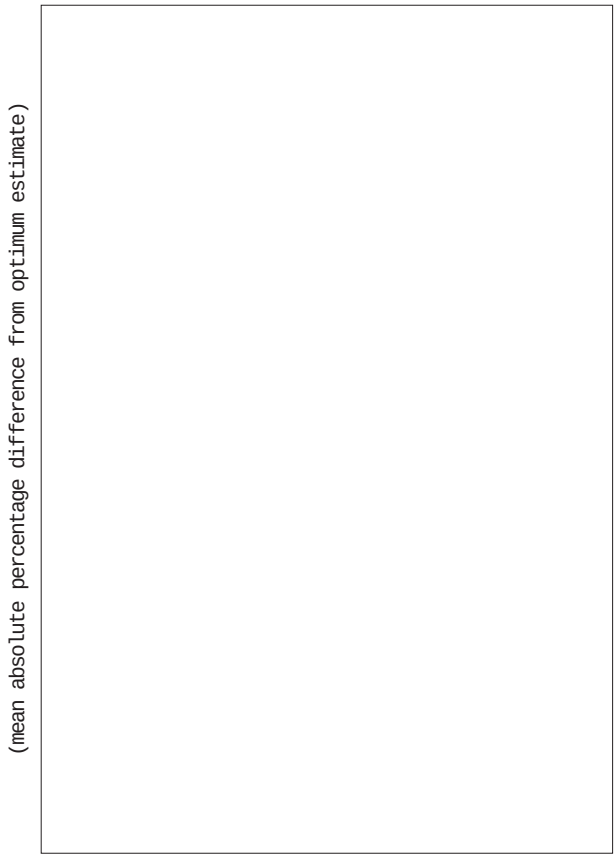

Figure 5.13 — Differences between estimates of hourly sub-catchment rainfall related to raingauge density (from DWRHP, 1977).

between the flux E of the kinetic energy of the hailstones and the radar reflectivity Z:

$$E = 5 \times 10^{-6} Z^{0.84} \tag{5.15}$$

where E is in W m^{-2} or J m^{-2} s^{-1} and Z is in mm^6 m^{-3}. On the assumption that radar reflectivities equal or less than 60 dBZ are caused by rain only and that radar reflectivities greater than 60 dBZ are caused by hail only, then fields of E may be evaluated. Good agreement between fields of E derived from radar reflectivities and those obtained from hailpad observations have been reported (for example Joss and Waldvogel, 1990).

Auer (1984) showed how infrared cloud-top temperature (T_B) and radar reflectivity (Z_e) can delineate between hail and rain (Figure 5.11). Figure 5.12 shows a curve relating Z_e to the hail diameter, D_H, given that hail is present. This curve is obtained from equation 5.13. It is assumed that the amount of melting in the hail is negligible.

The solid line separating hail from rain in Figure 5.11 was parametrized by Auer (1994) as:

$$2.6 \times Z_e + T_B = 857.15 \tag{5.16}$$

Where Z_e is in dBz and T_B is in 0°C. Figure 5.11 also has a broken line that separates rain and hail for T_B values less than –10°C. This may be represented (Hardaker and Auer, 1994) by:

$$0.75 \times Z_e - T_B = 38.75 \tag{5.17}$$

Defining a parameter h, which is positive or zero in hail and negative in rain, then using equations 5.16 and 5.17 it is possible to define:

$$h = \begin{cases} 2.6 \times Z_e + T_B = 85 & T_B \le 10°C \\ 0.75 \times Z_e - T_B = 38.75 & T_B > \pm 10°C \end{cases} \tag{5.18}$$

Equations 5.17 and 5.18 define the boundary between rain and hail and therefore one can use the boundary itself as an estimate of the maximum rainfall rate, above which one detects hail. Therefore, utilizing the boundary definition along with equation 5.11, assuming the temperature of the water in the rain-hail mixture is close to 0°C, a more accurate estimate of the surface rainfall rate contribution (in units of mm h^{-1}) in the measured Z_e value can be defined as:

$$\left(\frac{\left(10^{0.038 \times \left(85 T_B \right)} \right)}{280} \right)^{0.69} \qquad h \le 0 \text{ and } T_B \le -10°C$$

$$R = \left(\frac{10\left(0.135 \times \left(38.75 + T_B \right) \right)}{280} \right)^{0.69} \qquad h \le 0 \text{ and } T_B > -10°C$$

$$\left(\frac{10^{Z_e} / 10}{280} \right) \quad h < 0$$

In addition, equation 5.13 can be utilized to find the diameter of the hail in the rain and hail mixture. Here, the hail diameter, D_H, is estimated through:

$$D_H = \begin{cases} \left[\dfrac{10^{\frac{z}{10}}}{561} \right] & h \ge 0 \\ 0 & h < 0 \end{cases} \quad \text{mm} \tag{5.20}$$

Hardaker and Auer (1994) summarize the technique in the context of an operational system as follows:

(*a*) For each radar pixel, find the appropriate satellite pixel;
(*b*) Take the value of Z_e from the radar pixel and the corresponding value of T_B from the satellite pixel and evaluate equation 5.18;
(*c*) Use Z_e from the radar and T_B from the satellite, along with h, to determine surface rainfall rate in equation 5.19;
(*d*) Use the Z_e from the radar data and h in equation 5.20 to calculate the diameter of the hail present in the mixture.

This technique shows great promise, and is currently being tested in Europe and the United States.

5.2.9 Summary of accuracy of single polarization radar measurements of precipitation

So far in this chapter we have discussed the range of techniques used to transform radar reflectivity measurements to estimates of areal rainfall. In general, it is essential to apply physical corrections to the radar data, such as those for attenuation through rain, incomplete beam filling and vertical reflectivity profile variations, before using data from raingauges. Work is ongoing in many countries to optimize these techniques using sometimes complex mathematical procedures. Nevertheless, the current accuracy achieved operationally at best only approaches that defined in the Dee Weather Radar and Hydrological Forecasting Project (DWRHP, 1977), shown in Figure 5.13. The problem of the bright-band, however, remains the most important challenge in stratiform rain for those working in this field.

Recent work, discussed in section 5.2.3, promises a technique which could lead to significant improvement in the real-time estimation of Z_e-R relationships. The technique

Figure 5.14 — The relationship between Z_{DR} and D_0 at C-band frequencies (after Cherry and Goddard, 1983).

known as the Window Probability Matching Method (WPMM) allows the derivation of appropriate Z_e-R relationships for various rain types based upon a practically achievable sample size of raingauge and radar measurements. It may be summarized as follows:

Sets of Z_e-R relationships are calculated for various types of rainfall, using the WPMM procedure. The classification of the rain types is done by analysis of the three-dimensional reflectivity field in radar windows of 7 km by 11 rays. The classification criteria are:

(*a*) Horizontal radial reflectivity gradients $\bar{\nabla}_r Z$ (dB km^{-1});
(*b*) Cloud depth, as scaled by the effective efficiency E_e (see section 6.2.3);
(*c*) Brightband fraction BBF within the radar window; and
(*d*) The height of the freezing level H_f in kilometres above sea level.

The use of these Z_e-R relationships should result in considerable improvement of both point and areal rainfall measurements with respect to any other method using reflectivity-only radars. However, further studies with other datasets are necessary to confirm this. The accuracy of the radar estimates is masked, however, by the natural variability between the averaged rain intensity at the radar measurement volume and at the point of the rain gauge within the time window (Kitchen and Blackall, 1992). If this is the case, verification of the improvement in area-integrated rainfall requires a dense rain gauge network, with spacing of at most the radar horizontal beamwidth (i.e., about 1-km spacing at the range of 50 km).

5.2.10 Examples of operational systems

Over the last 20 years or so there has been a great increase in the deployment of digital weather radar systems world-wide. In Europe, between 1975 and 1992, the number of such radars increased from one to over 100 (Newsome, 1992), most of which are C-band. Accompanying such a deployment has been the development of comprehensive radar network systems for example in Switzerland and the United Kingdom (Joss and Waldvogel, 1990). International networking in Europe on a regional basis has been implemented with radar data being exchanged routinely between the United Kingdom, France, the Netherlands and Switzerland and between the Nordic countries Nordic Weather Radar System (NORDRAD) (Collier, 1995).

In the United States, the Next Generation Weather Radar (NEXRAD) programme has now come to fruition with the deployment of over 100 S-band high power Doppler WSR-88D radars. These radars provide a wide range of products to users (Klazura and Imy, 1993; Crum and Alberty, 1993). In parallel with this network, a large number of C-band Terminal Doppler Weather Radars (TDWR) have also been installed at airports.

Many other countries have also installed, or plan to install, weather radars. Japan has the densest radar network in the world operating in parallel with a very dense raingauge network (Tatehira, *et al*., 1982). While it is clear that total worldwide land coverage will never be achieved, it seems likely that digital radar data will be widely available in the years to come.

Figure 5.15 — Difference between disdrometer and radar values of Z_{DR} as a function of radar Z_{DR} (from Goddard, *et al*., 1982; Goddard and Cherry, 1984).

5.3 MULTI-PARAMETER TECHNIQUES

5.3.1 Basic theory

The departure of the shapes of precipitation particles from spherical gives rise to different radar reflectivity properties. Seliga and Bringi (1976) related signals in two orthogonal linear polarization planes, horizontal (H) and vertical (V), to two-parametric dropsize distributions. Likewise, circular polarization has also been used in this way by McCormick and Hendry (1972).

The oblateness of raindrops, when falling at terminal velocity in air, increases with drop volume. Since models for the sharp and minor-to-major axis ratio and fall speed data exist, it is possible to relate the dropsize distributions so measured to rainfall rates. If raindrop canting is neglected (mean observed canting angles are in most cases less than 20°, Brussaard, 1976), then the radar cross-section of the raindrops for horizontal polarization is expected to be higher than the cross-section for vertical polarization, that is:

Physical quantity	*Matrix element*	
Rainfall rate	$\bar{E}_1\bar{E}_1^*$	
Drop size resp. oblateness	$\bar{Z}_{\mathrm{DR}}$	$\bar{E}_2E_2^*$
Canting angle (0..... 45°)	$\bar{E}_2E_2^*$	$\bar{Z}_{DR}$
Degree of common orientation	$E_1E_2^*$	$\bar{Z}_{DR}$

$$\sigma_h(D) > \sigma_v(D) \tag{5.21}$$

where D is the equivolumetric sphere diameter of a raindrop.

With a dual polarization radar, both quantities, Z_H and Z_v, can be measured and used to calculate the so-called differential reflectivity, Z_{DR}:

$$Z_{DR} = \overline{Z}_{H,V} = \frac{\overline{Z}_H}{Z_V} = \frac{10^{18}\ \lambda^4\ No}{N^5\ \left|K_o\right|^2} \int_{D=0}^{D_{\max}} \nabla_{H,V} \left(D\right) \exp\left(\pm 3.67 D / D_o\right) dD \ \mathrm{mm^6 m^{-3}} \quad (5.22)$$

It is seen that Z_{DR} depends on D_0 only, and therefore can be used to determine D_0. After having D_0, (equation 5.22) it can be used to find the second unknown distribution parameter N_o.

Figure 5.14 shows in graphical form the relationships given by equations 5.21 and 5.22, for 5.5 Ghz (Cherry and Goddard, 1983). Z_{DR} has a dynamic range of the order of 5 dB, and a somewhat higher sensitivity with D_0 is evident for C-band. Z_{DR}, therefore, has to be measured to an accuracy of less than 0.2 dB (standard deviation), which is one of the main problems in practical implementations. If, for example, Z_H and Z_v are measured independently as means of 100 integrated independent single-pulse reflectivities, 10 per cent of Z_H and Z_V, are expected to be associated with fluctuation errors above 0.5 dB. This is clearly insufficient for deriving Z_{DR} with the stated accuracy. Improvements can be made by:

(*a*) Increasing the integration number, leading to single cell measurement times in the order of seconds;

(*b*) Acquiring single-pulse echoes for both polarizations nearly simultaneously, so that fluctuation errors in Z_H and Z_v cancel out when calculating $Z_{DR} = \overline{Z}_H / \overline{Z}_v$.

In practice method (*b*) is being applied, relying on the empirical relationship for the decorrelation time of single-pulse echoes at constant carrier frequency, due to drop rearrangement (Atlas, 1964).

5.3.2 Accuracy of measurements

Seliga, *et al*. (1981) report the results of limited comparisons of measurements made using this technique with those made using raingauge-adjusted reflectivity data. They found for convective rainfall that differential reflectivity rainfall measurements differed by about 22 per cent from raingauge measurements, compared with differences of 42 per cent using raingauge-adjusted reflectivity measurements, and 47 per cent using an appropriate mean relationship between Z and R ($Z = 187R^{1.27}$). It was noted that the lowest percentage difference (24 per cent) achieved using adjusted reflectivity measurements reported by Wilson and Brandes (1979) was obtained after the storm bias (adjusting the average radar-derived rainfall rates to the average raingauge-derived rates for each event) had been removed. Further excellent agreement between rainfall measurements made using the differential reflectivity technique, and measurements made using a distrometer (Joss and Waldvogel, 1967) have been reported by Goddard, *et al*. (1982) and Goddard and Cherry (1984) and are shown in Figure 5.15.

It would appear that the Z_{DR} radar technique has the potential for accurately measuring rainfall rate without any need for raingauge adjustment. However, as Jameson, *et al*. (1981) point out, single-point measurements of Z_{DR} may be associated with significantly diverse rainfall rates. Although two radar variables (Z_H and Z_{DR}) are used, two additional parameters (the maximum drop size and the drop shape) are considered, so that there is little net gain in quantitative information and further radar parameters are required (Atlas, *et al*., 1982), or temporal and areal averaging, perhaps even some form of adjustment in particular meteorological situations. Hence the technique could begin to suffer from the same kinds of problem as the reflectivity-alone technique. Goddard, *et al*. (1982) have addressed these problems and have suggested ways of empirically reducing the errors which result from them. Nevertheless, Hendry and Antar (1984) note difficulties caused by propagation effects, and Herzegh and Conway (1986) and Liu and Herzegh (1986) discuss problems arising from side-lobe effects.

Figure 5.16 — Polarization characteristics for various precipitation types. Partially based on results with 1.8 cm and 3.1 cm radars at elevations up to 20° (Hendry and Antar, 1984).

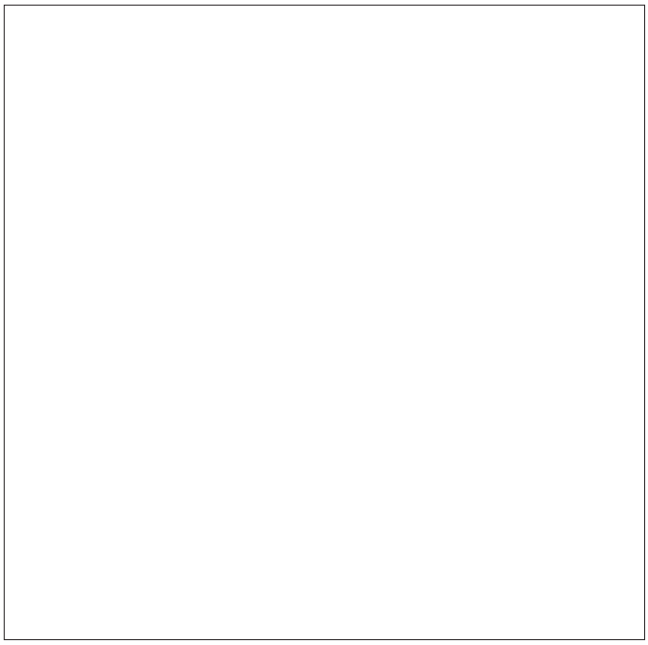

Figure 5.17 — (*a*) Geometry of scan for wind measurements by VAD technique; (*b*) Wind and fall speeds make up VAD pattern indicated by *V* when folding occurs (from Atlas, 1964, after Lhermitte and Atlas, 1961).

In summary, the over-estimation indicated in Figure 5.15 has been attributed to gradients in rainfall rate, dropsize departure from the exponential relationship, departure of drop-oblateness to the model used and drop canting effects due to wind shear and turbulence. The differential reflectivity technique, like other radar techniques, is adversely affected by the presence of reflectivity gradients below the radar beam, which may be significant in cases of isolated thunderstorms or orographic rainfall. In other words, even if the radar measures the rainfall rate accurately aloft within the beam, this measurement may still be unrepresentative of the rainfall rate at the surface. The use of a narrow beamwidth ($^1/_2$- 1°) helps but does not entirely overcome such problems, particularly where measurements of surface rainfall are required at ranges up to around 100 km from the radar, or in hilly areas of specific interest to hydrologists. The use of such narrow beamwidths and high power does increase system costs and adds to the complexity of the data processing, which result in a less attractive system for operational implementation. It is likely that dual-polarization radars will be restricted to making measurements of precipitation at close ranges if they are deployed at all operationally.

5.3.3 Other possible polarization techniques

The backscatter from precipitation particles in generally polarized, electromagnetic radiation can be represented by a "coherancy matrix" (Born and Wolf, 1964) where:

$$J = \frac{\overline{E}_1\ \overline{E}_1^* \times \overline{E}_1\ \overline{E}_2^*}{E_2\ E_1^* \times E_2\ E_2^*} \qquad (5.23)$$

where the overbar denotes the short-term average, and the asterisk indicates the complex conjugation (following the notation of Newsome, 1992). Taking the echoes are being the response to a transmitted signal with polarization state 1, then,

Figure 5.18 — Differential attenuation measurement.

$E_1E_1^*$ = mean power of the co-polar echo;
$E_2E_2^*$ = mean power of the cross-polar echo;
$E_1E_2^*E_2E_1^*$ = complex correlation between co- and cross-polar echoes.

The ratio $E_1E_1^*E_2E_2^*$ is, depending on the type of polarization used (linear, circular, or slantwise (±45°)), called linear de-polarization ratio (LDR), circular depolarization ratio (CDR) or slantwise depolarization ratio (SDLR).

For a radar with two transmitted polarizations (H and V, or RHC and LHC), two coherency matrices exist, but are not completely independent of each other. In the case of linear polarization $E_1E_1^*$ stands for Z_H in the first matrix and for Z_V in the second matrix, while $E_2E_2^*$ is the same for both matrices.

In the case of a linearly polarized radar with two transmitted polarizations and full coherency matrix calculation the physical meaning of the matrix elements with respect to the differential reflectivity Z_H/Z_V can be classified as follows:

The interpretation of the coherency matrix for circularly polarized radars has been pioneered by McCormick and Hendry, 1975). They introduced a special nomenclature, which has been widely accepted:

$$\text{CAN} = 10\log10\ (E_2E_2^* / E_1E_1^*) \qquad (5.24)$$

(The inverse of CDR)

$$\text{ORTT} = E_1E_2^* / (E_1E_1^* \times E_2E_2^*)^{1/2} \qquad (5.25)$$

(the degree of common orientation)

$$\text{ALD} = (\arg [\ E_1E_2^*\ ] - 180°) / 2 \qquad (5.26)$$

(the apparent mean orientation angle, now more often referred to as co-polar phase).

These parameters may be used to recognise canting effects and so correct Z_{DR}. In addition, the value of the cross polar reception lies in the possibility of identifying hydrometeor type as shown in Figure 5.16. Also Holt (1988) showed that the difference phase parameter (related to equation 5.27) may be estimated from non-switched circularly polarized systems, opening up new possibilities for more conventional radars. However, while radars having these facilities offer a range of possibilities they are not, at present, deployed extensively for the operational measurement of precipitation.

Figure 5.19 — The log ratio of reflectivity at 10 GHz divided by that of 3 GHz (against the mean diameter) (from Newsome, 1992).

5.4 DOPPLER RADAR

5.4.1 Theoretical framework

When the radar target is moving, the returned signal is shifted in frequency compared with the signal that would have been returned from a stationary target. Fourier analysis of the Doppler-shifted signal gives the power density, or Doppler, spectrum, *S(V)* of the velocities (see for example, Burgess and Ray, 1986). The integral or area under the spectrum is the reflectivity and the zeroth moment of the spectrum. The mean velocity V, is the first moment of the spectrum:

$$\overline{V} = f(V) = \frac{\int_{\infty}^{\infty} VS\,(V)\,dV}{\int_{\infty}^{\infty} S\,(V)\,dV} \tag{5.27}$$

Higher-order moments of the spectrum are given by:

$$f_n(V) = \frac{\int_{\pm\infty}^{\infty} \left(V - \overline{V}\right)^n S\,(V)\,dV}{\int_{\pm\infty}^{\infty} S\,(V)\,dV} \tag{5.28}$$

where n is the moment of the spectrum. The second moment (n=2) is the variance of the spectrum. The spectrum width is determined by a number of factors, the most importance of which are:

(*a*) The spread of the terminal fall velocities of the scatterers;
(*b*) Turbulence in the sampling volume;
(*c*) Shear of the wind along and across the radar beam;
(*d*) Antenna rotation rate.

The time of the return echo is fixed in the interpulser period between successive radar pulses. Any echoes which occur after the transmission of the next pulse, known as second-time-around echoes, will give a misleading range. The maximum unambiguous range is a function of the pulse repetition frequency, and gives rise to a phenomena known as velocity folding. Techniques to extend the unambiguous velocity range involve the use of two pulse repetition frequencies. Further discussion of these techniques can be found in Collier (1989) and, for the more advanced reader, Doviak and Zrnic (1984).

The Doppler spectrum may be analysed to give the distribution of hydrometeor fall speeds assuming still air if the radar is pointed vertically. It is also possible to derive vertical wind profiles using a method of data collection known as velocity-azimuth display (VAD) (Lhermitte and Atlas, 1961). Figure 5.17 shows the geometry of the VAD technique and how the wind and fall speeds may be derived using the following formulas:

$$\text{Wind velocity,} \quad V_h = \frac{\overline{V}_1 \overline{V}_2}{2\cos\alpha} \tag{5.29}$$

$$\text{Hydrometeor fall speed,} \quad V_f = \frac{\overline{V} + \overline{V}sub2}{2\sin\alpha} \tag{5.30}$$

5.4.2 Contribution of Doppler radar to precipitation measurements

Doppler radar provides a method of reducing the amount of ground clutter detected in radar images. The Doppler spectrum for rain and ground clutter are usually sufficiently separated for filters to be used to remove the ground clutter including any echoes due to anomalous propagation effects. This is the most important contribution that Doppler processing can make to precipitation measurement, although it should be noted that when rain echoes are stationary or moving tangentially to the radar then they will be regarded in the same way as ground clutter and be removed. In practice it is found that this problem is not serious.

There is some evidence (Crespi, *et al.,* 1995) that the nature of the Doppler processing can lead to improved sensitivity and therefore precipitation measurement. However, this effect is small and should not be overstated. Finally measurements of profiles of hydrometeor fall speed may be used to identify more clearly the brightband and to differentiate between snow and rain. While this may contribute to other techniques for improving measurement accuracy they are not procedures which offer complete solutions to the brightband or snow turning to rain problems.

5.5 FREQUENCY DIVERSITY

Measurement of the reflectivity at two frequencies producing different attenuation characteristics through precipitation can reveal a second characteristic of precipitation other than the reflectivity (Cherry, 1978). The power received from a pulse volume with reflectivity Z at a range R is given by:

$$P = \overline{Z}\frac{C}{R^2} \tag{5.31}$$

where C is a constant dependent upon the radar parameters. At a non-radar beam attenuation frequency (N) (Figure 5.18) the power ratio at two ranges R_1 and R_2 is given by:

$$\frac{R_{N2}}{P_{N1}} = \frac{C_N \overline{Z}_{N2}}{R_2^2} \times \frac{R_1^2}{C_N \overline{Z}_{N1}} = \frac{R_1^2}{R_2^2} \times \frac{\overline{Z}_{N2}}{\overline{Z}_{N1}} \tag{5.32}$$

For an attenuating frequency (A) there will be a two-way attenuation factor A_1 up to range R_1, and an additional two-way attenuation factor A_2 to range R_2:

$$\frac{P_{A2}}{P_{A1}} = \frac{R_1^2}{R_2^2} = \frac{\overline{Z}_{A2}}{\overline{Z}_{A1}} \tag{5.33}$$

The attenuation A may be determined from equations 5.33 and 5.34 provided that:

$$\frac{\overline{Z}_{N2}}{\overline{Z}_{N1}} = \frac{\overline{Z}_{A2}}{\overline{Z}_{A1}} \tag{5.34}$$

This equation requires that either the scatter at both frequencies is of the Rayleigh type, or that D_o, a parameter of the dropsize distribution:

$$N(D) = \mathrm{N}_o \exp(-3.67\, D/D_o)$$

is the same for both distributions at ranges R_1 and R_2. If one of these conditions is met, it follows that:

$$\frac{P_{A1}}{P_{A2}} = \frac{P_{N2}}{P_{N1}} \tag{5.35}$$

As noted in Newsome (1992) there are the following problems in measuring A:

(*a*) A number of system parameters have to be matched for both frequencies used. These are the antenna polar diagram, pulse length and shape, and polarization. Solving this problem is in principle possible by careful engineering and calibration procedures;
(*b*) The equality stated by equation 5.33 may not be true. Here again, assumptions have to be made;
(*c*) A would have to be measured to an accuracy of + 0.1 dB/km (two-way for λ = 1.2 cm (Cherry, 1978)), in order to arrive at interpretable values.

These problems limit the practicability of using dual frequency measurements to estimate rainfall. However, for large ice particles such as hail, the departure from Rayleigh scattering at the attenuating wavelength is a useful indicator of the presence of large scatters within the echo cell. This is illustrated in Figure 5.19 and has been discussed by Eccles and Atlas (1973) and Carbone (1972). This technique has been developed in Eastern Europe (Brylev, *et al.,* 1995).

Figure 6.1 — (*a*) Meteosat-derived infrared cloud-top temperatures for 0900 UTC 28 July 1988, light blue colder than –15°C. Radar rainfall intensity (mm h^{-1}) and pink <1, green 1-3, yellow 3-10, red > 10 mm h^{-1}. Coastlines of NW Europe, national boundaries and radar network boundaries are shown in black; (*b*) Location at 0900 UTC of the depression, surface fronts and warm conveyor belts W1 and W2. The area of heavy rain origination from W2 is stippled.

CHAPTER 6

SATELLITE MEASUREMENTS

6.1 INTRODUCTION

Browning (1990) discusses the role of precipitating clouds in climate stressing the importance of obtaining better observations globally and the need to parametrize the cloud and precipitation processes within general circulation models. Rain is a key component of the hydrological cycle, and the key to global rainfall measurement lies in space-borne techniques. However, the measurement and sampling problems are so great that there is no single or complete solution in sight, and the requirement is for a combination of complementary techniques. These topics form an important part of the World Climate Research Programme (WCRP) Global Energy and Water Cycle Experiment (GEWEX) (WMO, 1988*b*).

The status of the application of space-based remote sensing techniques for precipitation estimation was discussed by Kuittinen in WMO (1988*a*). This report contained no mention of the use of the SSM/1 instrument (85.5 GHz), the Global Precipitation Climatology Project (GPCP) and several other developments which occurred during the following seven years. Only one year later, Arkin and Ardanuy (1989) were able to illustrate how rapidly advances were occurring by discussing plans for the GPCP and GEWEX.

The GPCP is an attempt to make the best possible use of currently available data and algorithms (WMO, 1986*b*). The Project comprises several principal centres each of which will use existing observations and techniques to produce rainfall estimates and/or analyses for the period 1986–1995. The Geostationary Satellite Precipitation Data Center (GSPDC) located at the NOAA Climate Analysis Center in Washington D.C. acquires data from all the geostationary satellite systems. The algorithm used to derive rainfall is the global precipitation index (GPI) used by Arkin and Meisner (1987) (see section 6.2.1). The Polar Satellite Precipitation Data Center (PSPDC) located at the Goddard Space Flight Center of NASA uses radiometric observations from SSM/I to derive rain rates over oceans. The Surface Reference Data Center (SRDC) operated by the National Climate Data Centre of NOAA uses ground-

based measurements from weather radars and raingauges to validate and calibrate the satellite estimates. Finally, the Global Precipitation Climatology Center was discussed in section 3.5.

As part of the GPCP three (so far) Algorithm Intercomparison Projects (AIPs) have been organized over Japan (1989), over north-west Europe (1991) and over the tropical Pacific Ocean as part of TOGA-COARE (1993). These AIPs should help us to understand a wide range of algorithms and new satellite instruments. One challenge in the future is to assimilate global rainfall estimates from space in numerical forecast models. Work is currently under way in several countries. For example, Filiberti, *et al*. (1994) discusses the use of SSM/1 data in this way and demonstrates the feasibility of so doing. In the following sections, we discuss the wide range of satellite-based techniques currently available and assess their advantages and disadvantages.

6.2 USE OF VISIBLE AND INFRARED TECHNIQUES

Visible/infrared techniques derive qualitative or quantitative estimates of rainfall from satellite imagery through indirect relationships between solar radiance reflected by clouds (cloud brightness temperatures) and precipitation. A number of methods have been developed and tested during the past 15 years with a measured degree of success.

There are two basic approaches, namely the "life-history" and the "cloud-indexing" techniques. The first type makes use of data from geostationary satellites which produce images usually every half hour. It has been mostly applied to convective systems. The second type, also based on cloud classification, does not require a series of consecutive observations of the same cloud system.

It must be noted, however, that up to now none of these techniques has been shown to be "transportable". In other words, relationships derived for a given region and a given time period may not be valid for a different location and/or season. Other problems include difficulties in defining rain/no rain boundaries and inability to cope with the rainfall patterns at the meso- or local scales. An example of cloud not producing rainfall in close proximity to cloud producing rainfall is shown in Figure 6.1. Scientists working in this field are perfectly aware of these problems, and this is why it is current practice to speak of the derivation of "precipitation indices" rather than rain rates.

6.2.1 Cloud indexing methods

Cloud indexing was the first technique developed to estimate precipitation from space. It is based on the assumption that the probability of rainfall over a given area is related to the amount and type of cloudiness present over this area. Hence, one may postulate that precipitation can be characterized by the structure of the upper surface of the associated cloudiness. In addition, in the case of convective precipitation, one may also postulate that a relationship exists between the capacity of a cumuliform cloud to produce rain and its vertical as well as its horizontal dimensions. The vertical extent of a convective cloud is related to the cloud top brightness temperature (higher cloud tops are associated with colder brightness temperatures).

The approach is, therefore, to perform a cloud structure analysis (objective or subjective) based on the definition of a criterion relating cloudiness to a co-efficient (or index) of precipitation. This characteristic may be, for instance, the number of image pixels above a given threshold level. Hence, the general approach for cloud indexing methods involving infrared observations is to derive a relationship between a precipitation index (PI) and a function of the cloud surface area, S(TBB), associated with the brightness temperature (TBB) colder than a given threshold T_o. This relationship can be generally expressed as follows:

$$PI = A_0 + \sum_i A_i \times S_i \left[TBB_i\right] \qquad (6.1)$$

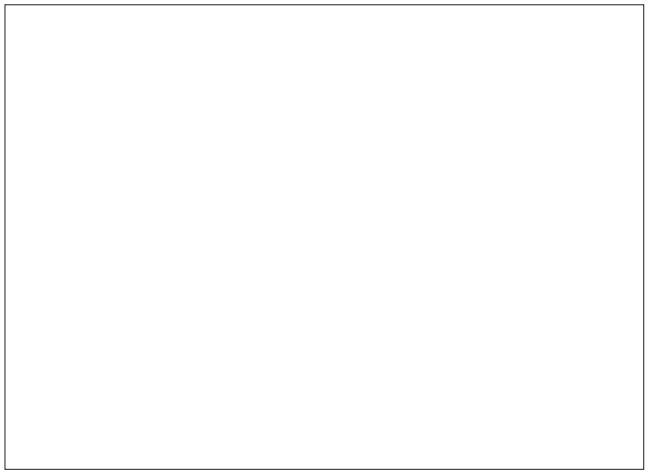

Figure 6.2 — Lognormal cumulative distributions of rain area (dashed curve) and volume (solid curve) similar to those observed in GATE, Texas and South Africa as shown by Rosenfeld, *et al*. (1990). For a rain rate threshold of τ, the fractional rain volume and area encompassed within τ are ϕ and $A(\tau)$, respectively; the average areal rain rate within that area is R_c. The curves correspond to a lognormal distribution with mean and standard deviation of log R equal to 1.1 mm h^{-1} (from Atlas, *et al.,* 1990).

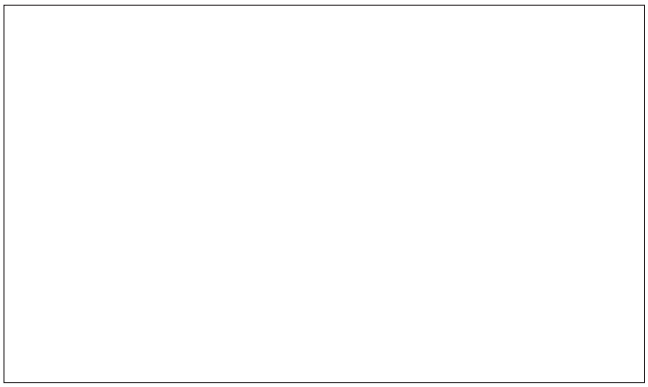

Figure 6.3 — The PDF of the rain intensities as derived from high-resolution radar data between 31 and 90 km, for convective rain situations having different average depth, denoted by E_e intervals of 0.1. These intervals range from 0.5 for the shallowest convection to 1.0 for the deepest convection (from Rosenfeld, *et al.,* 1990).

where A_0 and A_i are empirically-determined constants.

If desired, an additional term related to the visible image can be included on the right hand side of equation 6.1. The next step is to associate *PI* to a physical quantity related in some way to rain. This is done by adjusting the coefficients *A* and the threshold level T_o by comparison with independent observations such as raingauge or radar data (see for example Arkin, 1979).

One of the problems inherent to this technique is the bias created by the potential presence of high level non-precipitating clouds such as Cirrus. Another limitation resides in the fact that the satellite measurement represents an instantaneous observation integrated over space, while raingauge observations are integrated over time at a given site.

6.2.2 Life-history methods

Life-history methods, as indicated by their name, are based on the observation of a series of consecutive images obtained from a geostationary satellite. It has been observed that the amount of precipitation associated with a given cloud is also related to its stage of development, therefore two clouds presenting the same aspect (from the VIS-IR images point of view) may produce different quantities of rain depending on whether they are growing or decaying.

As with the cloud indexing technique, a relationship is derived between a precipitation index (PI) and a function of the cloud surface area, S(TBB), associated with a given brightness temperature (TBB) lying above a given threshold level, T_o. In addition, the cloud evolution is taken into account and expressed in terms of rate of change of S(TBB) between two consecutive observations.

An equation, as complex as desired, may be derived between PI and functions of S(TBB) and its derivative with respect to time:

$$PI = A + A \times \mathrm{S(TBB)} + A^1 \frac{d}{dt}\,\mathrm{S(TBB)};\ for\ \mathrm{TBB} < T_o \quad (6.2)$$

Here also, another step is necessary in order to relate the precipitation index defined by the equation to a physical quantity related to rain.

Many such relationships have already been published. These publications have been extensively discussed and it was demonstrated, at least for one instance, that taking into account the cloud evolution with time added unnecessary complexity and that comparable success could be obtained with a simple cloud indexing technique.

Recently, more physics has been introduced to the various schemes. Improvements include:

(*a*) Use of cloud models to take into account the stratiform precipitation often associated with convective rainfall and to help with the cloud classification;

(*b*) Introduction of simultaneous upper tropospheric water vapour observations;

(*c*) Introduction of a time lag between the satellite observations and ground-based measurements.

It has also became evident that satellite data could be used in conjunction with radar observations, not only to validate a method, but as a complementary tool. The forecasting rain optimized using new techniques of interactively enhanced radar and satellite (FRONTIERS), developed by the UK Meteorological Office, represents an example of combined use of satellite imagery and radar observations (see Browning and Collier, 1989).

Quite a few comparisons between different methods over the same test cases have now been performed and published, but one must remain extremely cautious about any final statement concerning the success (or lack of it) of VIS-IR methods. The degree of success is very strongly related to the space-time scales considered, and one cannot expect that a regression developed and tested for use in climate studies will also be valid for estimation of mesoscale precipitation. One must also keep in mind that it is always easy to adjust regression coefficients for a particular case and claim that the method has been validated.

6.2.3 Height-area-rainfall threshold (HART) technique

Doneaud, *et al*. (1981, 1984) derived the volumetric rainfall, *V*, from:

$$V = \int_\tau \int_A R\, da\, dt = R_c \int_\tau \int_A da\, dt = R_c \sum_i A_i\, \Delta t_i \quad (6.3)$$

where: R = the instantaneous local rain rate;
da and dt = incremental elements of area and time, respectively;
R_c = the average rain rate.

The integrals are taken over the entire area *A* for duration *T*. The double integral is the area-time integral (ATI).

Following this work, Chiu and Kedem (1990) developed a logistic regression model to estimate the fractional rainy area, which estimates the conditional probability that rain rate over an area exceeds a fixed threshold given the values of related covariates. Tests showed that this approach is superior to multiple regression. However, variabilities of meteorological parameters must be accounted for if this technique is to be applied to estimating rain rate from space.

Atlas, *et al*. (1990) developed a unified theory for the estimation of both the total rainfall from an individual convective storm over its lifetime, and the area wide instantaneous rain rate from a multiplicity of such storms, by use of measurements of the areal coverage of the storms within a threshold rain intensity isopleth or the equivalent threshold radar reflectivity. Equation 6.3 was generalized to:

$$V = \left[\overline{A}(\tau)\, T\right] S(\tau) \quad (6.4)$$

where the double integral,

ATI = $A(\tau)\, T$

τ = threshold

$S(\tau)$ = $R_c(\tau) / \phi$ and may be defined in terms of the proba-

Table 6.1
Coefficients used in the *K-R* and *Z-R* models

(C)	*E*	*B*	*C*	*F*
0.86	0.66×10^6	1.50	0.209	1.0
2	0.66×10^6	1.50	0.181	1.11
3.2	0.66×10^6	1.50	0.139	1.169

bility density function (pdf) $\int_{\infty}^{\infty} RP(R)dR \Big/ \int_{\tau}^{\infty} P(R)dR$

ϕ = the fraction of the total volumetric rate as shown in Figure 6.2

Sauvageot (1994) found that $P(R)$ can be represented by a lognormal distribution, and explained the stability of $S(\tau)$.

Divide (8.4) by total area observed A_0 then V_t/A_0 is the average area wide rain rate $<R>$ and $A(\tau)/A_0$ is the fractional area, $F(\tau)$, covered by rain within the threshold, τ. Thus,

$$<R> = F(\tau).R_c(\tau)\,\phi \qquad (6.5)$$

Rosenfeld, *et al*. (1990) examined the generality of the instantaneous area wide method and developed the method of utilizing measurements of storm height to enhance the accuracy of the rain estimates relative to that which is attainable with storm areas only. They defined a parameter E_e, the "effective efficiency" as:

$$E_e = (Q_b - Q_t) / Q_b \qquad (6.6)$$

where Q_b and Q_t are the water vapour mixing ratios at the base and top of the storm, respectively. Hence, E_e is the fraction of the water vapour carried up through the cloud base which is potentially available for precipitation. Q_t is determined by the actual height which is reached by the storm. As E_e increases from one class to another the corresponding probability density functions (PDFs) move to larger rain rates in a systematic manner as shown in Figure 6.3. Therefore, it is possible to stratify the $<R>$ versus $F(\tau)$ relationships according to both E_e and the corresponding best correlated τ.

Errors over the whole observing area are 5–10 per cent. The method is called the "height-area rainfall threshold" or HART method. Morrissey (1994) examined the effect of data resolution on this and the ATI techniques. The results indicated that significant biases and random errors can arise when using radar or satellite data having spatial resolutions different from those used to calibrate the method.

Figure 6.4 — Illustration of the surface reference method of using radar to measure rainfall intensity, showing the echo from the surface attenuated by an amount A which depends on the attenuating path H and the rainfall rate along that path (Meneghini, *et al*., 1983).

6.3 USE OF PASSIVE MICROWAVE TECHNIQUES

VIS-IR measurements represent observations of the upper surface of clouds only. In contrast it is often believed that microwave radiation is not affected by the presence of clouds. This statement is not generally true. Its degree of validity varies with the microwave frequency used as well as with the type of cloud being observed.

One major difference between infrared and microwave radiation is the fact that while the ocean surface emissivity is nearly equal to one in the infrared its value (although variable) is much smaller in the microwave region (from 5 to 200 GHz here). Therefore, the background brightness temperature (TBB) of the ocean surface appears much colder in the microwave. Over land, the emissivity is close to one, but varies greatly depending on the soil moisture.

As far as microwaves are concerned several different effects are associated with the presence of clouds over the ocean. They are highly frequency dependent, and include:

(*a*) Absorption by cloud droplets is roughly proportional to the square of the frequency. A 2-km thick (non-precipitating) cumulus cloud transparent at 18 GHz may be totally opaque (through absorption) at 160 GHz, the resulting effect being an increase of brightness temperature (through emission) over the cold background;

Table 6.2 Summary of the performance of satellite rainfall estimation techniques (partly after Browning and Collier, 1989)

Technique	*Area over which estimates are assessed (km^2)*	*Period of integration (hours)*	*Per cent errors*
Cloud indexing	10^5	24	122
	10^4	$^1/_2$	40
Area-average	10^5	Inst - 30×24	14
Life history	10^4	1	85
	10^5	24	55
	10^4	$^1/_2$	50
	6×10^3	$^1/_2$	65
Bispectral visible/infrared	10^5	$^1/_2$	50
Passive microwave	10^3	24	70
Active microwave	10^3	12	20
(not yet implemented)			(when combined with bispectral technique)
	10^3	30×24	10

(*b*) The increase of cloud water content associated with the presence of raindrops in a cloud produces an enhanced absorption-emission effect. The 2-km thick precipitating (a few mm hr^{-1}) Cumulus cloud will this time be detected over the cold surface background at 18 GHz, and the observed TBB will increase with the amount of "vertically integrated" raindrops contained in the cloud. This is the dominating effect below about 22 GHz, and the basis for estimation of rainfall at these frequencies;

(*c*) When the amount of rain present in the cloud becomes sufficient to absorb totally incoming radiation, the value of TBB reaches a value close to the cloud's infrared (or thermal) temperature. This is referred to as the "saturation" effect;

(*d*) Scattering by raindrops increases with drop size. The effect of scattering is to reduce the apparent TBB and is also frequency-dependent;

(*e*) The presence of ice in a precipitating cloud results in a decrease of TBB through scattering (ice particles do not absorb microwave radiation). This effect increases with frequency and particle size, and is used to delineate indirectly rain over the Earth's surface.

Measurements of rainfall using passive microwaves falls into one or two classes depending on the particular effect used to detect precipitation (i.e. absorption or scattering). To exploit absorption, a cold background is necessary. Thus, techniques based on this effect can be applied only over the ocean using frequencies below 10 GHz.

6.4 ACTIVE RADAR SYSTEMS

Measuring rain from a space radar is very attractive because this instrument is potentially able to provide the most thorough investigation of the precipitation field one can presently imagine from space. Two strong arguments mitigate in favour of the radar: its ability to discriminate in range (i.e. in altitude when operating from space), and the fact that the measured parameters like radar reflectivity, or radar attenuation, are directly related to the rainfall rate.

In the present section we will review the main techniques that have been envisaged up to now for measuring rain using a space-borne radar. The basic theory on which all these techniques are based was outlined in section 5.1.

The total attenuating cross-section, $\sigma_a\ (D) = cD$ where the c coefficients are tabulated as functions of λ and ambient temperature. The linear attenuation, K, of the incoming microwave radiation within a volume characterized by the mean drop size distribution $N(D)$ is given by:

$$K = c\int N(D)\, D^a\ Dd \tag{6.7}$$

where a is a coefficient also dependent on λ and ambient temperature.

Similarly, the rainfall rate R may be expressed as a function of $N(D)$ as:

$$R = \pi c_1 / \alpha \int_0^\infty N(D)\, D^3 + a_1\, dD \tag{6.8}$$

where c_1 and a_1 are the coefficients defining the power law relationship for the terminal fall velocity v_t of a raindrop as a function of its diameter D: $v_t\ (D) = c_1 D_{a1}$.

If we now assume that $N(D)$ can be described by an exponential function of the form $N(D)$ - N_o exp $(-\Lambda D)$, the

Figure 6.5 — Schematic portrayal of the tropical rainfall measuring mission (TRMM) spacecraft and instruments showing the relative coverage of each instrument. Acronyms are explained in text (from Browning, 1990, after Simpson, *et al*., 1988).

integrals in equations 5.1, 6.7 and 6.8 may be integrated analytically. Subsequent elimination of A produces the following two relations between Z, R and K:

$$Z = EN_o\,(1\text{-}B)\,R^B \qquad k = CN_o\,(1\text{-}F)R \tag{6.9}$$

where coefficients E, B, C and F may be expressed analytically as functions of c, a, c_1, a_1.

Table 6.1 specified the numerical values of coefficients E, B, C, and F at 3 cm, 2 cm and 0.86 cm wavelengths appropriate for a spaceborne radar; assuming an ambient temperature of 0°C. It should be remembered that equation 5.1 assumes the Rayleigh approximation. The introduction of the Mie correction (i.e. of the Z_e parameter) complicates the relation (without changing it qualitatively) and reveals a Z_e/λ dependence (not apparent in Table 6.1).

When using a radar for estimating rainfall rate, the reason for measuring two independent parameters, like Z_e and K, simultaneously is to minimize the dependence of estimates of rainfall rate, R, on the variability of the droplet size distribution (the N_o parameter may be eliminated between equations 6.3 and 6.4 allowing R to be expressed as a function of Z and K). The variability is a major source of error when estimating R from a single measurement of Z.

Another multiparameter technique currently used from the ground (section 5.3) is the dual polarization radar, measuring the differential reflectivity ZDR, between vertically- and horizontally-polarized waves. Because the raindrops are not spheres, but are oblate spheroids with axes aligned vertically, the equivalent reflectivity at vertical polarization, Z_v, is smaller than that at horizontal polarization Z_H. ZDR is defined as:

$$ZDR = 10 \log_{10} (Z_H/Z_v) \tag{6.10}$$

The eccentricity of the spheroid increases with the raindrop diameter D. This relationship is known. ZDR provides an estimate of the median volume diameter D_o, which is related to the Λ parameter of the distribution. It can be shown that the knowledge of the two parameters (Z, Λ) provides an unique determination of R. However, although this technique is attractive from the ground, it cannot be used from space as the angle of incidence is then too close to the vertical, making the determination of the ratio Z_H/Z_V very inaccurate (or even impossible at vertical incidence). None of the techniques that have been proposed up to now for use from space have envisaged the use of dual polarization measurements. All the techniques are based on measurements of Z_e, K, or both, as follows:

(*a*) Direct method: rainfall rate R is estimated using standard Z_e-R relationships empirically determined;

(*b*) Surface reference technique (SRT): the scattering properties of the ocean surface vary on a much larger horizontal scale than the rain rate field does. Hence the level of the signal received from the ocean surface through the rain cell relative to that outside the rain cell provides a means of monitoring the two-way attenuation along the ray path. Using an attenuation to rainfall relationship, rainfall can be estimated;

(*c*) Dual wavelength technique: the apparent reflectivities at the separate wavelengths are compared within the same resolution cell and the differential attenuation estimated. This is illustrated in Figure 6.4;

(*d*) Dual-beam technique (or stereo radar): stereoscopic observations are made from the same space vehicle using two antennae operating at the same frequency.

None of these techniques is yet used operationally, although a rain radar is planned for the joint United States–Japan tropical rainfall measurement mission (TRMM) (section 6.6).

6.5 SUMMARY OF ACCURACY

Table 6.2 gives a summary of the performance of satellite rainfall estimation techniques. It is clear that areal rainfall can be measured with acceptable accuracy for some applications from space. However, this conclusion only applies at present to measurements over areas greater than 10^4 km^2 for integration periods of less than 24 hours. Over smaller areas, errors are, in general, larger, although high accuracy can be achieved by careful "tuning" on specific datasets.

All satellite techniques suffer to a greater or lesser degree from errors arising from sampling. Indeed, these errors can be greater than all the other errors if accumulations are improperly computed. In tropical regions, there can be a significant diurnal cycle in rainfall activity and the phase and intensity of the cycle may increase the errors due to sampling as discussed by Oki and Sumi (1994). Lauglin (1981) has calculated the resulting sampling error for a range of sample intervals when measurements are averaged over periods of one week, two weeks and one month. For monthly averages over a 280 km square and a sampling interval of 10 hours, appropriate for the TRMM satellite (section 6.6), the sampling error is about 10 per cent. This analysis was carried out using GATE tropical rain data, but Seed and Austin (1990*a*) have pointed out that for convective systems in other regions which have shorter decorrelation times than observed for tropical rain, it might be misleading to apply GATE statistics universally.

Ground-based radar offers higher accuracy than satellite techniques over small areas and small time periods. Fabry, *et al*. (1994) (see section 5.2.2) found that the best accumulations are obtained with very high time resolution data. Krajewski, *et al*. (1992) estimated that, when the exponent parameter in the Z-R relationship has small uncertainty (about ± 10 per cent), radar techniques based upon averaging point observations work better than techniques based upon the area-threshold method. This conclusion is not inconsistent with the expected performance of ground-based radar versus satellite techniques whose best performance is achieved with the area-threshold method.

Raingauges remain the best method of estimating point rainfall. Although data from raingauges have been used

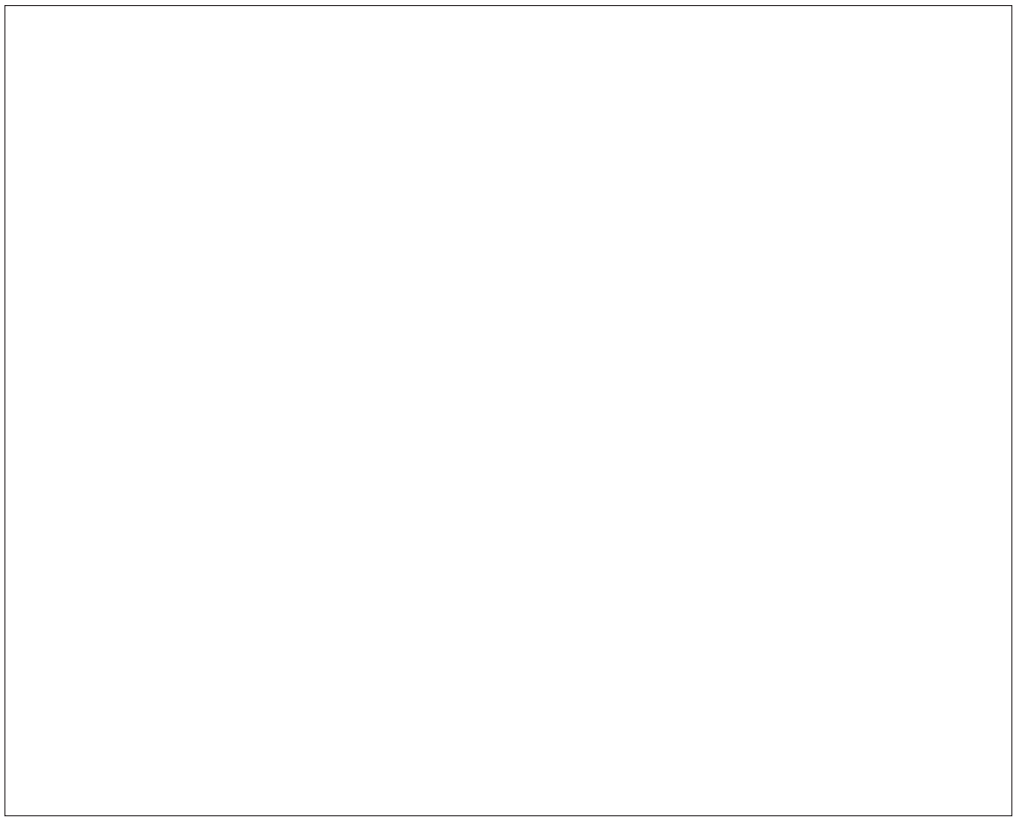

Figure 7.1 — The probability of precipitation as a function of infrared temperature and visible class (dashed line). The percentage of precipitation pixels, relative to the total number of precipitation pixels, normalized to a maximum value of 100 (solid lines) (from Cheng, *et al.,* 1993).

to calibrate both radar and satellite estimates, there are those who feel that it is unsound to force remotely-sensed measurements to be compatible with raingauge measurements. Further work on retrieval methods for remotely-sensed data is necessary in order to ascertain the correct balance between techniques. Finally, it is most important that techniques using remotely-sensed data are tested against numerical model products. There is little point in persisting with a method which does not outperform operational models.

6.6 TROPICAL RAINFALL MEASURING MISSION (TRMM)

In order to estimate rainfall over the tropics, the tropical rainfall measuring mission (TRMM) satellite programme has been developed jointly by Japan and the United States (Simpson, *et al.,* 1988; Theon, *et al.,* 1992). The satellite was launched in 1997 and is the first satellite with a precipitation radar operating at 14 GHz with a swath width of 220 km. This radar is part of a package of instruments containing two microwave radiometers — a standard SSM/I radiometer (four frequencies) with a swath of 580 km and a 19 GHz ESMR with a swath of 700 km and a visible/infrared radiometer (AVHRR) with a nominal swath of 1 100 km (Figure 6.5). With its swath of only 220 km the radar will provide three-dimensional information of fairly high horizontal resolution (4 km) over the innermost portion of the radiometer swaths. Many algorithms are being developed to make use of the variety of measurements. Some of them are physically based. Some of them exploit the fact that there are fairly stable statistical relationships (probability density functions) that characterize mesoscale convective systems in particular regions. The height-area rain threshold (HART) method discussed in section 6.2.3 will be of particular use for processing the data from this satellite. Since the satellite will fly in a non-Sun-synchronous orbit at 35° inclination each area of the Tropics will be visited about twice a day at local times which change slowly from day-to-day.

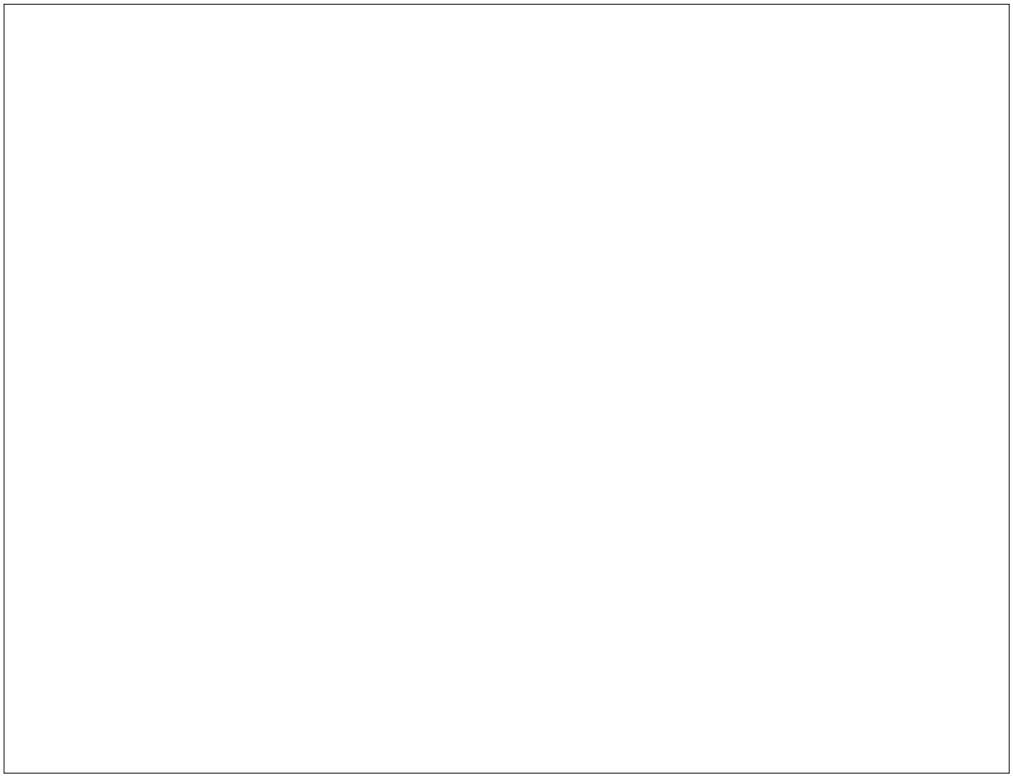

Figure 7.2 — Monthly rainfall fields derived from the United Kingdom mesoscale model compared with fields derived from raingauges (from Golding, 1986).

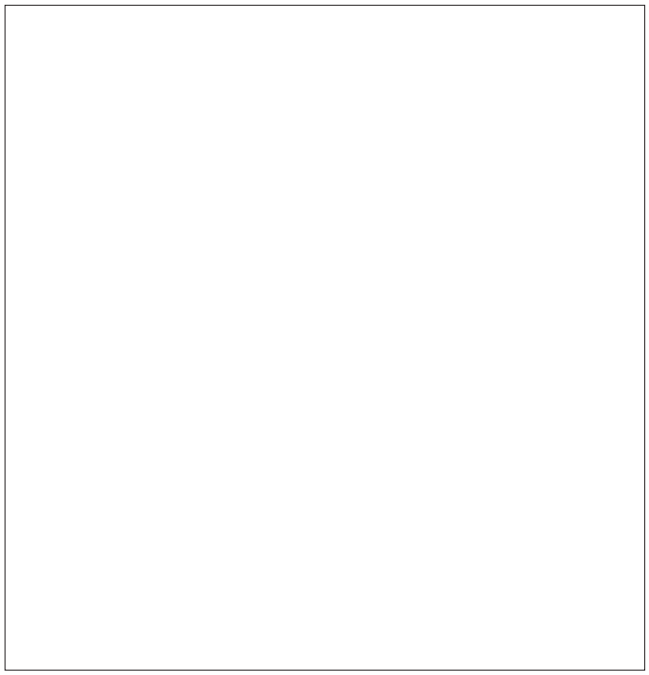

Figure 7.3 — Requirement for precipitation measurements (from Collier, *et al*. 1990).

CHAPTER 7

COMPLEMENTARITY OF GROUND-BASED AND SATELLITE MEASUREMENTS OF PRECIPITATION: THE RELEVANCE OF CURRENT PERFORMANCE TO SATISFYING THE HYDROLOGICAL REQUIREMENT FOR MEASUREMENT

It is evident that there are limitations with both existing and planned techniques for precipitation measurements from space based upon direct sensing of the visible, infrared and microwave properties of cloud and precipitation. This has prompted investigation of the contribution that ground-based measurements of precipitation and independent measurements of cloud characteristics might make to these methods.

So far, the blending of data from different sources has received restricted application as effort has concentrated on the estimation of precipitation over oceans and other data-sparse areas. One exception has been in satisfying the requirements of nowcasting. Here the need to extend the area of ground-based radar coverage has encouraged attempts to combine satellite data with surface observations and ground-based radar data. More recently, as part of the World Climate Programme (WCP), the Global Energy and Water Cycle Experiment (GEWEX) has been proposed in which the importance of combining ground-based and space-based measurements of precipitation is recognized.

7.1 USE OF GROUND-BASED WEATHER OBSERVATIONS

Although ground-based manual and automatic observations of cloud and precipitation have been used for some time to assess the performance of space-based techniques, there have been few attempts to devise objective procedures for combining these data with the precipitation estimates produced from satellite data. This is probably because of the limited coverage provided by conventional observations from raingauges and from human observers.

While there are clearly problems in many parts of the world, there are areas, for example the United States and Europe, which do have extensive coverage (even in real time). Work is under way in Europe, as elsewhere, to make better use of these observations including both manual and automatic measurements of present weather on land and from merchant ships and buoys. Areas of none precipitating cloud are identified from the surface observations and then removed. The removal process is usually subjective, although objective methods may be possible in areas where the observation density is high. This possibility has been exploited most extensively in attempts to blend surface-based weather radar data with satellite data.

Within the last few years, encouraging developments have taken place in the use of microphones and acoustic techniques generally do detect and measure rainfall at the surface of the oceans. Considerably more work remains to be done in this area before a fully operational system can be deployed.

7.2 USE OF GROUND-BASED RADAR OBSERVATIONS

Radar systems can make measurements of precipitation over wide areas from a single location in real time, and are easier and more cost effective to operate than extensive raingauge networks. It is therefore attractive to design procedures to combine the radar data with satellite data in order to understand better the relationships between variations in visible brightness and infrared or microwave brightness temperatures and rainfall,. However, care must be taken as measurements of precipitation made using radar data are subject to various errors which may produce spurious correlations (Chapter 5). Therefore most of the work to date has used radar data in a relative sense to locate areas of precipitation. The type of algorithms used range from simple insertion techniques to procedures developed to use radar data to derive visible or infrared rainfall relationships and algorithms using bispectral satellite data.

Perhaps the most widely applicable technique is the bispectral technique. The procedure exploits information on the height of clouds derived from infrared measurements and information on the depth of clouds derived from visible measurements. The visible and infrared data are each divided into a number of classes and a table of "probabilities" of rain for each class produced by comparison with radar data. Examples of tables for frontal rain are shown in Figure 7.1. These are then applied to the satellite data beyond the area of radar coverage.

Early work on this type of technique encountered problems arising from registration errors between visible and infrared images, instrument calibration, time difference between images and illumination geometry. However, these problems were overcome by Lovejoy and Austin (1979). Nevertheless, care must be taken to eliminate those areas of poor radar coverage before constructing the look-up table.

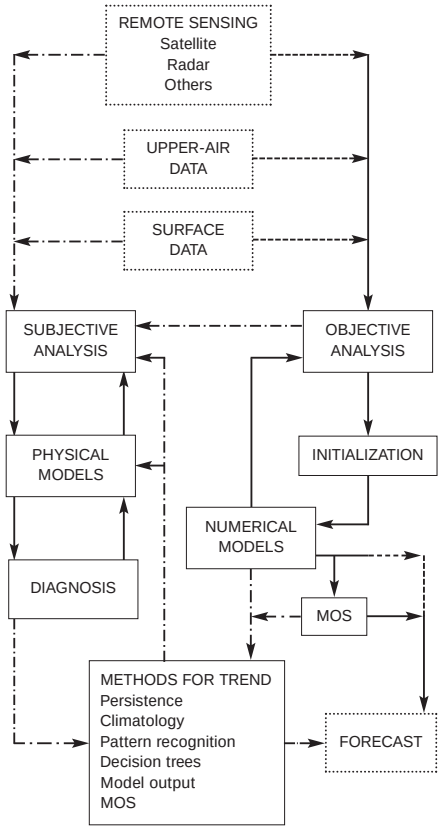

Figure 8.1 — The forecasting process (left) for humans (right) for a numerical prediction model (from Doswell, 1986).

Also, average rainfall rates of less than 0.5 mm h^{-1} that are derived from visible/infrared pairs corresponding to warm temperatures and low visible counts, are mainly a result of improper radar-satellite matching caused by the problems mentioned above. The rainfall rates at these pairs are set to zero to avoid the generation of spurious areas of small or trace rainfall amounts.

The rainfall probability maps derived using this technique have been verified with radar and surface data. A useful skill in estimating rain areas has been identified, although experience indicates that the probability of rain table should be changed seasonally. The radar verification shows that the main skill lies in identifying three classes, namely clear, cloudy with low probability of rain, and cloudy with a significant probability of rain. The accuracy of the results diminishes with increasing distance from the training radar. However, it was pointed out that use of a coarse resolution might allow the introduction of texture matrices. Rainfall over periods from $^1/_2$ to 2 hours may be estimated with an accuracy of around 49 per cent over areas of 10^5 km^2. However, more extensive assessments for different rainfall types are required to confirm this performance.

7.3 USE OF NUMERICAL MODELS

Given precipitation estimates from satellite data, procedures are being devised to use the estimates as input to numerical models. However, studies to use numerical models to aid the estimation of precipitation from satellite data are limited. Indeed, operational approaches to this problem exist in which the satellite-derived moisture fields are

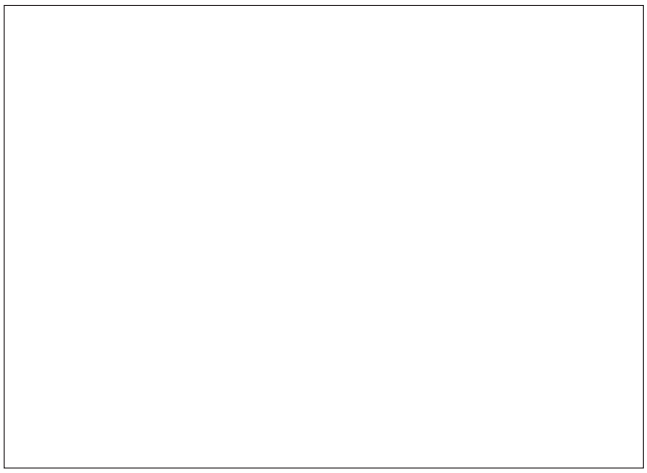

Figure 8.2 — The quality of weather forecasts, defined as the product of the accuracy and detail achievable, shown as a function of lead time for three different forecasting methods. The figure is highly schematic and the stage at which the quality of one technique becomes superior to another will not only change over the years with the development of the different methods, but will also depend on the particular phenomenon being forecast (from Browning, 1980).

interactively balanced with respect to other model fields even though relative humidity and vertical velocity should be well correlated. Currently, climatological rainfall fields and orographic rainfall derived from models approach the accuracy of observed fields (Figure 7.2), but numerical models do not yet reproduce convective rainfall with the spatial accuracy necessary for most hydrometeorological studies.

7.4 SATISFYING THE HYDROLOGICAL REQUIREMENTS FOR MEASUREMENT

Collier, *et al*. (1990) classified these requirements as shown in Figure 7.3. It is clear that the requirements for hydrology are more stringent than for meteorology, a point also illustrated by the recommended accuracies noted by Rodda (1977). For meteorology and climatology, the shorter the integration period and the smaller the area over which the measurements are made, the more tolerant is the requirement of errors in the data. This is not possible for hydrology, probably because there is no linkage provided by an energy cascade through physical systems of large to small scale as there is in the atmosphere.

Both radar and satellite systems provide measurements of precipitation. There are advantages and disadvantages of both, although the use of radar and satellite systems should be regarded as complementary. Depending on the application to be addressed, a choice can be made taking into account these advantages and disadvantages. There are, for example, situations where the lower cost satellite estimates of precipitation are adequate, e.g. over large areas where low spatial and temporal resolution are sufficient.

Where high spatial and temporal resolution are important for operational management purposes, a radar, even though it is more expensive, offers significant advantages. Moreover, radar data can be used to satisfy a variety of customer needs, e.g. they can be used for aviation severe weather warnings. The advantages and disadvantages of each system are as follows (compiled with the help of Professor D. H. Newsome, personal communication, CNS Scientific Services, Reading, United Kingdom).

Satellite precipitation estimation

Advantages

(*a*) Relatively inexpensive when compared with weather radar;
(*b*) Easy to operate and maintain;
(*c*) Tried and proven — but mainly in tropical zones;
(*d*) In convective rainfall, accurate monthly totals can be obtained, daily totals less so and subdaily totals much less accurate.

Disadvantages

(*a*) At night, no visible data are available therefore precipitation estimates are achieved using infrared and, perhaps, microwave data — less accurate — as cold, high level Cirrus cloud is not related to heavy rain;
(*b*) Techniques based upon assignment of temperature and/or brightness thresholds to rainfall amounts, vary in performance with season and, therefore, have to be adjusted regularly;
(*c*) Sampling problems for subdaily totals using images every half hour;
(*d*) Subdaily totals are likely to be very inaccurate, particularly in stratiform rainfall associated with mature thunderstorms, mesoscale convective complexes (MCSs) or frontal systems i.e. the rainfall regime in temperate zones;
(*e*) Estimates of snow cover are only possible in cloud-free periods;
(*f*) No estimation of the presence of hail is possible in thunderstorms;
(*g*) No estimation of low-level winds or severe weather is possible; therefore advice to aviation is limited to cloud type and approximate height;
(*h*) Multi-layer cloud decks prevent the reliable monitoring or orographic rainfall enhancement;
(*i*) Data may be unavailable for many hours during solar eclipses and sensor decontamination activities; usually these periods cannot be chosen to avoid severe weather occurrence;
(*j*) If satellite sensors fail, there is no possibility of repair until another satellite is launched.

Weather event	*Time scale for linear extrapolation validity*	*Non-linear predictive capability*
Downburst or microburst	≈ 1 to a few minutes	Very limited
Tornado	≈ 1 to a few minutes	Currently very limited
Individual thunderstorms or heavy shower	5 - 20 min	Very limited
Severe thunderstorm	10 min–1 h	Very limited
Thunderstorm organized on the mesoscale	≈ 1 to a few hours	Some
Flash-flood rainfall	≈ 1 to a few hours	Very limited
Orographically-triggered showers	≈ 1 h	Very limited
Lake-effect snowstorms	A few hours	Very limited
Heavy snow, winter storm or blizzard	5–20 min	Some
High wind gusts accompanying shallow showers	Many hours	Very limited
Hurricane	Many hours	Fair
Frontal passage		Fair to good

Table 9.1
Examples of typical linear extrapolation time-scales for precipitation fields associated with various weather events. (partly from Doswell, 1986, after Zipser, 1983)

Figure 9.1 — (*a*) An example of a simple non-linear model that is much worse than a linear one; (*b*) An example of a very good non-linear model. Such models are usually complex and hard to find (after Doswell, 1986).

Estimation of precipitation and weather by radar

Advantages

(*a*) Temporal resolution very high; updates as frequently as desired at no extra expense;
(*b*) Spatial resolution very high;
(*c*) Accuracy of sub-catchment rainfall totals good;
(*d*) No sampling problems using 5-minute (or better) intervals at no extra expense;
(*e*) Snowfall can be measured in near-real time in all cloud situations;
(*f*) Height of melting level can be measured accurately; this is useful for assessing low-level icing conditions (useful aviation advice especially for helicopters);
(*g*) Detection of hail occurrence and measurement of the size of hail stones is possible;
(*h*) Estimate of the occurrence of high winds and other severe weather can be made; very useful for aviation and public service forecasting;
(*i*) Very short period forecasts can be made;
(*j*) Very useful for operational management of hydropower and irrigation schemes;
(*k*) Orographic rainfall enhancement can be monitored provided an appropriate radar site is chosen;
(*l*) Equipment faults can usually be rectified within a few hours during which data may be available from the adjustment raingauges;
(*m*) Satisfies a wide range of customer requirements;
(*n*) Provides real-time data for operational management, e.g. flood warning and routing.

Disadvantages

(*a*) Total system is expensive;
(*b*) Requires maintenance and electronic calibration on a monthly basis — although downtime can be chosen to suit appropriate weather conditions;
(*c*) Requires a higher level of operator knowledge than the satellite technique;
(*d*) More extensive (than most other systems) technical training is required.

CHAPTER 8

APPROACHES TO, AND REQUIREMENT FOR, QUANTITATIVE PRECIPITATION FORECASTING (QPF)

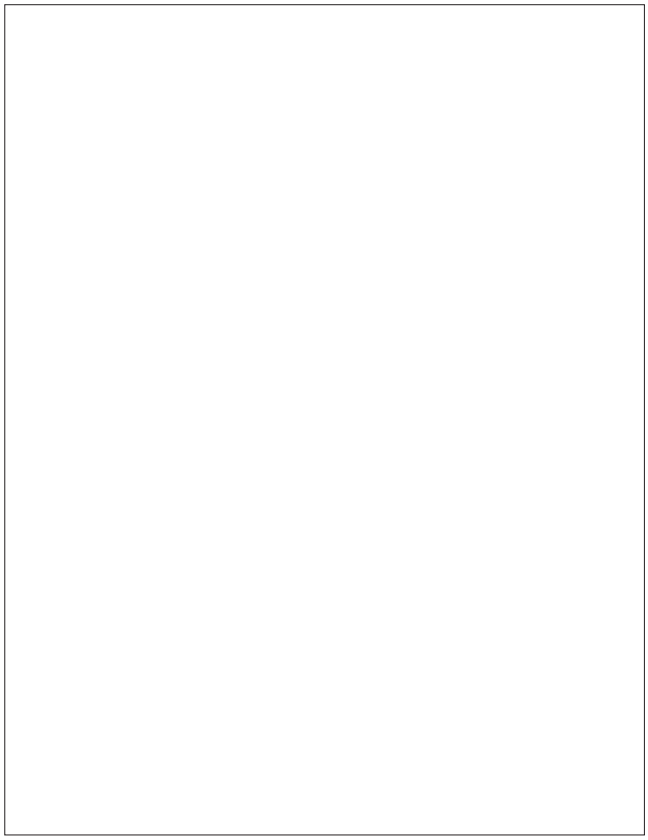

Figure 9.2 — (*a*) The elementary boundary vectors defined for each element E_{if} of a radar picture as used by Duda and Blackmer (1972); (*b*) A radar echo-contoured picture derived objectively by Duda and Blackmer (1972). The letters and characters represent various configurations of the boundary vectors.

Figure 9.3 — Fourier approximations to a digital contour (*a*) one harmonic; (*b*) two harmonics; (*c*) five harmonics; (*d*) nine harmonics (after Duda and Blackmer, 1972).

Weather may be defined as the detailed behaviour of the atmosphere on appropriate (to the particular application) space- and time-scales expressed in terms of the distribution of variables such as temperature, pressure, wind and precipitation. While precipitation is a single variable, its forecasting depends intricately upon the other variables. Indeed, precipitation is the most difficult atmospheric parameter to forecast on all time-scales.

Forecasts of the weather still depend upon a blend of manual subjective and numerical objective techniques. A variety of

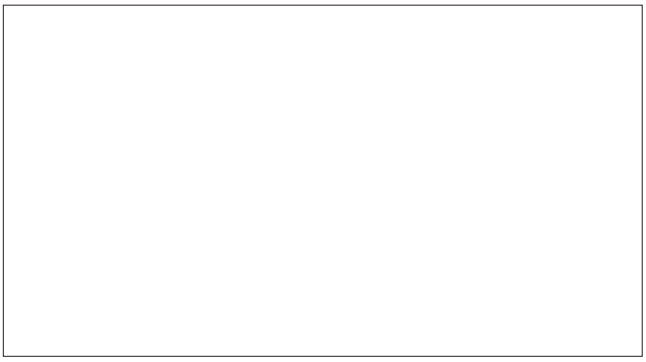

Figure 9.4 — The objective technique used by Muench (1976) for obtaining echo position. The values of the row j are replaced by the average of the three rows $j-1, j+1$. The left edge is half a grid to the left of the first non-zero value of the three-row average, and the right edge is similarly defined. Arbitrary intensity values are given along row j.

different types of data provide the input to both approaches, and it is recognized that numerical weather prediction requires subjective intervention in order to produce optimal forecasts (Figure 8.1). However, the large advances which have occurred during the past 20 years or so in weather forecasting have only been possible because of the use of mathematical models (Houghton, 1991).

Within an atmospheric model, the atmosphere's behaviour is represented by values of appropriate parameters at a grid of points. The models in operational use range from systems covering the globe with grid spacings of about 90 km to mesoscale models covering individual small countries having grids of a size around 15–20 km. All models have about 20 levels in the vertical. The dynamics included in the model are described by the horizontal momentum equations, the hydrostatic equation and the continuity equation. In addition, the models include the equation of state, thermodynamic equations and parametric descriptions of moist processes, radiative and convective processes, and the exchange of momentum, heat and water vapour with the underlying surface. Parametrizations of motions occurring on scales smaller than the grid size are also included. Assimilation, or model initialization, involves various types of filtering and smoothing, but may benefit from data only indirectly providing information about the basic variables of temperature, humidity, pressure and wind such as radar reflectivity data.

Weather forecasting may be divided into short-, medium- and long-range forecasting, where short-range forecasting is less than about two days ahead, medium-range forecasting is two days–two weeks ahead, and long-range forecasting is months ahead (Bengtsson, 1985). Browning (1980) has sub-divided short-range forecasting as shown in Figure 8.2. Here, forecasts for a few hours ahead, often referred to as nowcasts as they are based upon the extrapolation of current weather, are distinguished from forecasts based upon mesoscale (horizontal scale, 20–50 km; lifetime, 2–50 h) numerical weather prediction. In addition, forecasts based upon synoptic scale (horizontal scale, 500–5 000 km; lifetime, 50–500 h) models using model output statistics (MOS), are also identified. Beyond the time-scales shown in Figure 8.2, both dynamic and statistical techniques are used. The dynamic approach based upon numerical model runs involves considering the atmosphere as a chaotic system such that ensembles of model

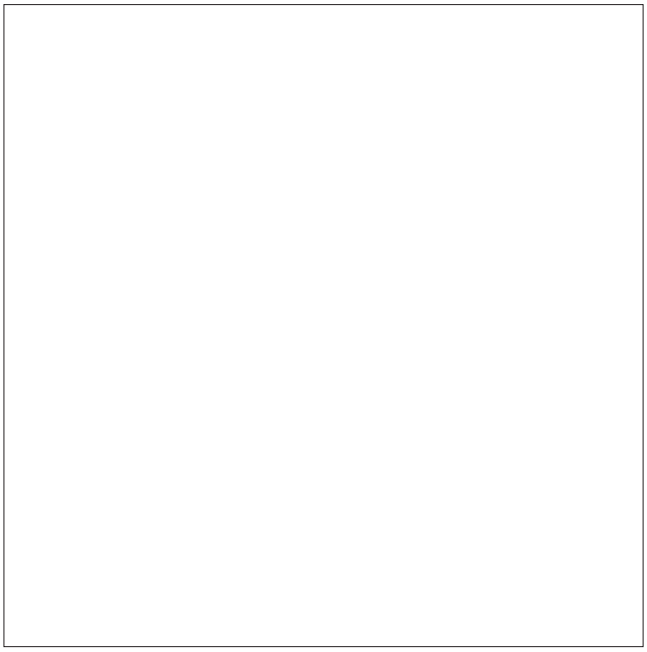

Figure 9.5 — Echo isolation using a bivariate normal distribution (From Wiggert, *et al*., 1976).

forecasts are analysed. Seasonal forecasting may be based upon this approach, but also upon statistical relationships developed between atmospheric parameters and specific observations.

The requirements for weather forecasts have been discussed extensively in the literature (see for example Harrison and Smith, 1989; Maunder, 1986). More specifically, the requirements for forecasts of rainfall cover all time-scales.

CHAPTER 9

EXTRAPOLATION FORECASTING: NOWCASTING

9.1 CHARACTERISTICS OF PRECIPITATION AND CLOUD, AND THE BASIS OF NOWCASTING

Observations for nowcasting must have high resolution, be delivered quickly and be updated frequently. Nowcasting therefore depends heavily upon the interpretation of remotely-sensed observations, which may be either wide-area or localized. Weather radars and satellite images are able to map rainfall and cloud fields in detail over hundreds of kilometres.

The distribution of precipitation and cloud in both space and time is extremely variable. In thunderstorms, rainfall rates may vary by tens of millimetres per hour from minute to minute and over distances of a few hundred metres (for example, Bader, *et al*., 1983; Hill, 1984). Cloud height too varies enormously over short distances in convective systems. Even in frontal rainfall, which is often assumed to be widespread and uniform, there are considerable variations (for example Browning, *et al*., 1993; Houze 1981). No economic network of manual observations, or even automatic weather stations, can hope to observe, in real time, precipitation distributions and their variations sufficiently reliably for operational weather forecasting. Clearly this is true over sea areas, but even over land large areas of rainfall often occur between conventional observations.

The use of data from a radar network is the only way of observing the detailed structure and behaviour of precipitation fields. Cloud imagery certainly allows rain-no rain areas to be defined with some reliability and for convective rainfall provides estimates of rainfall amount (Chapter 6). However, as yet no one technique or combination of techniques provides precipitation measurements of acceptable accuracy under all weather conditions. Indeed, ground-based radar data are an important element in several satellite-based rainfall estimation procedures (Chapter 7).

Short-range forecasts of precipitation are based upon the timely acquisition of radar data and the extrapolation of those data for a few hours ahead. The quality of the forecasts depends upon the time ahead for which linear extrapolation is valid. This varies for different weather systems as shown in Table 9.1. For convective systems, it is clear that linear extrapolation beyond 1 or 2 h is unlikely to provide good forecasts on its own. However, it should be noted that larger-scale systems often trigger small systems which produce severe weather. Therefore linear extrapolation for several hours ahead of larger systems may be an extremely important part of a procedure for forecasting severe weather associated with smaller systems.

Where linear extrapolation ceases to produce a good forecast, a non-linear forecasting procedure must be applied. However, the application of a non-linear model can produce a worse result than linear techniques as shown in Figure 9.1(*a*). The best approach is to use a mesoscale numerical model to provide forecasts beyond the region where linear extrapolation is applicable as shown in Figure 9.1(*b*). However, such forecasts are far from perfect and it remains necessary for forecasters to interpret the model output to improve the numerical output.

9.2 CHARACTERIZATION OF RADAR ECHOES AND CLOUD: FEATURE EXTRACTION

Several methods of describing radar echoes and cloud have been proposed, mainly with the purpose of the eventual use of the objective description within statistical analyses or forecasting procedures. To a lesser extent, these descriptions have also been used to provide a basis for condensing the volume of data sent from radars to users by data transmission systems. More recently, attempts have been made to use descriptions of echo structure to indicate likely rainfall types.

During the late 1960s, satellite technology had reached the stage where high-resolution cloud imagery was available, and pattern recognition techniques were developed in response to this new form of data (Leese, *et al*., 1971; Smith and Phillips, 1971). Radar meteorologists recognized the applicability of this work to radar data and based initial work on radar pattern recognition on these techniques.

The detection of radar echoes and cloud may be considered within the following categories (Pankiewicz, 1995) which are interrelated:

(*a*) Spectral: intensities and multispectral characteristics;
(*b*) Textural: statistical measures of the local neighbourhood (including spatial frequencies and frontal dimensions);
(*c*) Spatial: size and shape;
(*d*) Contextual: relationship with other radar echo or cloud systems.

The most obvious features of satellite emagery are spectral or multispectral grey-level intensities (see for example Arking and Childs, 1985) giving cloud fraction, optical thickness, cloud-top temperature, etc. Further spectral features may be derived by considering a variety of statistics such as the mean, standard deviation, maximum, or minimum (see for example Ebert, 1987).

Haralick (1986) listed the following as possible statistical textural parameters: grey-level co-occurrence, gradient analysis, orthogonal transformation, autocorrelation, mathematical morphology of tonal primitives and relative extreme density. Pankiewicz (1995) discusses these measures, reviewing the derivation of contrast, homogeneity, correlation and other parameters.

In pattern recognition, context is defined as the dependencies between various pixels, groups of pixels or larger scale attributes (Seddon, 1983). For example, cellular convection generates a characteristic, very variable, cloud or radar pattern, which is quite different from that associated with fronts. The use of conditional probability of obtaining a particular class given a feature enables class membership to be allocated.

Unfortunately as the method of classifying an image increases in complexity, it becomes necessary to make decisions only upon the most essential, discriminatory information. Likewise, reducing the number of dimensions examined may lead to a decrease in the error rate of recognition (Duda and Hart, 1973; Kittler, 1986). The most complex procedure may not always be the most successful! Clearly, the aim in designing a pattern recognition system is to classify unknown patterns with the lowest probability of misclassification. In the

following sections, some examples of techniques which have been applied are outlined.

9.2.1 Contouring

The most conceptually simple method is that of contouring. A single selectable cloud or echo intensity threshold is used and must be repeated if several thresholds are needed for a complete description of an echo. Duda and Blackmer (1972) have investigated a technique, originally proposed by Brice and Fennema (1970), which computes the "directed" boundaries for a digital picture. For each element E_{if} of a picture there are four elementary boundary vectors V_1, V_2, V_4, V_8, defined in Figure 9.2(*a*). These vectors encircle the element in a counterclockwise fashion as shown in Figure 9.2(*a*) and are known as the "directed" boundaries of each picture element. A four-bit binary number V_{if} indicates the presence or absence of each boundary vector. Initially, all vectors are absent and the program scans the picture inserting vectors whenever there is a transition from a zero to a non-zero value across the boundary. The picture may be displayed using certain line printer characters (letters, arrows, dashes, etc.) to represent various configurations of vectors, for example L to represent $\downarrow\rightarrow$, and V to represent $\downarrow\rightarrow\uparrow$(Figure 9.2(*b*)). Similar techniques have been described by many workers in connection with the contouring of a variety of fields of meteorological data.

9.2.2 Fourier analysis

A description of the contours of a digitally-defined echo area may be derived from a Fourier series expansion (Duda and Blackmer, 1972; Östlund, 1974; Zittel, 1976). Consider *x(s)* and *y(s)* to be the *x* and *y* coordinates of a point on the arc length s measured from some arbitrary initial point. The *x* and *y* are periodic functions, repeating when the arc length equals the perimeter *P*, and they can be expanded in a Fourier series:

$$x(s) = a_0 + \sum_{n=1}^{\infty} a_n \cos(nws - \theta_n) \qquad (9.1)$$

$$y(s) = b_0 + \sum_{n=1}^{\infty} b_n \cos(nws - \theta_n) \qquad (9.2)$$

where $w = 2\pi/P$, a_n and b_n are the amplitudes of the nth harmonic (for example Duda and Blackmer, 1972). Figure 9.3 illustrates Fourier approximations to a digital contour, and it can be seen that as few as five harmonics may be used to provide quite a detailed description of an echo if only one intensity level is used. Using a multiple-thresholding technique (see section 9.2.4), it is possible to give a complete three-dimensional description of a radar echo (Barclay and Wilk, 1970), which may be used for transmitting the radar information from a radar site to a user.

Fourier analysis is used within pattern recognition procedures which require knowledge of the shape of the echo for the purpose of assessing pattern motion. An example of such a procedure has been described by Muench (1976), in which a harmonic analysis of the pattern between the edges is made, and the phase angles of significant amplitudes are stored (Figure 9.4). The analysis provides the locations of the edges and peaks in the harmonics which, when matched with corresponding edges and peaks at a later time, give echo displacement vectors.

9.2.3 Bivariate normal distribution

A further technique for describing cloud areas or radar echoes has been proposed by Wiggert, *et al*. (1976). This techniques uses an unnormalized bivariate normal distribution *f(x,y)* where:

$$f(x,y) = \exp\left\{-\frac{1}{2(1-p^2)}\left[\left(\frac{x-\mu_x}{\sigma_x}\right) + \left(\frac{y-\mu_y}{\sigma_y}\right) - 2\frac{x-\mu_x y-\mu_y}{\sigma_x \quad \sigma_y}\right]\right\} \qquad (9.3)$$

where p is the correlation coefficient, μ_x is the average x value $\equiv\bar{x}$ (that is the average echo or cloud area km^2), μ_y is the average y value $\equiv\bar{y}$ (that is the average rain rate mm h^{-1}), σ_y is the variance in y.

$$W = \sum f_{i,j} = weight, \quad \bar{x}^2 = \frac{1}{W}\sum_{i,j} x^2 f_{i,j} \qquad (9.4)$$

In three dimensions, a bivariate normal distribution has contours that are ellipses and has cross-sections that are normal distributions. The description of the echo or cloud area is contained in the weight of centroid, together with the second moments of the bivariate normal distribution of the echo area. All local maxima are found within each echo (Figure 9.5). It is claimed by Wiggert, *et al*. (1976) that this technique is better than simple Fourier analysis, as it gives a method of describing the interior of an object. However, its added complexity is really useful only in dealing with large intense thunderstorms which have well-defined interior maxima and is not practical for frontal rainfall which may be very uniform or contain complex cells within a large-scale fragmented rain area. More recently, Ebert (1987) has used textural features of cloud images to classify the images into cloud and surface types. Similar techniques could be extended to radar data.

9.2.4 Clustering

When objects are well separated, for example in the case of some thunderstorms, there is no difficulty, in principle, in defining them objectively using a threshold technique such as that proposed by Barclay and Wilk (1970) or Crane (1976). However, there are many occasions when object areas are very complex and a simple intensity threshold does not isolate individual objects clearly for analysis. This is especially true in the case of widespread frontal rain.

To overcome this problem, clustering procedures aimed at isolating data into homogenous subcategories, such as particular cloud types or particular shapes of rain area, have been proposed (Ball, 1965; Haralick and Kelly, 1969; Endlich, *et al*., 1971) and implemented (Duda and Blackmer, 1972; Wolf, *et al*., 1977). Such techniques are also referred to as supervised classifiers. However, difficulties arise in defining an initial grouping in which to begin allocating

areas of cloud or radar echoes and in determining the true number of clusters.

Duda and Blackmer (1972) have suggested a method of clustering based on the sequential lowering of an initially high intensity threshold, this being referred to by them as hierarchical clustering. The technique has been developed by Smith (1975), although not all clusters recognized undergo a matching procedure as to do so increases computation time significantly. Clusters smaller than a predefined size are ignored. Östlund (1974) and Wiggert, *et al*. (1976) use an "eight-surrounding-points" search (within a radius of height points) to isolate cluster areas. For each point above a threshold, a search within a radius of eight surrounding points is made to see whether any of these points are occupied by echo above the threshold. This is repeated until no such points are found. On finding such an echo in the surrounding area, the central echo is assumed to belong to the same cluster as the echo so found. A grid length of about 1.6 km was used, so that echoes within about 13 km of each other were regarded as belonging to the same echo cluster. Wolf, *et al*. (1977) have adopted a "touching" algorithm, that is members of a cloud (in their case) group must touch at least one other member of the group. This is a simple form of hierarchical clustering (Anderberg, 1973) known as single-linkage clustering and depends on the details of the application and the weather types. Collier (1981) found that allocation of echoes to a particular cluster if they were within 40 km of other echoes led, for frontal rainfall in the United Kingdom, to one cluster being identified for 63 per cent of the time, and two clusters for 34 per cent of the time.

Developments of this technique aim to improve the reliability of the cluster allocation. For example, some sensitivity to the variance of features or objects in a cluster may be achieved by considering the value significance or the range of values over which data may fall into a particular cluster. This is implemented by using small connected parallelepipeds having stepped borders (Lillesand and Kiefer, 1987). Another approach is to use discriminate functions, the value of which guides allocation to a particular cluster.

If some echoes are not to be considered for allocation to a particular cluster then some measure of echo significance is required. At its simplest level, echo significance may be based on echo size only, that is echoes smaller than a predefined size are ignored.

Duda and Blackmer (1972) have pointed out that, in considering echo significance, the following parameters can be examined: intensity, size, height, shape, motion, rapid changes in intensity, shape and size, and merging with or splitting from other echoes. Intensity and size are probably the most important parameters. For radar, they have suggested the following empirical weighting factor, based on an assumed $Z^{R1.6}$ relationship, as a first step towards the evolution of a complete significance parameter:

$$weight = 100 \log_{10}\left[\left(\frac{Z_{max}}{Z_{ref}}\right) 0.5 \frac{\sum Z^{1/1.6}}{Z_{ref}^{1/1.6}}\right] \qquad (9.5)$$

where Z_{max} is the largest reflectivity factor measured and Z_{ref} is a reference value arbitrarily defined. The echo size is contained in Z. Although this weight does not take account of all the parameters mentioned above, it nevertheless was found to produce plausible results, when objective forecasts prepared using it were compared with actual echo patterns. Most subsequent work has not taken the problem of echo significance much further. Muench and Lamkin (1976) and Wolf, *et al*. (1977) have developed further empirical techniques, which are claimed to be very effective in providing objective "guidance" for operational forecasters. However, such a procedure can be misleading as echoes may travel in what Hill and Browning (1979) refer to as "skeletal" form — low intensity and variable size and shape — and yet develop later to produce significant rainfall over areas of high land.

Much of the discussion in this section so far has been concerned with supervised classification which will fail when development of the echo or cloud occurs. Hierarchical techniques may be extended to include unsupervised classification procedures based upon some form of learning from the characteristics of the data. At its simplest level, this approach uses a technique for partitioning the data and associating features to the partition centre. The analysis compares the new image with these partition characteristics in order to allocate radar echo or cloud. This allows features to move between clusters. Seddon and Hunt (1985) and Farki, *et al*. (1992) use supervised minimum-distance-to-means classifiers after the classes have been identified.

All these approaches to identifying echo significance are not unambiguous and careful data training is needed. Nevertheless, the implementation of some measure of echo significance is necessary. Recently, neural networks have been considered as providing the potential to improving these techniques (Lee, *et al*., 1990). This approach models the perception capabilities of the human brain (Beale and Jackson, 1992). So far, the results are mixed (see for example Liu and Xiao, 1991; Peak and Tag, 1994), although the potential has certainly been demonstrated. This will be discussed further in section 10.3.

9.3 PATTERN MATCHING PROCEDURES AND MOTION DERIVATION

Tracking individual echo or cloud areas, or large areas of echo or cloud from one image to the next, involves some kind of matching or correlation. Once the movement is defined, then short-period forecasts may be made (neglecting development and decay of course).

Some work (for example Parsons and Hobbs, 1983) has been reported in which regression relationships between radar echo movement and wind velocity have been identified. Tatehira, *et al*. (1976) have used the 700 hPa wind velocity to advect echo areas and have claimed a distinct improvement over persistence forecasts, while indicating that such forecasts were not as good as those made using a pattern-matching procedure.

Smith (1975), in a study of a variety of echo patterns, and Shearman (1977) (see also Niemczynowicz, 1987), in a study of rainfall patterns, defined using a raingauge network report that no reliable correlations were found between rain area movement and wind velocity at any level. Indeed, Bond,

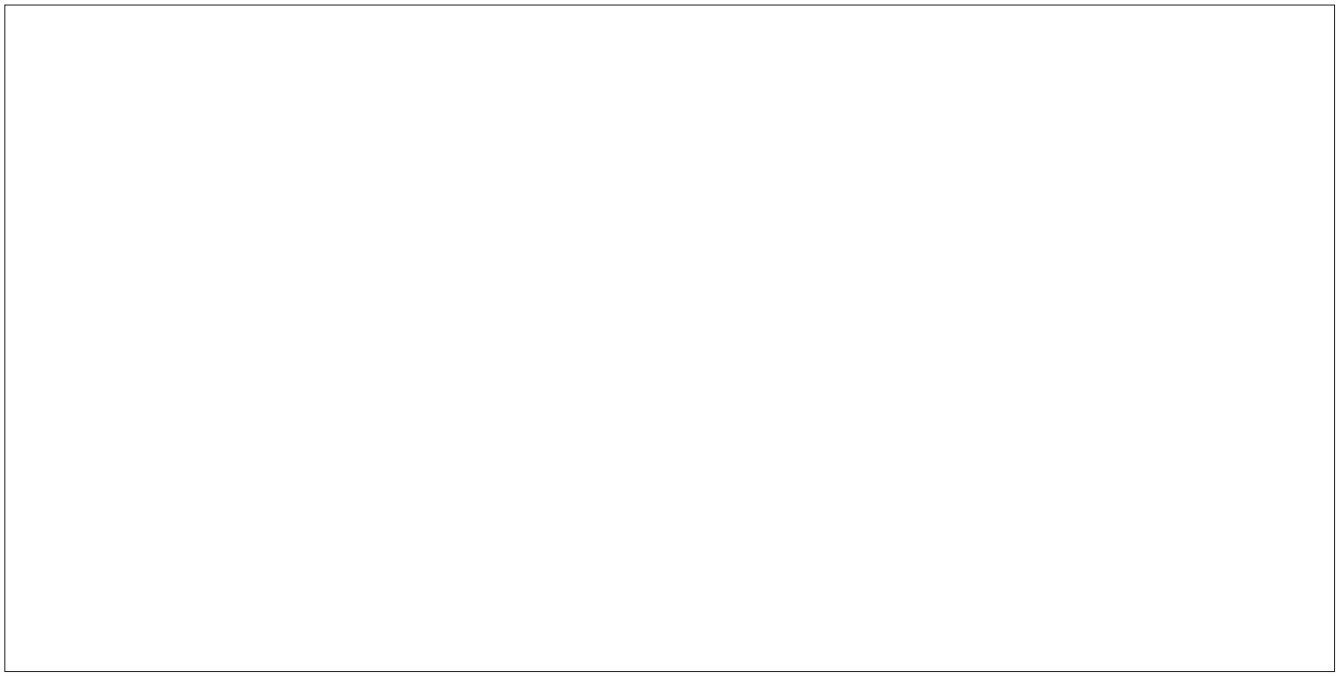

Figure 9.6 — Illustraing (*a*) The mean error regardless of sign in the forecast hourly rainfall for the 20 km square (400 km^2) centred on Malvern, plotted as a function of the lead time of the forecast, for light rain (trace -1 mm h^{-1}) and moderate-heavy rain (more than 1 mm h^{-1}): — results of objective forecasts (without manual modification); - - - results of subjective forecast; numbers in parentheses denote number of cases; (*b*) The percentage error for the cases of moderate-heavy rain: — results of objective forecasts (without manual modification); - - - results of subjective forecast; arrows show the radar measurement errors found in the DWRP; x – x, performance of the cross-correlation technique described by Bellon and Austin (1984) for a 600 km^2 area; + – + performance of the cross-correlation technique described by Bellon and Austin (1984) for a single point (gauge site); *dB* + *A*, error of the radar estimates of rainfall derived by Bellon and Austin. BB = brightband (from Collier, 1989; after Browning, *et al*., 1982).

I	Errors in measuring the actual spatial distributions of surface rainfall intensity	Deficiencies of initial observations
II	Errors in estimating the actual velocity of the rainfall pattern	
III	Errors due to non-linear temporal changes in the intensity of the rainfall pattern	Deficincies of forecasting by linear extrapolation
IV	Errors due to non-linear temporal changes in the velocity of the rainfall pattern	

Table 9.2 Categories of errors in forecasts of rainall produced using linear extrapolation (after Browing, *et al*., 1982)

et al. (1981) tracked a number of weak, but rapidly moving, shallow shower cells and found that the speed of movement was very closely related to the speed of maximum wind gusts at the surface. This was confirmed by Monk, *et al*. (1987), who also found that an operationally-useful indication of the speed and direction of movement of two cyclonic vortices was provided by radar echoes. Therefore care must be taken in associating radar echo or cloud movement with wind velocity at particular heights as the success or not of such attempts will depend upon the type of precipitation. Nevertheless, procedures for advecting radar echoes using numerical model winds at specified levels have met with some success (Brown, *et al*., 1991; Andersson, 1991). In the following sections, we outline some of the techniques which have been used to define objectively radar echo or cloud motion.

9.3.1 Centroids

If echoes or cloud can be isolated easily, then the simplest pattern-matching procedure is one using the centroid of each feature. Echo centroids at one time may be matched with those at a subsequent time (Walton and Johnson, 1986). Constraints are usually applied to the calculated echo motion to aid the matching procedure; for example echoes are not normally considered to move at speeds greater than 120 km h^{-1}.

This technique has been developed by Wilk and Gray (1970) (for radar echoes) and Endlich, *et al*. (1971) and Wolf, *et al*. (1977) (for clouds) with some success for weather situations characterized by isolated echo or cloud, for example isolated thunderstorms. Barclay and Wilk (1970) and Zittel (1976) have used a linear least-squares positional fit through

Table 9.3
Principal sources of error in the subjective rainfall forecasts for Malvern during 29 frontal rainfall events
(after Browning, *et al*., 1982)

Source of error	*Type (see Table 9.2)*	*Number of rainfall events affected*	*Measure of importance of the errors (summation of mean forecast errors rounded to the nearest 5 mm)*	
			Before making subjective corrections	*After making subjective corrections*
Development or decay of rain areas	III	16	20	20
Beam overshooting shallow precipitation	I	14	20	10
Difficulty in defining motion due to amorphous structure of rain areas	II	9	15	10
Radar adjustment changes and drop size variability (discounting known long-term errors)	I	10	10	10
Low-level evaporation	I	14	10	5
Bright band	I	8	10	5
Changes in velocity of rain areas	IV	5	5	5

the centroid positions of echoes as a function of time to specify displacement vectors. Difficulties arise when echoes (or cloud areas) split or merge, and clustering techniques (see section 9.2.4) have been developed which show some success in overcoming this problem.

9.3.2 Cross-correlation

Cross-correlation techniques may also be used to match portions of one radar picture with portions of subsequent pictures (see Wilson, 1966 for radar data, and Leese, *et al*., 1971 and Smith and Phillips, 1971 for clouds). This procedure has the advantage of taking into account the detailed shape of the echo being tracked and decreases the chances of mismatching echoes, although the procedure uses only one level of intensity at a time. Thresholding may be used to identify particular features or scales of motion (Yoshino and Kozeki, 1985).

If all the echoes in a radar picture move together, and if there are no significant size, shape or intensity changes from one picture to the next, then conceptually the simplest matching procedure is to cross-correlate an entire picture with an entire picture at a subsequent time. This technique has proved to be very successful within these limitations (Zawadzki, 1973; Austin and Bellon, 1974; Hill, *et al*., 1977; Bellon and Austin, 1984). Cases of developing convective activity and orographic rainfall are not suited to this technique but widespread rainfall over lowland areas on occasions may be analysed successfully. By identifying precipitation "objects" in the image, as discussed in section 9.2, it is possible to cross-correlate each image in turn. Using the formulation from Schmetz and Nuret (1987), the cross-correlation equation is:

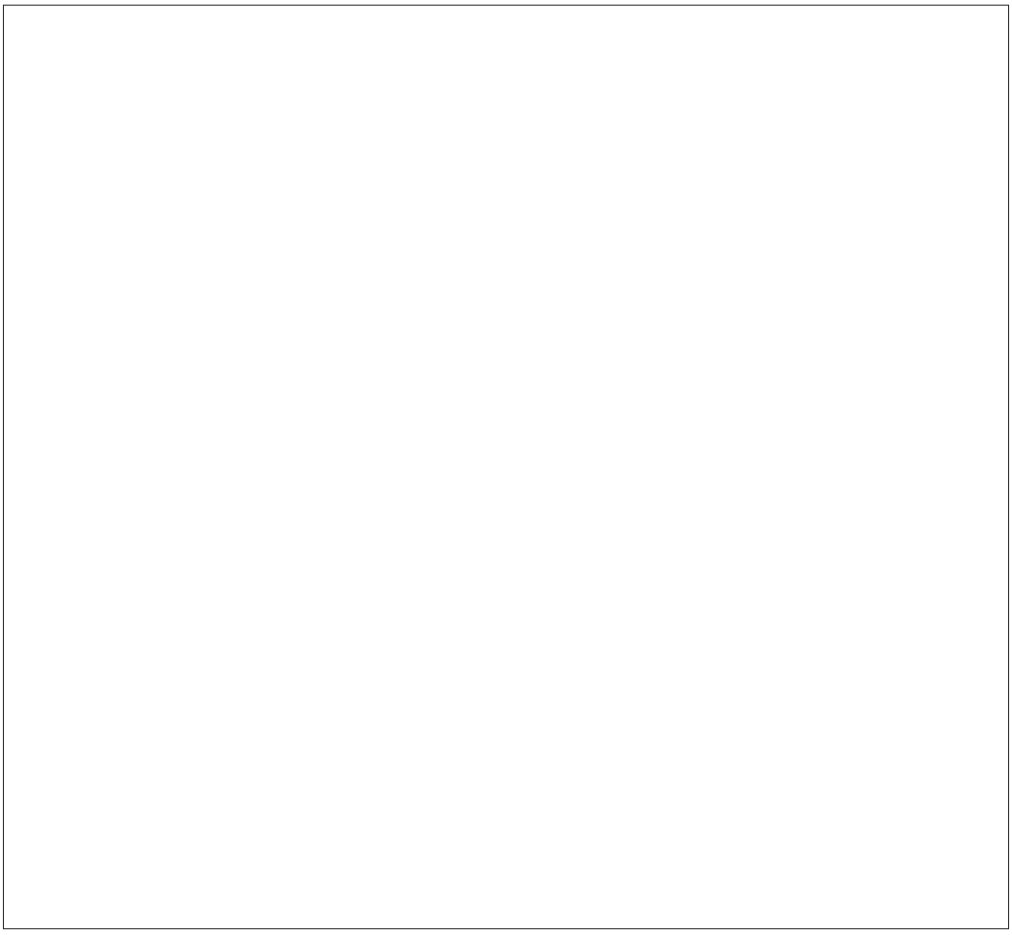

Figure 9.7 — Example of the SHMI reliability diagram (from Andersson, 1991).

$$PCC(i) = \sigma_{sr}(i) / \{\sigma_r \sigma_s(i)\} \quad (9.6)$$

where $PCC(i)$ represents the pattern cross-correlation coefficient for the ith translation of the precipitation object in question, $\sigma_r(i)$ is the standard deviation of rainfall rates or accumulations (R) in the object, and $\sigma_s(i)$, the standard deviation of Rs in an equivalent area in the second image, translated by the ith translation vector from the objects' centre of gravity. $\sigma_{sr}(i)$ is the co-variance of the object with its ith equivalent area in the second image, and is given by:

$$\sigma_{sr}(i) = \frac{1}{n} \sum_{x=1}^{n} \sum_{y=1}^{n} \{R_s(x + j_i, y + y_i) - R_s(j_i, k_i)\} \{R_r(x, y) - R_r\} \quad (9.7)$$

where n is the number of pixels in the precipitation object, x and y describe the location of object pixels in the first image, and j_i and k_i, the x and y components of the ith translation vector.

The procedure of this type used in the GANDOLF system (Collier, *et al*., 1995) may be summarized as follows:

(1) Read two, sequential images.
(2) Threshold the two images, such that pixels with precipitation rates (R_s) less than the threshold rate are set to a value of 0.0 mm hr^{-1}. This serves to delimit precipitation objects. A more complex procedure could be used, but is unlikely to be justified in terms of improved performance.
(3) Search for the maximum R in the image. This will be associated with one of the precipitation objects defined in (2).
(4) Generate a template for the object associated with the maximum R in (3). This template is an array of the same dimensions as the original radar image, but consisting only of ones (the object) and zeros.
(5) Find the centre of gravity of the object.
(6) Calculate an array of all potential translation vectors for the object. This is done by finding the coordinates of all pixels which lie within a semi-circle whose radius of curvature is

centred on the centre of gravity of the object. The size and orientation of this semi-circle are defined with respect to a representative, true motion vector for the object, as inferred by an appropriate steering level wind. The radius of the semi-circle is set as being equal to 1.5 times the distance moved by an object moving at the steering level wind speed. The orientation of the semi-circle is defined such that its vertices are at angles of -60 degrees and + 60 degrees to the steering level wind direction (input from independent data or mean movement from previous analyses).

(7) Calculate a pattern cross-correlation coefficient between the object in the first image and an equivalent, translated area in the second image. Repeat this for each translation vector derived in (6).
(8) From the array of pattern cross-correlation coefficients in (7) find the maximum realistic correlation coefficient, hence find the probable optimum translation vector for the object.
(9) Erase the object from the first radar image using the object template.
(10) Repeat steps (3) to (9) until all objects in the first image have been accounted for.
(11) Repeat steps (2) to (10) for a range of thresholds R_s.

9.3.3 Complex methods

The description of echoes using Fourier analysis techniques provides the locations of the edges and peaks in the harmonics, which may be matched at separate times to give echo displacement vectors (Muench, 1976). Similarly, analyses using other statistical echo distributions may also be used to match echoes.

These techniques often use all the intensity information within an object area to obtain a match. For example Duda and Blackmer (1972) and Blackmer, *et al*. (1973) minimize the following expression when searching for two matching echoes or echo areas:

$$\sum_x \sum_y \left[I_n(x,y) - I_o(x - x_d,\ y - y_d) \right]^2 \qquad (9.8)$$

where I_o (x,y) and $I_n(x,y)$ are the intensity integers in the old and new radar pictures, respectively. I_o $(x–x_d,\ y–y_d)$ corresponds to displacing the old echo x_d to the east and y_d to the north. Various modifications were made to this expression to cater for echoes moving into and out of the picture and to allow for occasional large errors by examining the sum of the magnitude of the errors. The latter modification provided the means of iterative echo matching so that merging and splitting could be allowed for. After matching cloud centroids, Wolf, *et al*. (1977) derived a measure of "goodness of fit" based upon an empirical formula relating statistics of the distribution of derived vector displacements to the intensity and size of cloud areas. This appears to work well for isolated cloud areas, but it is doubtful to what extent it would be effective for more uniform frontal cloud.

A different approach has been adopted in the Nimrod system in the United Kingdom (Golding, 1995). Here the vectors derived from cross-correlation and centroid matching are compared with the winds forecast by a mesoscale numerical weather prediction model. The optimum wind height (or heights) is selected and forecasts made. While this procedure works well when the model performs well it is necessary to revert to the observations only approaches when it does not although this situation does not occur very often.

Table 10.1
Storm types (after Dixon and Wiener, 1993)

Type	*Reflectivity threshold/dBz*
Individual convective cells	40–50
Convective storms	30–40
Mesoscale convective complexes	25–30
Snow bans	15–25

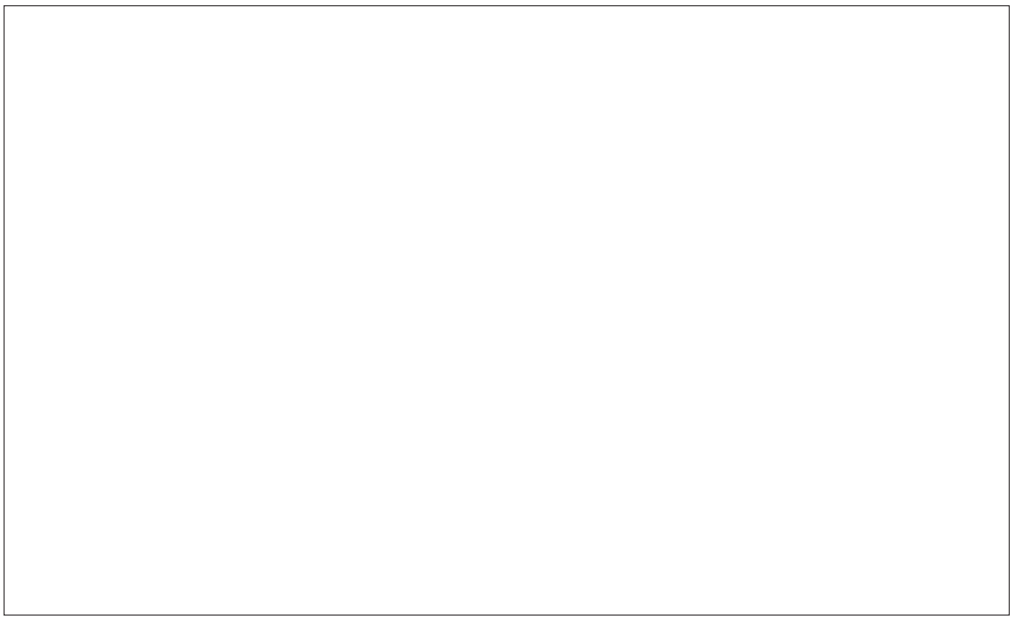

Figure 10.1 — The interrelationships between observer system within an expert system (from Campbell and Olson, 1987).

9.4 ALLOWING FOR PATTERN DEVELOPMENT

When echoes have been identified, and their displacement vectors deduced, then a quantitative forecast based purely on extrapolation may be made. Unfortunately, echo areas change their size, intensity, speed and direction of movement on timescales from hours to as short as a few minutes, depending upon the synoptic situation and the local orography.

Wilson (1966) and Austin and Bellon (1974) have indicated how the maximum cross-correlation coefficient, derived by comparing objective forecasts based purely on extrapolation with their corresponding actual patterns, decreases with time for compact storms, scattered echo and squall lines. They suggest that useful forecasts may only be made for in excess of 30 minutes ahead when radar echoes (or cloud objects) are well defined and their movement is uniform. Hill, *et al*. (1977) and others have demonstrated that extrapolation forecasts up to 6 hours ahead can be made for frontal rainfall, and Hill and Browning (1979) have shown that individual echoes (with dimensions of the order of tens of kilometres) associated with weak convection aloft could be tracked for several hours within the warm sectors of depressions. This variability has been quantified by Zawadzki, *et al*. (1994) who computed the following regression relationship between the decorrelation time to 0.5, T_L, convectively-available potential energy (CAPE) and helicity (H_r):

$$T_L = 114 - 1.3\left(\frac{CAPE}{H_r}\right) \tag{9.9}$$

This relationship has a correlation coefficient of $r = 0.92$ and a significant level better than 5 per cent. An increase in the ratio of convection energy to shear energy leads to a decrease in the precipitating cell's longevity.

By moving the echo contours individually, instead of the whole echo, changes of the echo shape can be forecasted. This principle, however, is purely formal. Such techniques have been developed by Kavvas and Chen (1989), Heideman, *et al*. (1990), Foufoula-Georgiou and Kumar (1990) and Bianco and Huang (1990). A verification of those methods (Ruggiero, *et al*., 1991) showed no apparent improvement over moving the unchanged echo field. In a study using various schemes to extrapolate the evolution of radar echoes over the tropical Atlantic, Tsonis and Austin (1981) also found at best only minor improvements over simple extrapolation. Many schemes gave even worse results. The physical processes causing echo changes are probably not observable in the past history of an echo. Simple orographic effects can be invoked in the FRONTIERS system (Brown, *et al*., 1991). To get a real improvement, and also to make somewhat longer forecasts possible, use must be made of information from conceptual meso- or microscale models (Wright and Golding, 1990; Collier, 1991).

9.5 OPERATIONAL ACCURACY ACHIEVED

It is difficult to assess objectively the relative performance of the several different methods of extrapolating echo movement, as most of the techniques claim to be successful in a limited sense and have been used in different weather situations. However, Elvander (1976) (see also Alaka, *et al*., 1977) has described a series of experiments using the following three different techniques:

Model A: A cross-correlation technique similar to that used by Austin and Bellon (1974) and referred to by Elvander (1976) as the Canadian model;

Model B: A technique involving the tracking of individual echoes using a linear least-squares extrapolation of the motion of the echo centroid as described by Barclay and Wilk (1970) and Wilk and Gray (1970) and referred to by Elvander (1976) as the National Severe Storms Laboratory model;

Model C: A technique involving the tracking of individual echoes by considering the entire echo complex and some measurements related to individual echoes as described by Duda and Blackmer (1972) and refined by Blackmer, *et al*. (1973). This technique was referred to by Elvander (1976) as the Stanford Research Institute model.

It was concluded by Elvander (1976) that the simple cross-correlation model was most effective when used with zero-tilt (that is low-altitude) reflectivity data, but the linear least-squares interpolation of echo centroids was the most effective method when the data on the vertically-integrated liquid (VIL) water content were used. The data used in the experiments were representative only of convective rainfall; no stratiform rainfall cases were considered.

The conclusions of Elvander (1976) were based upon forecasts up to 90 min ahead, using instantaneous pictures at both 10 min and 30 min intervals. Forecasts made using input data at 10-min intervals were usually about 20–30 per cent more accurate than forecasts made using data at 30 min intervals for models B and C. The increase in accuracy for model A using the more frequent data was about 10–20 per cent. However, the differences between all three techniques were generally small for forecasts using data at 10-min intervals, and the cross-correlation technique was significantly better only using zero-tilt reflectivity data when the data were input at 30-min intervals.

No assessment of the three models specified above has been carried out using radar echo data obtained from observations of stratiform rainfall. Hill, *et al*. (1977) have demonstrated that a version of model A does provide quite successful forecasts up to six hours ahead for one case of frontal rainfall using data smoothed over a grid length of 20 km. However, both Browning, *et al*. (1974) and Hill and Browning (1979) have presented data showing significant differential motion of mesoscale precipitation areas within frontal systems which model A is not suited to coping with. More recently Ciccione and Pircher (1984), using a sample of 15 frontal events, found that forecasts using cross-correlation performed better than forecasts using their version of echo tracking.

The improvement that can be achieved using subjective techniques has been examined by Browning, *et al*. (1982), who compared forecasts for a 400 km^2 area made using data from four radars in the United Kingdom. The forecasts derived during a total of 29 frontal events between November 1979 and June 1980 were prepared using both a totally objective echo centroid technique (Collier, 1981) and subjective linear extrapolation. Figure 9.6 shows the percentage error, regard-

less of sign in the forecast hourly rainfall for the 400 km^2 area centred on Malvern (located in the middle of the radar network), plotted as a function of lead time. Various errors in the forecasts were identified, as discussed above and partially corrected such that the subjective forecasts were considerably better than the objective forecasts. However, comparable data for totally objective cross-correlation forecasts up to three hours ahead assessed by Bellon and Austin (1984) are also plotted on Figure 9.6 and show that objective procedures may approach the performance of subjective techniques.

Bellon and Austin (1984) (see also Austin and Bellon 1982) used data recorded in the Montreal (Canada) area during the summers of 1978–1981. Although Bellon and Austin point out that summer convection in the study area is often caused by the passage of large-scale low-pressure centres, or of frontal systems steered by a strong jet stream, there are likely to be significant differences between their data and that used by Browning, *et al*. (1982). Many of the United Kingdom rainfall data were influenced by low bright-band effects and the rainfall was of limited vertical extent. Indeed, the radar composite images used in the study provided data mostly below 3 km elevation (Browning, *et al*., 1982) and yet were still subject to considerable errors due to the beam overshooting the precipitation and other measurement problems (Tables 9.2 and 9.3). Such errors were less important in the Montreal data as evidenced by the use of constant altitude plan position indicator (CAPPI) data at an altitude of 3 km. This difference may explain why the objective procedure of Bellon and Austin (1984) performed almost as well as the subjective procedure recorded by Browning, *et al*. (1982).

The performance of the FRONTIERS operational forecasting procedures and existing rainfall forecasts have recently been analysed by Brown, *et al*. (1994). Forecast accumulations were evaluated by comparison with raingauge data in two regions of the United Kingdom. The operational forecasts were significant over-estimates (average bias +250 per cent) but were issued more reliably than were the FRONTIERS forecasts, which were much closer to ground truth for the same cases (average bias –29 per cent). Comparison with a dense gauge network in south-east England shows that the accuracy of the forecasts increases with increasing accumulation period and river catchment size.

While most work to date has used categorized forecasts, giving expected rain amount, some investigators have considered probability forecasts.

A probabilistic model for radar forecasts of rain was developed by Zuckerberg (1976). However, building upon the Poisson distribution, it only gives the probability of rain/no rain. A model by Andersson (1991) gives probabilities for different rain amounts. The latest available 850 hPa wind from the high resolution limited area model (HIRLAM) (Kållberg, 1989) is used to steer the echoes. The 850 hPa wind is chosen since rain cells over Sweden generally move with that wind (Wickerts, 1982).

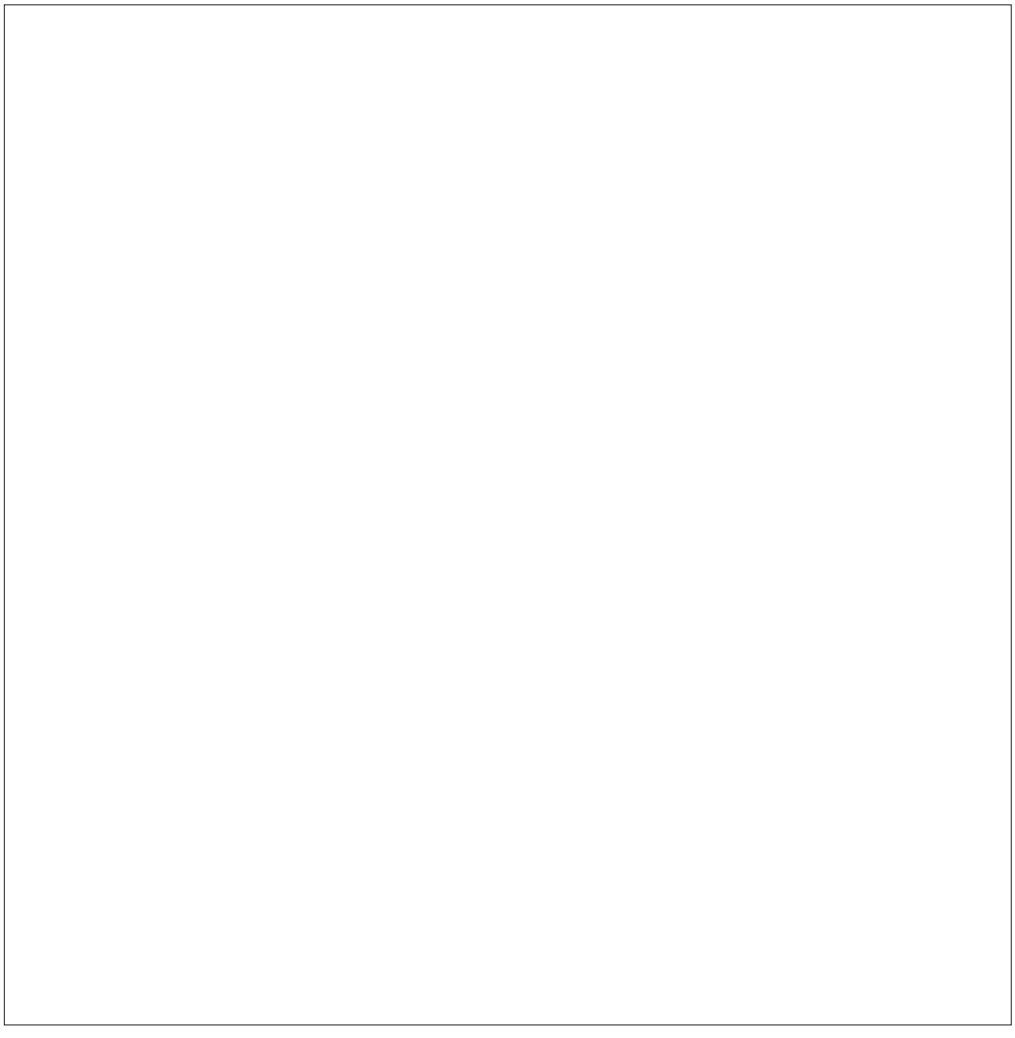

Figure 10.2 — Cell stages identified at 1000 UTC 12/8/93 from Hameldon radar, United Kingdom
+ = d cel; * = m;
triangle = M;
diamond = E; and
square = D.

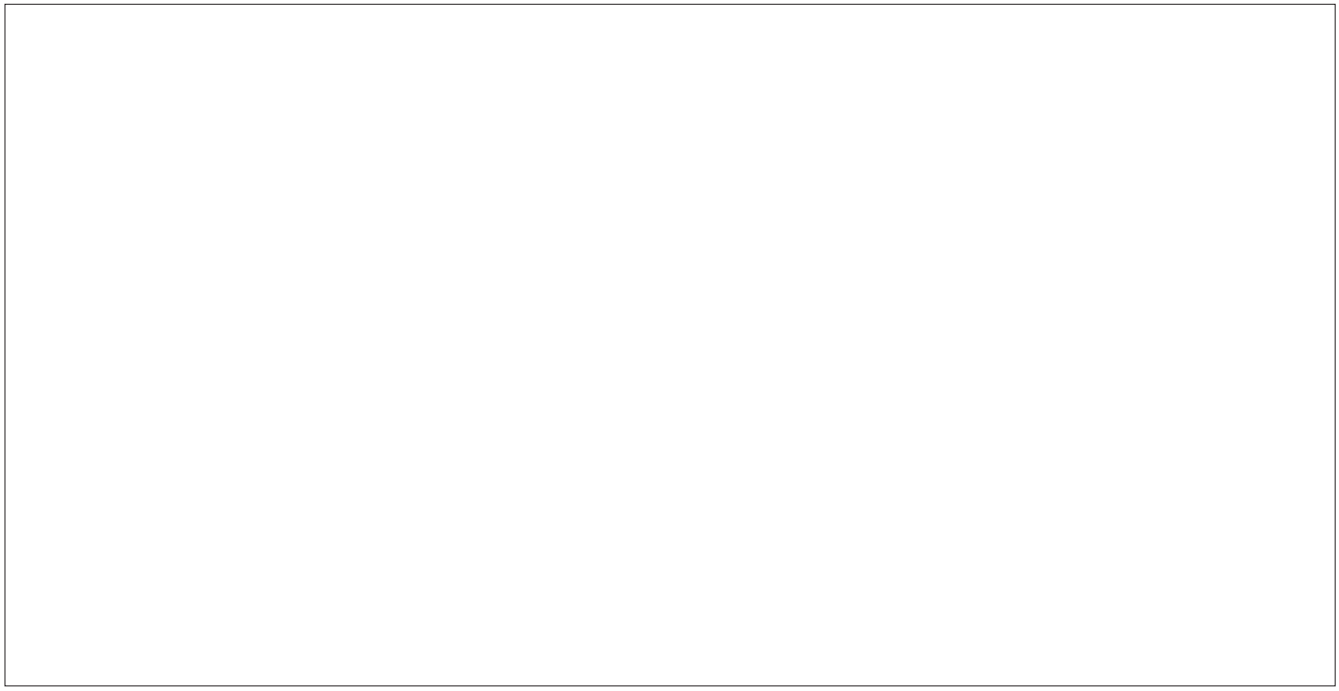

Figure 10.3 — (*a*) A multilayer network. The information coming to the input units is recoded into an internal representation and the outputs are generated by the internal representation rather than by the original pattern. Input patterns can always be encoded, if there are enough hidden units, in a form so that the appropriate output pattern can be generated from any input pattern (from Rumelhart, *et al*., 1986); (*b*) A single unit u_i, with inputs y_i, adjustable weights w_{ij} (from input y_i) and threshold weight θ_j (from Sutton, 1989*b*).

A source area upwind of the forecast target area is selected. With a wind speed *ff*, a distance *ff** (forecast time duration) passes over the forecast spot during the forecast. This distance is used as length for a line giving the middle of the source area. The width of the source area is 20 km (it is possible to select this) and it begins with a triangle having its apex at the forecast target area. The idea is that, though the pixels change their reflectivities before reaching the forecast location, the distribution of reflectivities should remain fairly constant. Each pixel within the source area is therefore assumed to have the same probability of hitting the forecast target area.

If a single probability forecast can be verified, the result tells us even less of the performance of our method than in the case of categorical forecasts. For verification, the probability forecasts need a larger set of forecasts than the categorical ones. The Swedish forecasts have been verified using a skill score which is a function of the Brier score, BS:

$$BS = \sum \left(P_r - Obs\right)^2 / N \qquad (9.10)$$

where P_r is the probability given by the forecast (0 to 1); *Obs* is the outcome of the event (1 if the event occurred and 0 if it did not); *N* is the number of events. The skill score used was:

$$\text{SKILL} = 100 \times (1\text{-}\text{BS}_{\text{TEST FOREC}}/\text{BS}_{\text{REFERENCE FOREC}}) \qquad (9.11)$$

The assessment results are presented on reliability diagrams as shown in Figure 9.7.

In summary, it must be stressed that the performance of any extrapolation procedure will depend upon the type of precipitation being forecast. Useful forecasts for several hours ahead can be achieved in frontal rainfall, but forecasting convection is problematic and other techniques discussed in the following chapters need to be used in conjunction with extrapolation for this type of precipitation system. It is necessary to calculate continually parameters such as T_L (equation 9.9) to assess the likely reliability of forecasts.

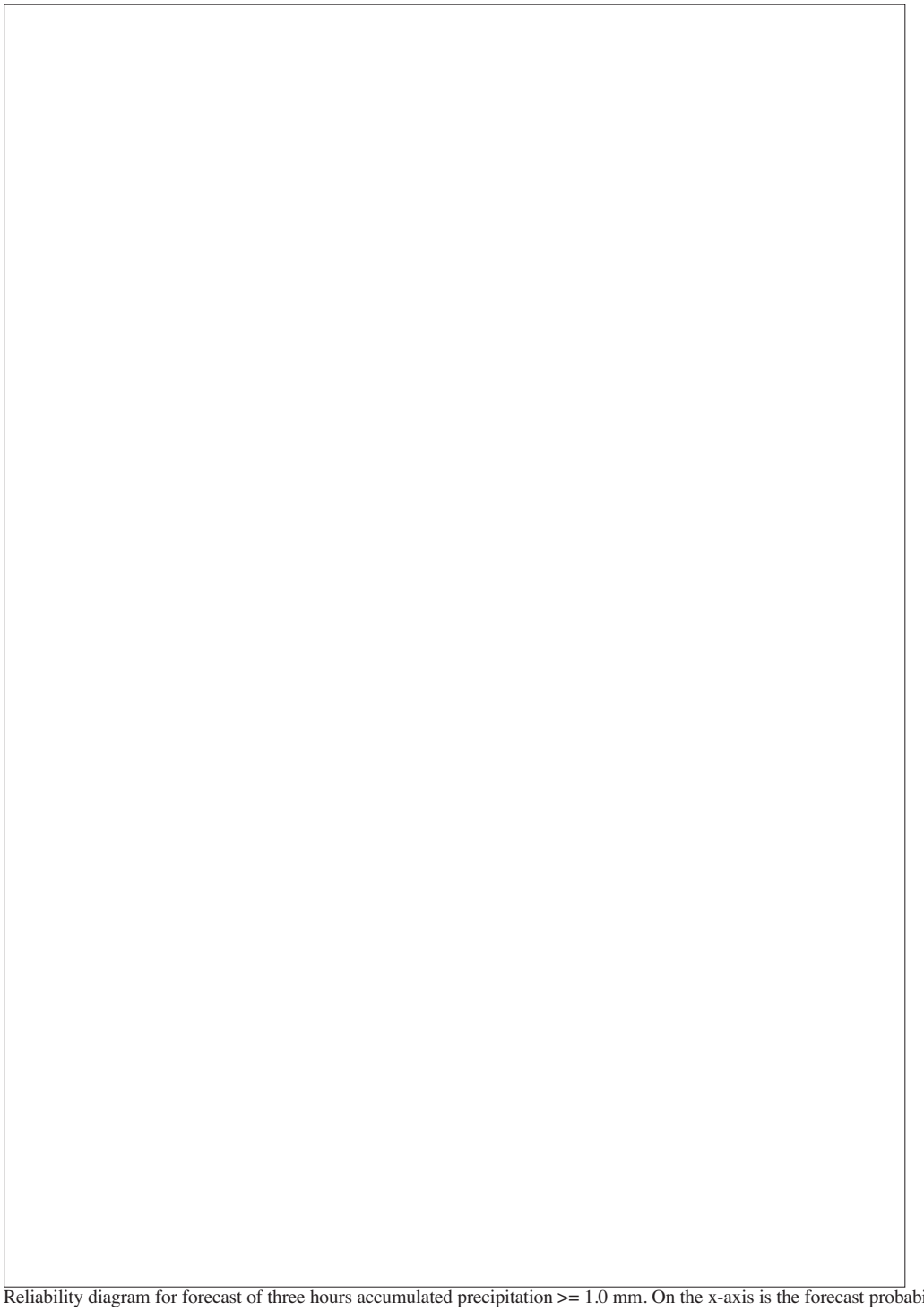

Figure 10.4 — Plots of CSI for the object-oriented forecasts (solid) and FRONTIERS forecasts (dashed) using FRONTIERS radar actuals as truth. The CSI was calculated for all rainfall rates greater than 1/32nd mm hr^{-1}. The results from nine data times from 1600 to 2000 UTC at half-hourly intervals are plotted. The top plot shows T+3 scores, the middle T+2 and the bottom plot T+1 (from Collier, *et al.,* 1995).

Reliability diagram for forecast of three hours accumulated precipitation >= 1.0 mm. On the x-axis is the forecast probability, on the y-axis the observed frequency of hits. Figures in the diagram give the number of cases. For instance, there were 59 forecasts giving the probability 0.9 (90 per cent) of precipitation >= 1.0 mm. For 79 per cent (46 cases) of these 59 forecasts precipitation >=1.0 mm were observed by a conventional gauge at the forecast spot. The reference forecast gives a frequency of 0.097, i.e. the sample mean frequency. Good forecasts are not only characterized by observations close to the 45° line, but also and mainly by having many forecasts far away from the reference forecast. The skill, in this case 53 per cent, is the skill relative to a climatological forecast, which has skill = 0.

The Norrköping Doppler weather radar, October–November 1992. The forecast spot was about 200 m from the atenna.

CHAPTER 10

ARTIFICIAL INTELLIGENCE

Much of what was described in Chapter 9 can be categorized as the application of primitive artificial intelligence techniques to short-period forecasting. Pattern recognition algorithms have been used to diagnose radar echo motion and severe weather has been inferred from radar databases. These techniques have levels of success which may be enhanced by blending data from different sources. In practice, how this is done will depend upon the meteorological phenomenon being forecast and how the observing systems contribute to this application.

Humans are particularly adept at using their experience to associate apparently unrelated pieces of information in ways which enhance their appreciation of a situation. However, this often leads to a lack of reproducibility in weather-forecasting procedures with a concomitant unreliability of forecast products. An attempt to reproduce human logic patterns is to establish a decision tree which considers aspects of an observational database and, based upon the logical outcome of a series of questions, leads to the prediction of a weather event. Colquhoun (1987) describes a method of forecasting the severe weather associated with thunderstorms based upon a decision tree. It is suggested that such procedures could be incorporated into computer-based interactive analysis systems, such as outlined in WMO (1983), which may use Doppler radar data. Given an adequate observational database, it is a small step to attempt to use a computer to implement the decision tree automatically, as described by Elio, *et al*. (1987). This then becomes one form of knowledge-based expert system. Dixon and Wiener (1993) describe the TITAN system which seeks to recognize particular types of storm defined as contiguous regions exceeding thresholds for radar reflectivity and size (Table 10.1). This is a very simple form of knowledge-based system.

10.1 EXPERT SYSTEMS

A different use of artificial intelligence is to attempt to analyse meteorological situations in ways which would not be possible otherwise. For example Campbell and Olson (1987) extract significant features from Doppler radar data in a manner, and within a time, not possible for a human forecaster. This involves a careful blend of software representing observer system and an expert system in the way shown in Figure 10.1. Here the working memory contains a set of facts which represent symbolically the contents of the radar and feature databases. The inference engine performs the task of matching these facts to the condition part of production rules and instigates tests of any matches with the radar image-processing element. The production rules contain knowledge of the weather phenomena and radar artifacts which the system can recognize in addition to how the phenomena relate to radar image features and their evolution (see for example Waterman, 1986).

McArthur, *et al*. (1987) adopt this approach in developing a scenario-driven automatic pattern recognition procedure. A scenario is defined as a "multidimensional hypothesis that describes the expected patterns of a change in various weather systems across a varying number of meteorological data streams or sets". This approach is almost, although not quite, an expert system. However, Stewart, *et al*. (1989) go further in developing a hail forecasting system. It was found that forecasts made by meteorologists were closely approximated by the expert system. The conclusion drawn was that the intuitive processes that weather forecasters use to aggregate information into a forecast can be analysed and described in this way.

Most of the work so far has concentrated on severe weather phenomena, tornadoes, microburts and gust fronts (Zubrick and Riese, 1985; Elio and de Haan, 1985). While there is a view that these systems will underpin operational forecasting in the future (Bullock and Heckman, 1986), it will be important to blend the expert system approach with more conventional extrapolation techniques in a way which results in definition of both movement and development. Of particular importance will be the mix of mesoscale numerical model output, such as the divergence field, and the image fields.

10.2 THE OBJECT-ORIENTED APPROACH

Object-oriented programming (see for example Winston, 1984) describes an application domain as a population of objects of various sorts. These are often physical objects from the real world but may also be abstract concepts. Objects are collections of attributes (properties of the object and its current state, such as temperature, size, velocity, etc.,) and methods (processes that define and implement all the things that are allowed to happen to that object).

A class is a template for a particular kind of object. All the objects in a class have the same list of attributes. Individual objects are instances of the class and differ from one another in values assigned to their attributes. In particular each object (instance) has a unique identifier or name. Objects have lifetimes — they may be created and destroyed during the execution of the program.

This approach differs from conventional structured programming where the emphasis is usually either on processes or on data but without a tight, ownership relation between these and specific real-world entities. In object-oriented programming, processes and data are not public property, but are encapsulated within individual objects.

Encapsulation renders the contents of an object (attributes and methods) inaccessible to the outside world except through pre-defined transactions. Objects communicate with each other via messages. The messages that an object-class may send or receive are pre-defined and a class has at least one method associated with each allowed message. Messages may seek to alter the values of attributes or to elicit information about them. However, changes to the object are

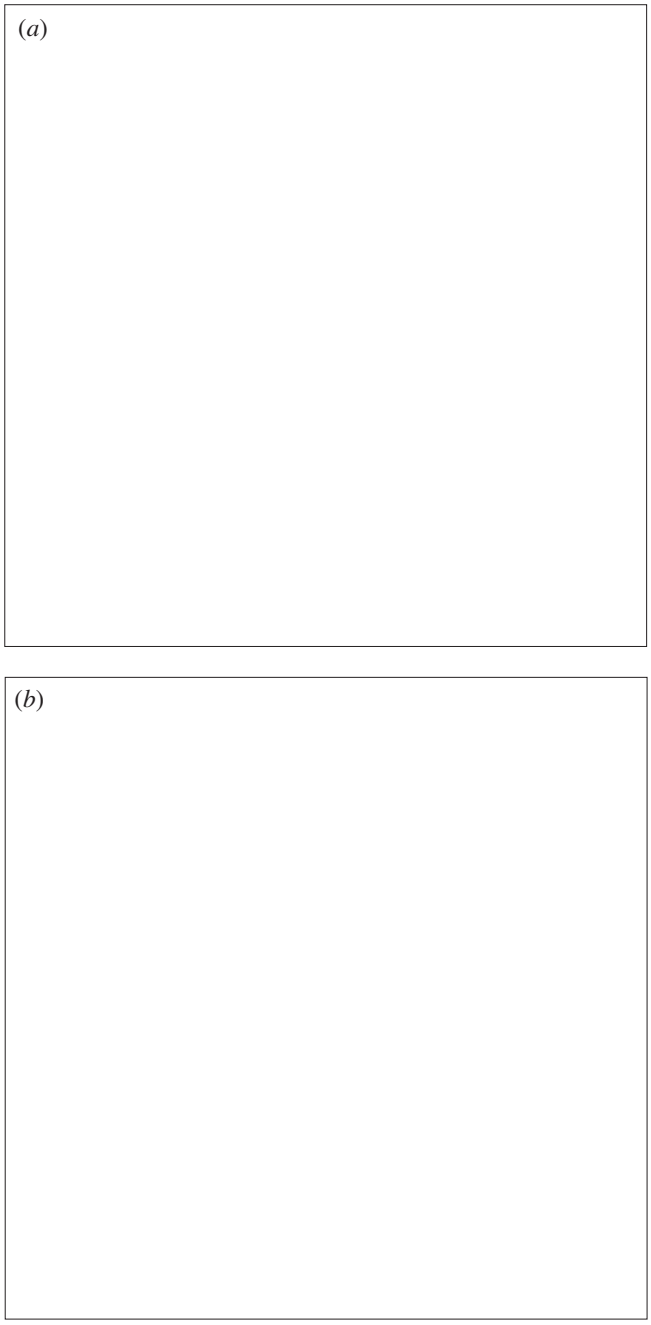

Figure 11.1 — (*a*) Model excluding lee drying and hydrometeor drift; (*b*) Model with lee drying and hydrometeor drift; (*c*) Actual rainfall 00Z 7 March 1988, Gisborne region, New Zealand (after Sinclair, 1994).

effected exclusively by the internal methods of that object in response to a message — external processes cannot directly access or change an object's attributes.

This technique was first developed in meteorology for use in the design and implementation of meteorological workstations (Cooper and Smiley, 1990), but has recently been employed to forecast the development of convection using radar, satellite, sferics (lightning flashes) and mesoscale model data by Hand and Conway (1995). The latter attribute the class of convective cell objects as follows:

1. ident — This attribute identifies the object throughout its lifetime and incorporates the time and place of its creations. Its value, once set, remains fixed throughout the life of the cell.
2. stage — Stage of development of the cell (d, m, M, E or D defined below).
3. location — Current cell cloud base centroid location.
4. age — Age of the cell (seconds).
5. size — Radius of cell base area (metres).
6. top — Cell cloud top height (metres).
7. ctt — Cell cloud top temperature (°C).
8. velocity — Components of cell horizontal velocity (u, v) in metres per second.
9. ppn rate — Cell precipitation rate containing information on average, maximum and minimum rates within cell (mm h^{-1}).
10. ppn type — Phase of precipitation reaching ground (rain, hail or snow).
11. flashes — Lightning frequency (flashes per minute).
12. potential — Expected development of cell:
    - –1 = Unknown (this is default for d' cells);
    - 0 = Weaker developer, will quickly reach dissipating stage;
    - 1 = Moderate developer, will initiate further moderate development and then dissipate;

Figure 11.2 — Possible maximum intensity of rainfall as a function of updraft wind velocity and the temperature at the ground surface (from Yamada, *et al.,* 1993).

2 = Strong developer, will give heavy precipitation, perhaps lightning, and initiate new strongly developing cell;
3 = Cell which is about to initiate a daughter cell;
4 = A cell which has already initiated new cells.

13. ppn ratep Precipitation rate of parent cell (if applicable).

A number of messages may be sent to objects in this class.

Instantiation is the process of creating new instances of objects, in this case convective cells. Values for all the attributes are set initially to their default values corresponding to the analysed cell stages and are then adjusted using mesoscale model and satellite data.

This system is being developed for real-time use as the core of the GANDOLF system described by Collier, *et al*. (1995). The following cell stage classification is used:

d Large towering Cumulus or Cumulonimbus without anvil Cirrus which is producing precipitation but which evaporates before reaching the ground.
m Young and growing Cumulonimbus cloud which is giving precipitation at the ground.
M Fully mature Cumulonimbus cloud with pronounced Cirrus anvil and well developed updrafts and downdrafts. Often giving heavy (> 10 mm hr^{-1}) precipitation at the surface.
E Weakening Cumulonimbus cloud or less intense cell giving mainly moderate precipitation at the surface (2–10 mm hr^{-1}).
D Cell in a dissipating stage with downdrafts eventually predominating throughout the cloud giving mainly light precipitation at the surface.

Four meteorologically important layers (ground to cloud base, cloud base to freezing level, freezing level to –10°C level, above –10°C level) are examined, using principally radar data, in order to diagnose which of these cell stages is applicable at a given time, as shown in Figure 10.2. A forecast may then be made based upon the cell lifetime defined in

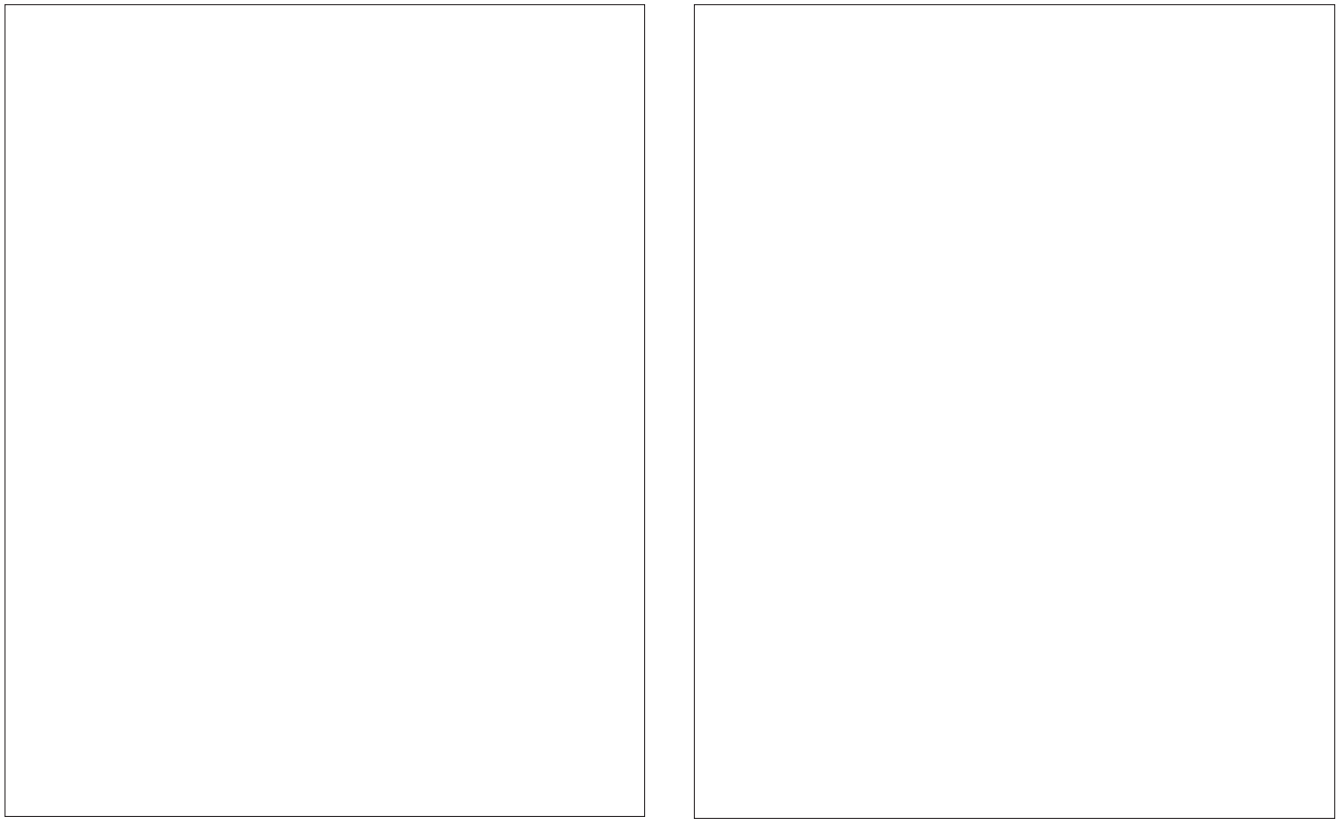

Figure 11.3 — Mesoscale model forecast of rainfall October to December 1993 compared with raingauge data (courtesy of the Meteorological Office, United Kingdom).

terms of the cell stages. This system is currently being tested, but early results outlined in section 10.4, are encouraging.

10.3 NEURAL NETWORKS

For many years behavioural scientists have attempted to reflect the logical reasoning of the human brain by developing "neural networks", networks of processors which represent neurons or nerve cells. Associative memory (the ability of apparently trivial facts to trigger a long train of detailed memories), pattern recognition, learning by example and tolerance of noisy (inexact) data are all possible with artificial neural networks. The application in meteorology is comparatively recent (Bowen, 1989; Sutton, 1989*a*), and as yet it is not clear to what extent such an approach will produce improvements over more conventional image processing.

The most common design of network has three layers with each neuron linked to those in adjacent layers. Those in the two layers are also linked to inputs and outputs. Software adjusts the strength of each link as the network learns the particular task it is asked to do. It recognizes particular patterns of inputs and produces consistent outputs in response. One way of doing this is known as "backpropagation", which is a pattern recognition technique for teaching an objective procedure how to deal with the future behaviour of particular meteorological situations or precipitation types (Rumelhart, *et al.,* 1986; Sutton, 1989*b*). Figure 10.3 illustrates the linkages in such a procedure. The approach certainly offers a new way of continuously teaching software systems the essential elements of the experience acquired by human forecasters. Whether or not the results will outperform an expert system remains an open question.

However, neural computing offers the following benefits:

(*a*) Ability to tackle new kinds of problems: Neural networks are particularly effective at solving problems whose solutions are difficult, if not impossible to define;

(*b*) Robustness: Neural networks tend to be more robust than their conventional counterparts. They have the ability to cope well with incompletor "fuzzy" data and can deal with previously unspecified or unencountered situations. Neural networks are particularly effective at solving problems whose solutions are difficult, if not impossible to define;

(*c*) Fast processing speed: Neural networks can potentially operate at considerable speed;

(*d*) Flexibility and ease of maintenance: Neural networks are very flexible in the way in which they are able to adapt their behaviour to new and changing environments. They are also easier to maintain, with some having the ability to learn from experience in order to improve their own performance.

In spite of these benefits it is important to note that neural nets have not yet been tested over a long period, although Peak and Tag (1994) have demonstrated the use of a neural net for the segmentation of cloud imagery, and McCann (1992) outlines the use of a neural network to forecast significant thunderstorms at the National Severe Storms Forecast Center, United States.

10.4 ASSESSMENT OF CURRENT PERFORMANCE

A comparative study of artificial intelligence (AI) systems was first proposed at the Second Workshop on AI Research in Environmental Science (AIRIES) in 1987. As a consequence an exploratory study of the efficacy of AI systems in the weather forecasting process, known as SHOOTOUT-89, was specified (Roberts, *et al.,* 1990). The following systems were tested:

(*a*) Knowledge augmented severe storms predictor (KASSPr), Canada — traditional expert system;

(*b*) GOPAD, United States — uses multiple discriminant analysis to make forecasts by analogy;

(*c*) GONVEX, United States — rule-based production system using backward-chaining interencing;

(*d*) Additive linear prediction system (ALPS), United States — judgement analysis;

(*e*) WILLARD, United States — structured hierarchy, expert system;

(*f*) Objective convective index (OCI), United States — indices of severe weather potential;

(*g*) Severe weather intelligent forecast terminal (SWIFT), Canada — early expert system.

Due to various difficulties SWIFT was not tested, but McLeod, *et al*. (1990) report the results of independent tests in Canada. They found that SWIFT has comparable skill to the human forecaster over its domain. Tests during SHOOTOUT 89 suggested that KASSPr exhibits more skill than the operational forecaster. It is clear from these experiments that expert systems can perform for severe weather warnings at a level which is operationally acceptable. However, they have not yet been used to forecast quantitative precipitation amounts.

Initial tests of the object oriented scheme in the GANDOLF system for a rapidly developing mesoscale convective system (MCS) are shown in Figure 10.4. The figure shows plots of Critical Success Index (CSI) for the object-oriented forecasts, and those produced by the FRONTIERS system (linear extrapolation of radar echoes using mesoscale model winds). The object-oriented forecasts are considerably better lead times beyond two hours ahead than the model extrapolation forecasts during the period when the MCS undergoes rapid development from about 1900 UTC. Note that the larger the value of CSI the better the forecast. While such analysis is encouraging, it is clear that any one system will not perform reliably on all occasions. There is a need to develop procedures for selecting which forecast will perform well in particular weather situations. Indeed, McCann (1992) concludes that neural networks are nothing more than pattern recognition diagnostic techniques with some short-term predictive skill.

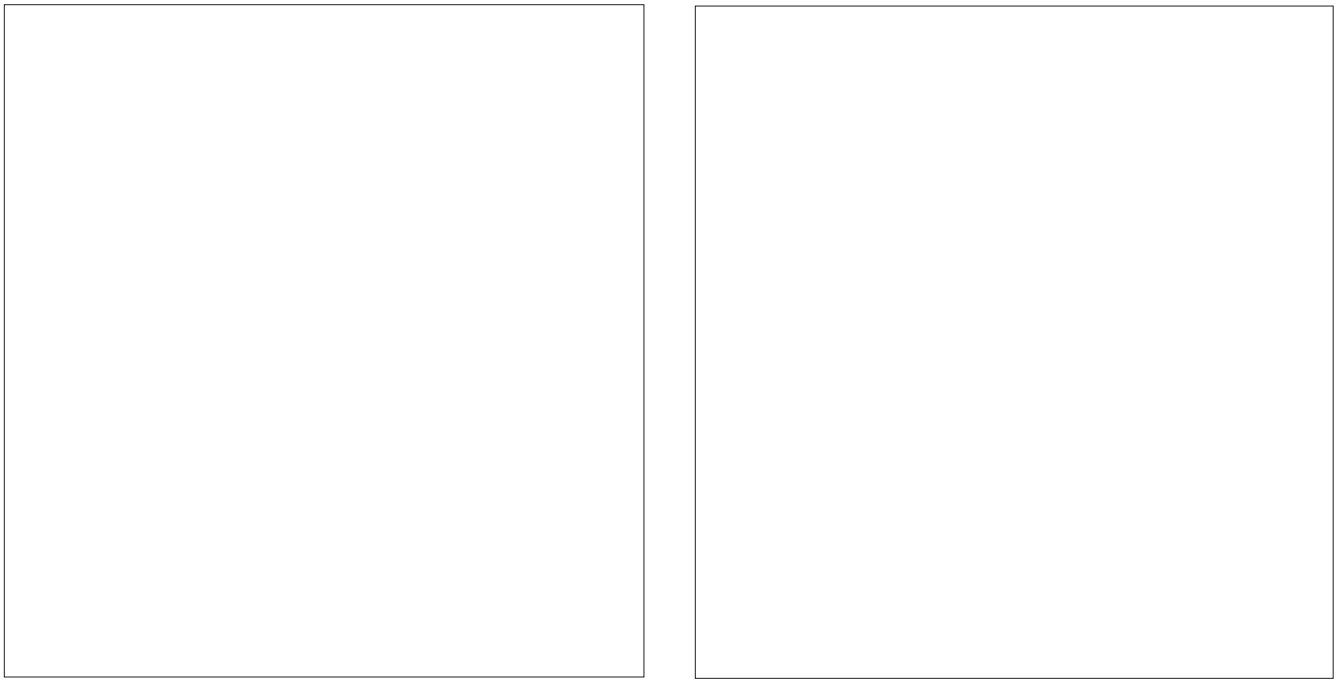

Figure 11.4 — Total model rainfall fields at 24h using (*a*) no bogus data (i.e. no artificial data inserted normally) and (*b*) not including mesoscale outflow data conditions. The rainfall is contoured every 1 cm (from Strensrud and Fritsch, 1994).

CHAPTER 11

HYDROMETEOROLOGICAL AND MESOSCALE NUMERICAL MODELLING

11.1 FORMULATION OF MODELS

Georgakakos and Lee (1987) classify numerical models used for precipitation forecasting as statistical, dynamical and statistical-dynamical models. They argue that current computer and sensor technology and networks do not allow precipitation forecasting in an operational environment for scales relevant to floods and flash floods (down to 100 km^2 in space and to one hour in time). They recommend (see also Georgakakos and Hudlow, 1984) that a viable approach at present is to use simplified parametrizations at scales relevant to hydrologic forecasting accompanied by statistical techniques. At present this approach offers the most reliable forecasts of rainfall, although the use of mesoscale data sources such as radar networks now offer the opportunity to explore the potential of the numerical prediction of thunderstorms (Lilly, 1990).

11.1.1 Statistical models

The space-time structure of rainfall has been investigated using a very wide range of statistical techniques with both raingauge and radar data (Crane, 1990). Models which view the rain process as being organized by two-dimensional turbulence in the atmospheric operating on scales about or larger than five kilometres have prompted further studies aimed at characterizing this variability using multifractial analysis (Lovejoy and Schertzer, 1990).

The development of predictive statistical models has led to the capability to make very short period forecasts of rainfall amount (see for example Krajewski and Georgakakos, 1985; Rodriguez-Iturbe and Eagleson, 1987; Cox and Isham, 1988; for a review see Georgakakos and Kavvas, 1987). Some of these models reproduce the general mesoscale and synoptic-scale features of mid-latitude rainfall as depicted by ground-based radar (Kavvas and Herd, 1985).

11.1.2 Dynamical models

The simplest type of dynamical model is based upon the estimation of topographically-forced vertical motion (Collier, 1975, 1977). Further sophistication may be introduced by incorporating cloud physics (Bader and Roach, 1977; Bell, 1978; Sinclair, 1994). Using large scale numerical model forecasts to provide the input parameters, these simple models may produce forecasts with considerable skill as shown in Figure 11.1. However, they are only capable of forecasting orographically-enhanced precipitation, although simple representations in one dimension of the parcel theory of convection can also produce orders of magnitude estimates of convective rainfall (Figure 11.2).

More complex one-dimensional models, incorporating cloud entrainment and mixing (Curié and Janc, 1993) are useful for forecasting cloud-top height and precipitation, and can be used operationally, particularly if they form part of convective parametrization schemes used in more complex models. However, they are not able to simulate realistically the convective dynamics in the presence of shearing winds.

Two-dimensional models, which are time-dependent, are able to forecast convective development (see for example Kopp and Orville, 1994). However, these models operate over limited domains and require powerful computing facilitates. Also they are found to be very dependent upon the initial conditions, particularly moisture availability, used in simulations. At present, their use is confined largely to use as diagnostic tools.

To capture fully small-scale weather systems, and hence produce reliable precipitation forecasts, it is necessary to

Figure 12.1 — The relationship between different configurations of the unified model.

employ four-dimensional models having fine spatial (10 km) and temporal (three hours) resolution, and comprehensive representations of physical processes. It was not until computer technology was able to cope with integrations of the approximate equations in the early 1970s, that mesoscale numerical models were developed (Tapp and White, 1976; Pielke, 1981).

During the 1970s a number of experiments were reported which demonstrated that mesoscale models could be expected to give good forecasts in situations in which local weather is determined as a locally-forced response to large-scale meteorology or to orography (see for example Carpenter, 1979, 1982). The results of these experiments allowed the parametrization of physical processes to be refined and the simulation of further weather phenomena to be successfully carried out (see for example Fritsch and Chappell, 1980).

In the United Kingdom, this work culminated in an operational trial of the mesoscale model from October 1984 to January 1986 (Golding, 1990). After further improvements the model was introduced on a semi-operational basis being used also for a number of detailed case studies (see for example Sanderson, *et al.,* 1990).

The present United Kingdom mesoscale model became operational in 1992, and is discussed further in what follows where we outline the structure of this type of model. The current Met Office mesoscale model is embodied within a software system referred to as the unified model which has been described by Cullen (1993). The structure of this system, highlighting the physical parametrization of particular relevance to hydrometeorological studies and noting some of the improvements planned for the near future, is as follows:

The equations used are an approximation to the atmospheric equations of motion. The integration scheme uses a quasi-hydrostatic form of the equations of motion, and a split-explicit time integration scheme, which is very efficient in the use of computer time. The quasi-hydrostatic approximation is suitable for use in models with a horizontal resolution of 5 km or greater. However, a fully non-hydrostatic version of the integration scheme is now under development which will allow the accurate modelling of much finer spatial scales.

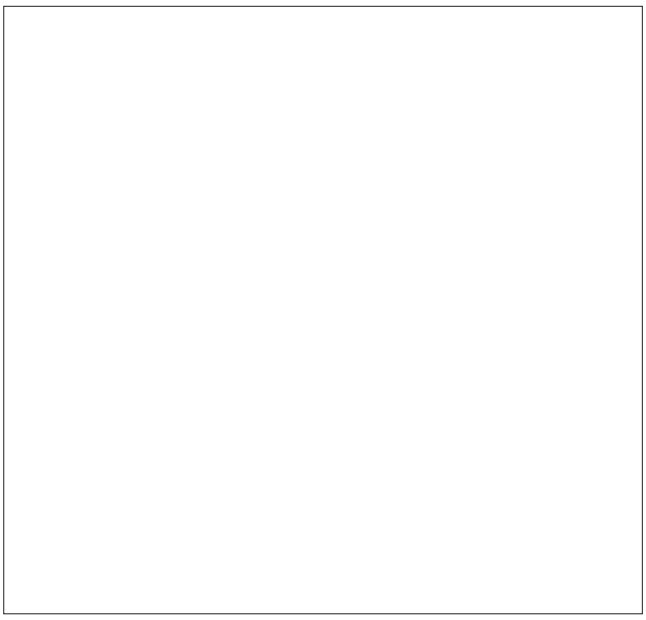

Figure 12.2 — Unified model eta (η) levels.

The equations are integrated in spherical polar coordinates, using a "hybrid" vertical coordinate. This is a function of pressure, equal to unity at the lower boundary, and equal to a multiple of pressure at the upper levels. It is chosen because terrain-following coordinate surfaces are much more convenient in the lower layers of the atmosphere, while pressure coordinates are more likely to give accurate results in the upper layers. The unified model code is designed to allow any distribution of levels. However, it is found in practice that the performance of physical parametrization schemes is very sensitive to the distribution of levels. The mesoscale model uses 31 levels, with extra levels between 10 metres above the ground and the tropopause.

In a limited area mode, an equatorial latitude longitude grid is used in the horizontal in which the coordinate pole is shifted. The code can be run at any desired resolution over any region of the globe, subject to computer resource restrictions. For operational running over the United Kingdom the mesoscale model has the coordinate pole at 37.5°N 177.5°E and a grid-length of 0.150 (16.8 km) and a coverage area of approximately 1 500 km^2.

A library of parametrizations is available for the unified model. Some of those that are being used at present are described briefly below:

(*a*) Land surface model. A multilayer soil temperature model and a soil moisture prediction scheme are included. Different soil types are specified and used to determine the surface albedo. A model of the vegetation canopy is included. Moisture can be retained in the canopy or transferred to the soil or atmosphere. Different vegetation types can be specified. Snow depth is predicted and used in the calculation of albedo;

(*b*) Boundary layer. Vertical turbulent transport of primary variables and tracers in the boundary layer depends on the local Richardson number. The presence or absence of cloud is taken into account in calculating the transport coefficients;

(*c*) Large-scale cloud and precipitation. Large-scale clouds are represented by their liquid water (or ice) content. The total optical thickness of the clouds is taken into account in the radiation calculations. Large-scale precipitation is calculated in terms of the water or ice content of the cloud; frozen cloud starts precipitating as soon as it forms. Cooling of the atmosphere due to evaporation of precipitation is included. Figure 11.3 shows an example of the precipitation field generated by the model;

(*d*) Convection. Sub-grid scale convective processes are modelled using a simple cloud model: convection affects the large-scale atmosphere through compensating subsidence, detrainment and the evaporation of falling precipitation. A treatment of the effects of the convective downdrafts is also included;

(*e*) Radiation. The radiation calculation uses six bands in the long wave and four in the solar calculation. It allows for water vapour, ozone, carbon dioxide and the large-scale and convective cloud distributions. Cloud radiative properties depend on cloud water and ice content.

11.1.3 Statistical-dynamical models

Georgakakos and Bras (1984*a*, *b*) describe what they called spatially lumped precipitation prediction models based upon the conservation of the mass of condensed water equivalent over the area of interest. Surface meteorological data are used as input and horizontal water transport due to cloud and rain movements is ignored. State estimators are developed for objective initialization in order to localize the predictions to specific locations using near time observation of precipitation. Lee and Georgakakos (1990) provide a detailed description of the equations used in this type of model.

The mass conservation equation is expressed in a state-space form necessary to enable the use of estimation theory for real-time state updating and characterization of the forecast errors (see section 14.3.1 and Gelb, 1974). The state-space form consists of a set of first-order differential or difference equations with the dependent variables representing the model states.

Lee and Georgakakos (1990) discuss prospects for further work with this type of model including calibration using merged fields of radar-rainfall and raingauge data and the use of the model as a means of integrating data from remote and on-site sensors for the real time forecasting of rainfall. However, as recognized by the authors this approach can only be justified in cases where (*a*) adequate observations of meteorological variables are available within the area of interest to define the initial and boundary conditions; and (*b*) adequate time and computer resources are available for timely integration of the governing equations. Since these conditions cannot in general be met, it was considered adequate to use only the governing equations corresponding to the conservation of water-mass-law together with adiabatic expansion. Spatial interpolation of either observed wind vectors or vectors from a numerical weather prediction (dynamical) model and objective interpolation of other data provide the model inputs. Unfortunately this approach is likely to lead to unreliable precipitation forecasts as we discuss in section 11.4.

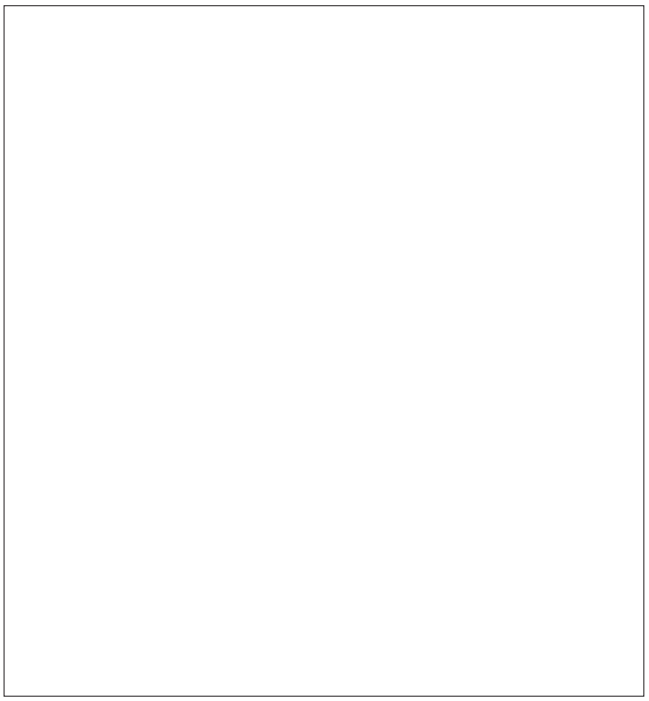

Figure 12.3 — Layer cloud processes.

11.2 INITIALIZATION PROCEDURES

As pointed out by Golding (1987) and others, since many mesoscale disturbances are forced either by the large scale flow or by the lower boundary, it is clearly necessary that this forcing should be correctly specified if a good forecast is to be obtained. For the large scale flow this requires a consistent specification of the temperature and velocity fields. However, the advecting velocities must be specified to a very high accuracy as must the model boundary conditions.

The lower boundary conditions, orographic height and land/sea contrast are relatively straightforward to specify, but the effect of the sub-grid scale variability of these parameters is more problematic. Since thermal forcing can occur at the edge of a cloud sheet, lying snow or moist ground, it is necessary to specify the initial moisture distribution in the atmosphere some hours ahead.

The primary response of the atmosphere to forcing occurs through condensation of water and the consequent release of latent heat. Hence, a detailed specification of the three-dimensional moisture distribution is required for the accurate prediction of the mesoscale response to forcing.

Initialization procedures to cope with conventional meteorological data have included a variety of techniques including the use of balance equations and normal mode initialization (see for example Baer and Tribbia, 1977; Leith, 1980), and semi-geostrophic approximation (see for example Hoskins and Bretherton, 1972; Cullen and Purser, 1984). Where synoptic-scale influences are not important, the details of radiation and precipitation processes must be represented in the initialization procedure. Such procedures are known as physical initialization, and involve the use of reverse algorithms consistent with the physics of the numerical model which can provide a modification of the initial state variables (see for example Krishmamurti, *et al.,* 1993). For example, the rain rates are assumed to be known, and are used to provide

Figure 12.4 — Convective cloud model.

Figure 12.5 — Atmosphere-land surface interactions.

the specific humidity and the potential temperature at the top of the constant flux layer (see for example Gal-Chen, 1978). Moisture variables are derived consistent with the imposed rain rate.

11.3 PRECIPITATION FORECAST SKILL

The performance of statistical models in predicting precipitation is variable. Waelbroeck, *et al*. (1994), using a model based on a local reconstruction of the dynamics in phase space, demonstrated a level of performance for which the mean-squared error in the prediction of the rainfall anomaly for 1982 in Mexico was 64 per cent of the variance, and the beginning of the rain season was correctly predicted.

The United States National Weather Service objective thunderstorm probability statistical forecasting guidance has a skill ranging from 37 to 45 per cent (daily) and 24 to 30 per cent (12-24 hours), (see for example Murphy and Sabin, 1986). Bosart and Landin (1994) have concluded from this level of performance, and from their own assessments that forecasts of the initiation and evolution of convection are very "perishable" and, by implication, not well suited to statistical approaches.

Simple models can reproduce orographic rainfall distributions very well (Figure 11.1). Likewise, mesoscale models can also forecast orographic and frontal rainfall with significant skill as shown in Figure 11.3. However, forecasts of convection are much less reliable. Intense convection can be forecast successfully over a wide area, but individual thunderstorms and convective cells are usually located incorrectly (Collier, 1990). However, Krishnamurti, *et al*. (1994) have demonstrated the improvement of forecasting tropical convective rainfall which can be achieved using physical initialization. Nevertheless, at present numerical forecasts of heavy convective precipitation show little skill (Dunn and Horel, 1994*a*, *b*).

11.4 LIMITATIONS AND FUTURE DEVELOPMENTS

It is clear that forecasts of precipitation, and indeed other parameters, depend critically on the initial conditions used in the model. This is illustrated in Figure 11.4 where two model rainfall fields are shown derived using two different sets of initial conditions for the same day. Similar results have been analysed by Berri and Paegle (1990), who found that the predictions of the sea breeze type of circulation in the boundary layer are sensitive to errors in the initial wind field. However, they also found that this result reversed where the local observation accuracy exceeds current observation accuracies by a factor of approximately three. Lee, *et al*. (1991) simulated observed mesoscale variations in boundary-layer moisture, wind speed and wind shear, and found that numerical simulations revealed large differences in timing the initiation of deep convection and some differences in the strength of the convection.

It seems clear that improvements in numerical forecasts of convective precipitation will depend upon the availability of mesoscale observations from, for example, Doppler radars and high resolution satellite data (Lilly, 1990; Lin, *et al*., 1993). As far as model structures are concerned, Zhang, *et al*. (1994) suggest that the greatest potential seems to lie in the coupling of parametrized convection with explicit moisture schemes.

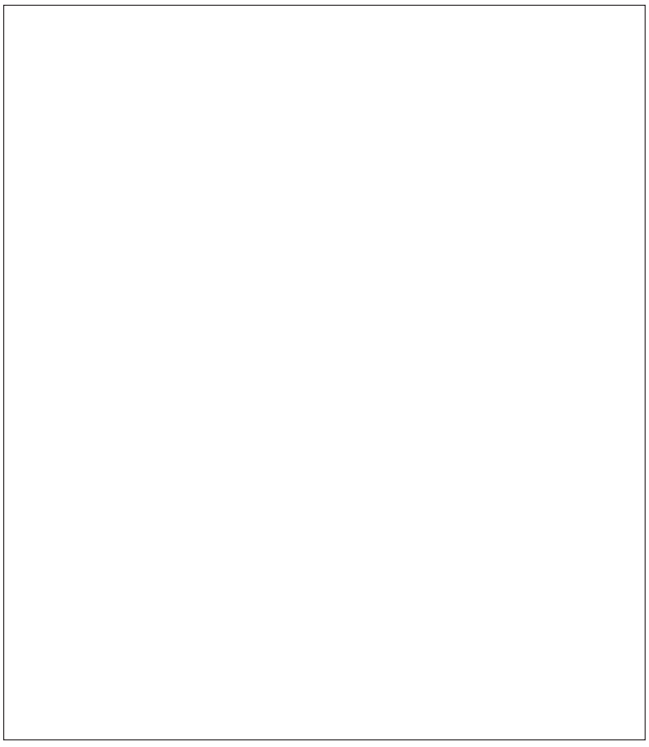

Figure 12.6 — United Kingdom Meteorological Office moisture diagnostics — monthly averages global (0°E-360°E, 90°S-90°N). Precipitation-evaporation (after Milton and Van der Wal, 1994).

CHAPTER 12

REGIONAL AND GLOBAL NUMERICAL MODELLING

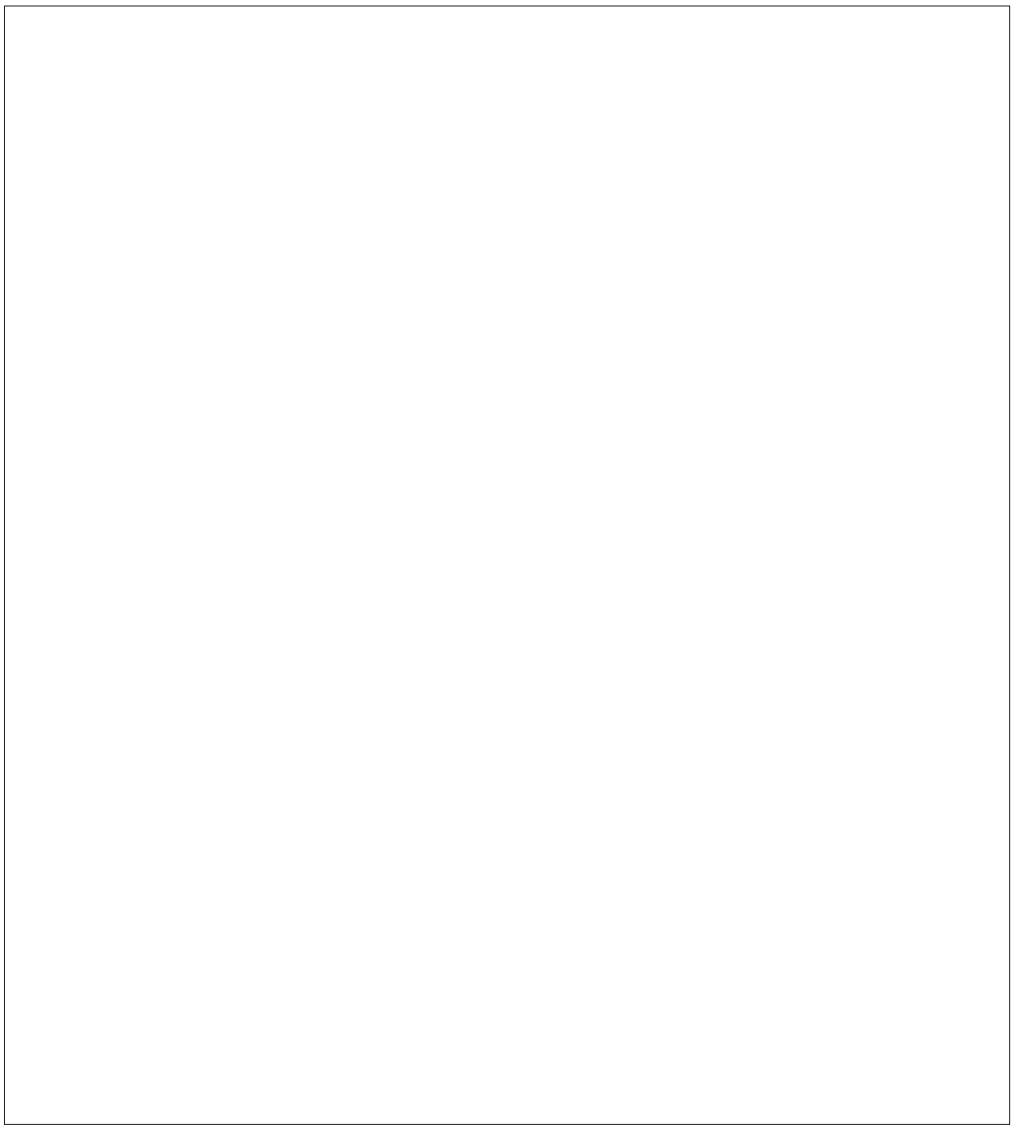

Figure 12.7 — Distribution of average rainfall rate in mm d^{-1} for December, January and February: (*a*) from a GCM control run; and (*b*) as observed (from Browning, 1990).

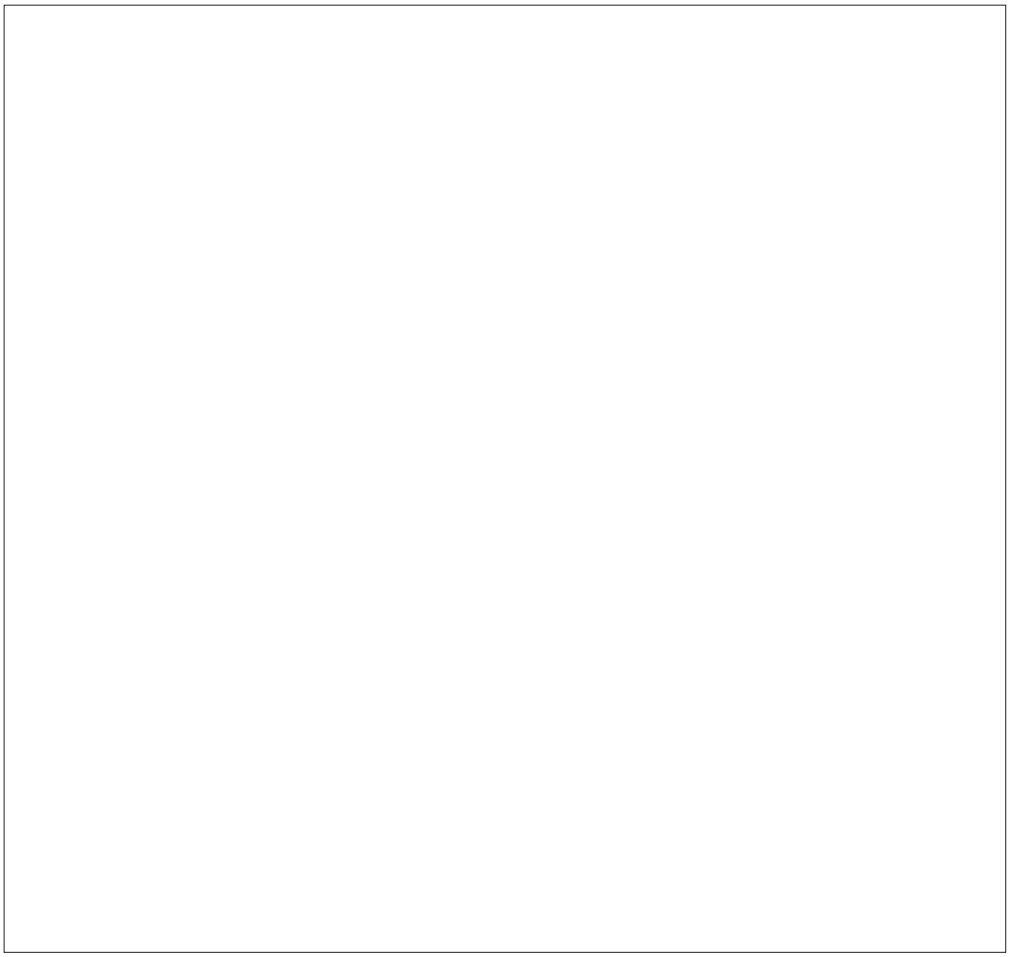

Figure 12.8 — Sample 'plume' diagrams and corresponding forecast probabilities across Europe for precipitation at T + 120 (five days) derived from the distributions of predictions across an ECMWF ensemble. Contours are at 5 per cent, 35 per cent, 65 per cent and 95 per cent (after Harrison, 1994*a*).

12.1 MODEL FORMULATIONS

The basis of global models, as for mesoscale models, is a set of equations known as the 'primitive' equations. These equations set out the basic dynamical, thermodynamically and conservation properties of the atmosphere. The conservation equations ensure that certain properties such as energy, mass and momentum are conserved as the model is operated. Gill (1982) and Harries (1994), for example, give the simplified basic equations which are used.

The United Kingdom Meteorological Office has developed a so-called unified model which combines and standardizes (Figure 12.1);

(*a*) Operational numerical weather prediction (NWP) in both global and limited area formats;
(*b*) Climate modelling;
(*c*) Ocean modelling.

In what follows we outline the structure of this model drawing upon a range of model descriptions prepared by Meteorological Office staff.

The model uses a single general purpose code and employs a modular structure which allows easy enhancements to, and interchange between, models. Furthermore, all the meteorological code has standard interfaces between subroutines as agreed by several centres in Europe and the United States to facilitate the exchange of schemes for intercomparison. The code has also been written so that it is not machine dependent, i.e. it will run on any future Super computer procured by the Meteorological Office.

The model may be run with either a global domain, or one that is limited in horizontal or vertical extent. For day-to-day NWP there are three atmosphere-only versions: a global model (GM) covering the whole world; a limited area model (LAM) covering much of Europe, the North Atlantic and North America; and finally a mesoscale model covering the United Kingdom and a small part of Continental Europe (Chapter 11). They all share the same physical parametrizations, a feature that was not the case with their previous counterparts.

The Meteorological Office wave models run in both global and European versions. The former assimilates ERS-1 (ESA remote sensing satellite) data and forcing data from the GM to produce a forecast to T + 120. The European version uses forcing data from a limited area run to produce forecasts to T + 36.

Boundary conditions for LAM are provided by GM forecast values from an earlier run interpolated onto the LAM coordinates. These are applied to the outermost four points around the boundaries, with weights given to GM values of 1, 0.75, 0.5 and 0.25. Similarly the LAM provides boundary values for the United Kingdom mesoscale model (Chapter 11).

A GM can be developed using a three-dimensional array of grid points, as in the case of the United Kingdom Meteorological Office model. This model uses a standard latitude/longitude coordinate system with grid points every 5/6 (0.833 3) degrees latitude and 5/4 (1.25) degrees longitude. This gives a north-south resolution of 93 km and an east-west resolution that decreases with increasing latitude. On the Equator, it is 139 km and at 50° latitude it is 89 km, so that in these regions the grid boxes are almost square. Poleward of around 55° the extra east-west resolution is not effective as the fields must be filtered to remove spurious small-scale variations that develop as a result of close grid spacing. This limits the effective resolution to around 93 km.

Instead of a grid base on actual latitude/longitude coordinates, the limited area version uses a rotated latitude/longitude coordinate system in which the computational north pole is shifted to an actual position of 30°N 160°E. This allows the regional area to take advantage of the even grid spacing enjoyed in equatorial regions and dispenses with the need to filter. It is sometimes referred to as an ELF grid (Equatorial lat-long fine-mesh). The rotated grid has a resolution of 0.442 5 degrees in both directions, which equates to about 50 km across the whole area. The model may be run in limited area format for any other part of the globe, as long as the coordinate pole is shifted to a position such that the area of interest has even grid spacing.

Both the GMs and LAMs have the same resolution in the vertical. The atmosphere is divided into 19 layers, with the winds and temperatures carried at 19 levels and humidity carried at the first 16 levels. A hybrid pressure based coordinate is used, referred to as η (eta) (Figure 12.2).

The bottom four levels are terrain-following sigma levels, which help in application of realistic boundary conditions. The top three levels are pressure surfaces, and in between the levels are a mixture of the two, so that they gradually follow the terrain less and less and become more uniform in pressure and height.

An alternative model structure is to use a spectral transform technique in which a parameter is described in terms of a series expansion of spherical harmonics around the Earth. It has been found that about 15 terms in the series expansion are required to achieve a reasonable representation of the parameter. This approach is used in the European Centre for Medium-range Weather Forecasts (ECMWF) model.

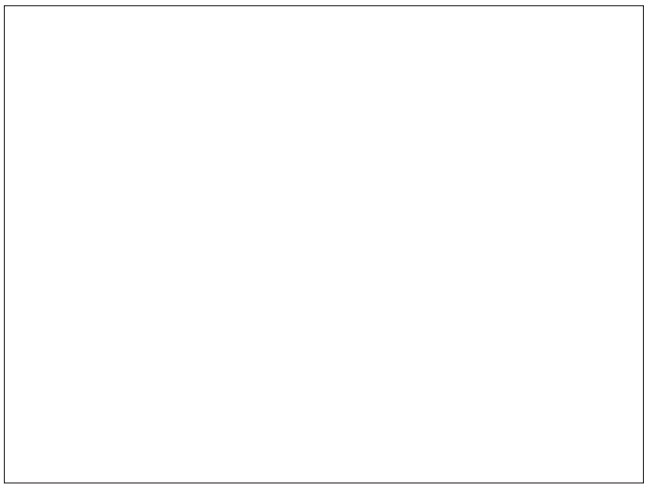

Figure 13.1 — Relationship between yearly anomalous rainfall (mm) over Zimbabwe and the production of maize (kg/ha) for the period 1970–1993. ENSO years (1972/1973, 1982/1983, 1986/1987, 1991/1992) are associated with a strong decrease in rainfall and maize production (after Buckland, 1993).

The United Kingdom Meteorological Office model predicts the following primary prognostic variables:

(*a*) Horizontal wind components (u, v);
(*b*) Potential temperature (θ);
(*c*) Specific humidity (q);
(*d*) Cloud water and ice (q_I, q_f);
(*e*) Surface pressure (P*);
(*f*) Soil temperature (T_S);
(*g*) Soil moisture content (SMC);
(*h*) Canopy water content;
(*i*) Snow depth (Snowdepth);
(*j*) Surface temperature (T*).

From which the following secondary prognostic variables may be diagnosed:

(*k*) Boundary layer depth (Z_H);
(*l*) Sea surface roughness (Z_O);
(*m*) Convective cloud base (Ccb);
(*n*) Convective cloud top (Cct);
(*o*) Layer cloud amount (Ca);
(*p*) Vertical velocity (h).

When run in coupled ocean/atmosphere configurations, the following are included as additional prognostic variables:

(*q*) Sea surface temperature (SST);
(*r*) Proportion of sea-ice cover (ICEc);
(*s*) Sea-ice thickness (ICEt);
(*t*) Sea surface currents.

Ancillary fields (i.e. those parameters that are not predicted and must be specified) include:

(*u*) Land/sea mask;
(*v*) Soil type;
(*w*) Vegetation type;
(*x*) Grid-box mean and variance of orography;
(*y*) Ozone mixing ratio.

When run in atmosphere only mode, parameters (*q*) to (*t*) are included as ancillary fields rather than prognostic variables and must be specified.

If the model is run with limited horizontal extent, boundary values of prognostic variables (*a*) to (*e*) must be supplied for the period of the integration.

If the model is run with limited vertical extent, for example as a stratospheric model, prognostic variables (*f*) to (*o*) are not used, and item (*y*) is the only ancillary fields used. For some applications item (*y*) may be a prognostic variable.

Over land, a geographical distribution of vegetation and soil types is specified. These determine soil conductivity and heat capacity, surface hydrology, albedo and roughness. The last two parameters are allowed to vary if the surface acquires snow cover.

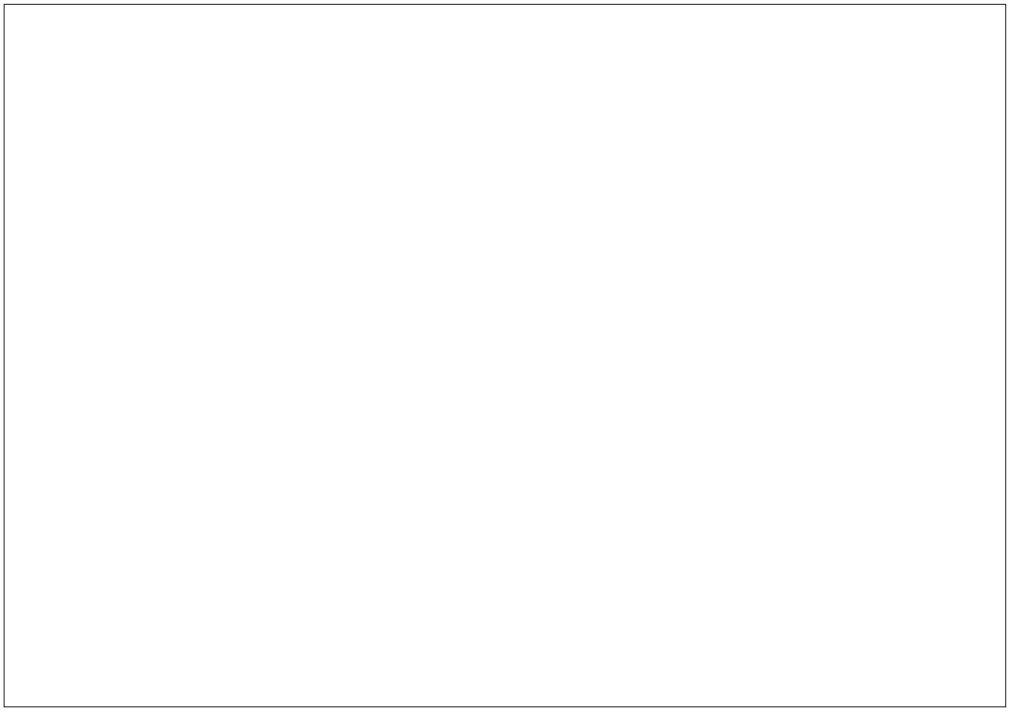

Figure 13.2 — Skill of monthly temperature and rainfall forecasts for 10 districts of the United Kingdom. Plots are four-year running mean skills, values being plotted at the end of each period. The Folland-Painting skill score is used (from Harrison, 1994*b*).

12.2 METEOROLOGICAL PARAMETRIZATIONS

In order to represent weather and climate it is necessary to parametrize atmospheric processes which include (after Harries, 1994),

(*a*) Heating, for example by solar radiation;
(*b*) Cooling;
(*c*) Evaporation;
(*d*) Condensation;
(*e*) Liquid water processes;
(*f*) Cloud formation;
(*g*) Cloud-radiation interaction;

(*h*) Sub-grid scale processes (for example turbulence, gravity wave drag).

To illustrate the complexity of these parametrizations we outline two types of process of particular importance to the hydrological cycle.

12.2.1 Large-scale cloud and precipitation

The model holds explicit values of fractional cloud cover, together with separate values for cloud water and cloud ice mixing ratios (i.e. kg of cloud water/ice per kg of moist air within a cloud). Cloud water is converted to precipitation by a process known as autoconversion, the rate of which increases with increasing cloud water mixing ratios. The autoconversion equation includes a term which increases the rate of conversion if there is precipitation falling into the grid-box from above, thereby simulating the processes of growth by accretion and coalescence. In this way, seeder-feeder enhancement of precipitation may be represented.

Frozen precipitation is assumed to start falling as soon as it is formed, simulating enhanced growth by deposition (Bergeron-Findeisen). Evaporation and melting of precipitation is allowed to take place to the extent that the temperature and humidity of lower layers allow, with the attendant cooling of the environment by latent heat exchange. At temperatures of –15°C and below, all cloud content is ice, with a mixture of water and ice between –15°C and 0°C, the proportion of ice decreasing with increasing temperatures.

Dynamical ascent is the most important process leading to cloud formation in the model, but cloud may also be formed by radiative cooling and turbulent transport. These processes are summarized in Figure 12.3.

12.2.2 Convection and convective precipitation

A cloud model is used to represent Cumulus and Cumulonimbus convection, in which an updraft and precipitation-induced downdraft are considered (Figure 12.4). A test is made for convective instability: if the potential temperature of any level is higher than that of the level above, convection is initiated. Convection will continue as long as the air within the cloud continues to be buoyant. Dilution of the cloud is represented by entrainment of environmental air. Before the cloud detrains completely at the level where the parcel of air ceases to be buoyant, the remaining mass, heat, water-vapour and cloud water/ice are completely mixed into the environment at the cloud top.

A single cloud model is used to represent a number of convective plumes within the grid square, and precipitation is diagnosed within that square if:

(*a*) Cloud liquid/ice content exceeds a critical amount; and

(*b*) The cloud depth exceeds a critical value.

This value is set to 1.5 km over the sea and 4 km over land. However, if the cloud top temperature is less than -10°C, the critical depth is reduced to 1 km over land or sea. As with large-scale precipitation, the convection scheme allows for evaporation and melting of precipitation.

12.3 ATMOSPHERE-LAND SURFACE INTERACTIONS

Land surface grid points are specified in a way which allows variations in soil and vegetation type.

A soil model containing four layers is used to represent the sub-surface heat fluxes. A heat balance equation is used to derive the surface temperature and contains terms for the fluxes of incoming solar radiation, outgoing long-wave radiation, sensible heat down into the soil and up into the atmosphere and latent heat due to the evaporation of water and the melt of snow. The presence of snow changes the surface albedo and roughness length, as well as insulating the soil. Surface water may be increased by precipitation, condensation and snow-melt, and decreased by evaporation, surface run-off and seepage into the deep soil.

The vegetation canopy plays a part in the hydrology of the model in several ways: it provides a source of moisture to the atmosphere through evapotranspiration; it acquires and stores water by intercepting falling rain and by direct condensation; it releases this water to the soil by the process of "throughfall". Sommeria (1994) provides a detailed description of the parametrizations used in the European Centre for Medium-range Weather Forecasts (ECMWF) model. Turbulent mixing plays an essential role in determining the structure of the boundary layer and occurs on scales far smaller than the models' resolution. It determines important fluxes of sensible heat, moisture and momentum between the surface and the atmosphere. Its effects are calculated using equations of diffusion (analogous to conduction) (see Figure 12.5).

12.4 PERFORMANCE OF CURRENT MODELS IN FORECASTING PRECIPITATION

The performance of mesoscale models was discussed in Chapter 11. Most numerical prediction models exhibit a characteristic known as "spin-up" when integrated from an initial state generated from an assimilation of observations and model background field. During the spin-up time the surface boundary layer is established, spurious gravity waves are damped and the model dynamics is established such that it relates to that of the true atmosphere.

Spin-up is most often associated with the model hydrological cycle. The initial adjustments represented by this phenomenon arise from both imbalance in the initial state and from deficiencies in modelling the physical and dynamical processes. For example, the thermodynamic state required by convection as represented in the model or the large scale cloud schemes may be incompatible with the initial input analysis.

Analyses of the spin-up in global forecasts of the United Kingdom unified model by Milton and Van der Wal (1994) show that the globally averaged large scale rain shows a 44 per cent increase between T + 00 and T + 72 hours, while the convective rainfall shows a 15 per cent increase. This work

Figure 14.1 — The unit hydrograph illustrating (*a*) a direct proportional relationship between the effective rainfall and the surface runoff; (*b*) two units of effective rainfall falling in time T produce a surface runoff hydrograph that has its ordinates twice the TUH ordinates; and (*c*) two successive amounts of effective rainfall, R_1 and R_2 each all in T producing a surface runoff hydrograph which is the sum of the component hydrograph due to R_1 and R_2 separately (superposition) (from Shaw, 1994).

also provides an indication of the success of the model in reproducing the global climatology of precipitation and evaporation. For long period time-means the global values of precipitation minus evaporation (P-E) should be close to zero if hydrological balance is achieved. The performance 1992-1994 is shown in Figure 12.6.

Numerical models can now reproduce the main features of the global precipitation climatology as shown in Figure 12.7. However, as discussed by Sommeria (1994), the way in which physical parametrizations are structured has a profound effect upon model output. For example, the inclusion of a shallow convection scheme in the ECMWF model allowed additional mixing at the top of the boundary layer which provided better conditions for the development of deep convection. The global convective precipitation was increased by approximately 7 per cent as a result.

There is now a gread deal of activity in numerical weather prediction in many countries (WMO, 1995*b*). From time to time, large differences in skill arise between models on individual days which can often be traced to seemingly small analysis differences. Improvements in analyses inherent in variational methods could lead to improved predictions (WMO, 1995*c*). Work to compare precipitation forecasts from different operational models is planned.

12.5 ENSEMBLE FORECASTING

Ensembles of predictions may be generated by setting off a numerical forecast model from a number of starting conditions, each slightly different from the others (see for example Shukla, 1981; Murphy and Palmer, 1986). The main hypotheses behind work so far are (Harrison, 1994*a*):

(*a*) That the grand ensemble mean provides a better forecast, on average, than any individual ensemble member;

(*b*) That the spread of solutions across the ensemble provides an indication of confidence in the prediction represented by the ensemble mean, a lower spread indicating limited sensitivity to errors in initial conditions and therefore higher confidence in the prediction.

The first regular operational use of ensembles started at the United Kingdom Meteorological Office in December 1988 (Milton, 1990). Harrison (1994*b*) poses two questions related to the use of ensemble forecasts:

(*a*) To what extent is variable model performance, based on single integrations, related to errors in initialization data, to specific performance of particular models within particular regimes or regime transitions, or simply to inappropriate model formulation itself?

(*b*) To what extent can a well formulated ensemble based on an imperfect model fully sample possible future atmospheric states in their correct proportions?

It is concluded that future model improvements and the application of ensembles are both necessary to provide the optimal strategy for forecast improvement. Further work is necessary to develop techniques to identify the fastest lineally growing perturbations relatiave to a short-range forecast trajectary (WMO, 1995*c*). Nevertheless, the application of ensembles can provide useful indications of forecast probabilities as shown in Figure 12.8.

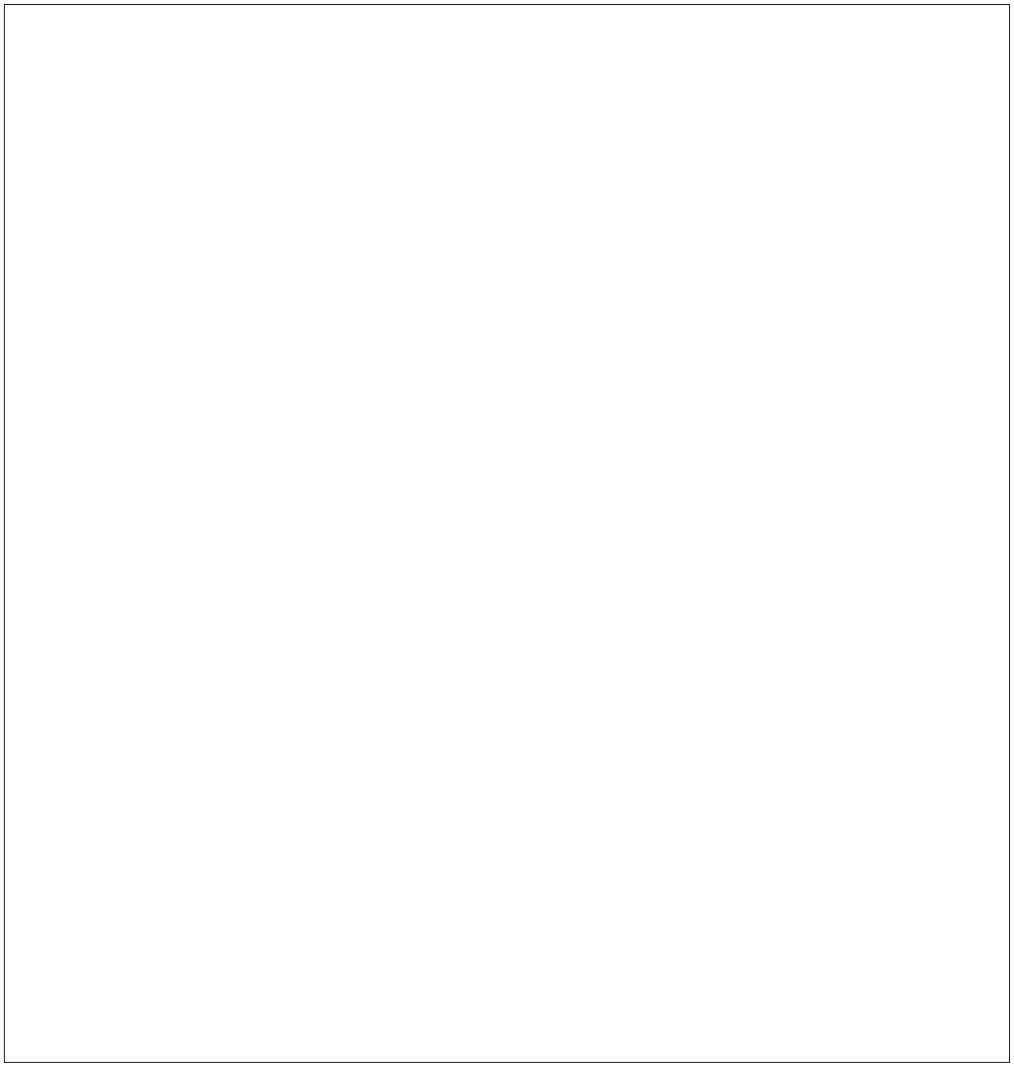

Figure 14.2 — Sub-watersheds 8 and 11 of the Walnut Gulch (Arizona) experimental catchment divided into model cells (from Karnieli, *et al*., 1994).

Figure 14.3 — Schematic representation of the structure of the *système hydrologique Européen* (SHE) model (from Abbott, *et al*., 1986*a*, *b*).

CHAPTER 13

SEASONAL AND CLIMATE PREDICTIONS

Moura (1994) notes that progress in predicting climate has shown progress on some scales only, notably seasonal (100 day) to interannual (1 000 day) time-scales, for which forecasting skills have been demonstrated mainly with regard to the *El Niño*/Southern Oscillation (ENSO) phenomenon. For example, Figure 13.1 shows the strong link between maize production and interannual precipitation fluctuations in Zimbabwe for the period 1970 to 1993 including ENSO years (1982/1983, 1991/1992). It is clear that seasonal-to-interannual changes in the tropical climate are largely caused by changes in the lower boundary forcings via changes in sea surface temperature (SST), soil moisture and ice and snow cover and seem to have a high degree of predictability (Shukla, 1993). The oceans cover 70 per cent of the surface and appear as a major forcing mechanism, determining, to a great extent, the thermal properties of the Earth's climate. They possess a total mass which is about 300 times larger than that of the atmosphere and a thermal capacity which is some 1 000 times greater.

According to current theories, ENSO has its origin in a dynamical instability of the coupled ocean-atmosphere fluid. Hence it is likely that global coupled ocean-atmospheric models offer the most promising approach to seasonal and interannual forecasting. However, during the last 20 years or so there has been a considerable amount of work on empirical-statistical techniques for monthly and seasonal forecasting (see for example Zhaobo, 1994; Harrison, 1994*b*).

A monthly forecast can follow the prevailing trend of evolution of the air in the range of several days to half a month and also use numerical weather prediction results. A seasonal forecast uses a mainly statistical approach. Most Meteorological Centres producing seasonal weather forecasts prepare temperature and precipitation forecasts directly.

Empirical-statistical methods in seasonal forecasting include:

(*a*) Regression analysis, which aims to establish a regression expression between a predictand and predictors;
(*b*) Discriminant analysis, in which a prediction is expressed as a category on the basis of an established discriminant equation;
(*c*) Cluster analysis, wherein the future likelihood of a category for the predictand is considered, i.e. to forecast the category;
(*d*) Analogue method — the previous-period evolution characteristics of the predictand and predictors under study are determined first, to which a close analogue is sorted out from historical cases whose subsequent-period features are taken to be those of the predictand in the following season;
(*e*) Time-series analysis — the series are constituted of historical observations of predictand and predictors and are then treated by the related analysis to establish an autoregression model for a predictive purpose;
(*f*) Period analysis — a type of time-series analysis which consists of extracting principal periods from the predictands' series, followed by their superimposition and extension for prediction.

Each of the statistical techniques can be used to prepare a prediction model in a direct fashion. It should be noted, however, that they are all based on the historical record and only when a regularity is found will an appropriate statistical scheme be of use.

The use of past data sequences to identify analogues with current conditions is still the basis of monthly and seasonal forecasting in some countries. Results are somewhat variable, however, and other countries such as the United Kingdom dropped this approach. However, with the advent of global computer models during the early 1980s the possibility of producing deterministic forecasts for weeks and even months ahead presented itself. Nevertheless, these model developments were accompanied by a realization of the importance of atmospheric predictability as implied by chaos theory. This theory suggested that small changes in model input conditions could result in widely differing forecasts. The use of analogues resulted in temperature forecasts having some skill but rainfall forecasts having very little skill. Methods based upon, automated numerical empirical techniques (see for example Folland and Woodcock, 1986) have shown improved levels of skill as shown in Figure 13.2.

Recently specific techniques have been developed for forecasting rainfall in the Sahel region of sub-Saharan Africa based upon sea surface temperature (SST) anomalies (Folland, *et al.,* 1991). Such forecasts are now made routinely by the United Kingdom Meteorological Office (Ward, *et al*., 1983) from the output of the unified model. A similar approach has been developed for forecasting rainfall over north-east Brazil (Ward and Folland, 1991).

Ensembles of predictions (section 12.5) are also being investigated for seasonal forecasting. However, it is possible for all members of an ensemble to make similar predictions, suggesting high confidence in the forecast, whereas the atmosphere ends up in a state far from that forecast. Also it is possible for two or more distinct outcomes to be present within an ensemble. Ensemble forecasting was introduced into the United Kingdom Meteorological Office in 1988, but any improvement from this time is not evident in Figure 13.2. However Harrison (1994*b*) indicates an improvement due to the use of ensembles of the order of five to 10 per cent.

CHAPTER 14

USE OF PRECIPITATION MEASUREMENTS AND QUANTITATIVE PRECIPITATION FORECASTING (QPF) IN FLOOD FORECASTING MODELS

14.1 MODEL FORMULATIONS

We may identify three generic types of rainfall-runoff model namely black box (or metric), conceptual (or parametric) and physics-based (or mechanical). These types are characterized by increases in the amount of information represented within the model formulation, model data requirements, their use of computer resources (much less of a problem now) and the range of scenarios to which the model can be applied.

Black box models are often linear, and may use time-series analysis techniques. The model parameters can be clearly identified, and there is an arbitrary separation into component parts such as input, storage and slow flow (base-flow). Initial conditions are modified according to observed records and model parameters are estimated using regression equations with streamflow records. These models are the only approach possible for ungauged catchments, and Burn and Boorman (1993) describe alternative methods to the use of regression equations which may be employed in such circumstances. The methods are based upon the assignment of ungauged catchments to a group based on the physical characteristics of the catchment and the use of similarity measures to transfer parameters.

Somewhat more complicated combinations of several linear models are sometimes referred to as “grey box” model. These simple models may work very well over restricted areas and time periods, but in general the rainfall run-off precess is non-linear and time variant. In addition, spatial complexities of the catchment topography, soils, vegetation and rainfall necessitate a more complex approach if many different types of event are to be simulated or forecast (Loague and Freeze, 1985).

Conceptual models take an assumed form whose parameters are meaningful, but not usually measurable and therefore are specified through an optimization process. A hydrological time-series is composed of the terministic components in the form of periodic parameters and of a stochastic component. Autoregressive models are commonly used (Box and Jenkins, 1970), and the parameters of such models are usually estimated by least square methods, the method of moments or the maximum likelihood method (for example Wang and Singh, 1994). The optimization process may be very subjective (e.g. based upon experience) or objective by minimization of an error function. Unfortunately, problems

Figure 14.4 — Minute by minute variations of rainfall rate derived using a dropsize disdrometer (after Chandrasekar and Gori, 1991).

arise when the optimization process identifies different parameter sets and it is unclear what set is optimum. One way of circumventing this problem is to modify model initial conditions according to observed data as an event proceeds so that the model can self correct. We discuss this later in section 14.3.

Physics-based models use quantities which are, in principle, measurable (see for example Beven and Kirkby, 1979). Model parameters have physical significance and the equations used represent the small scale physics of homogenous systems. Hereby lies a problem as highlighted by Beven (1989); in real applications of these models, an example being the *système hydrologique Européen* (SHE) model (Abbott, *et al*., 1986*a*, *b*), it is necessary to lump the small scale physics to the model grid scale typically 250 m × 250 m as in the SHE model applied with the Wye catchment (Bathurst, 1986*a*, *b*). There is no theoretical framework for doing this in just the same way as there is no theoretical framework for representing the effects of sub-grid scale convection in atmospheric numerical models. Beven (1989) concludes therefore that it will be necessary to proceed with physically-based models cautiously, employing programmes of field measurements to ensure that model predictions relate to real world process.

14.2 LUMPED AND DISTRIBUTED MODELS

Conceptual models may be either lumped, that is the characteristics of the whole catchment may be embodied in one set of equations, or distributed in which the spatial characteristics of

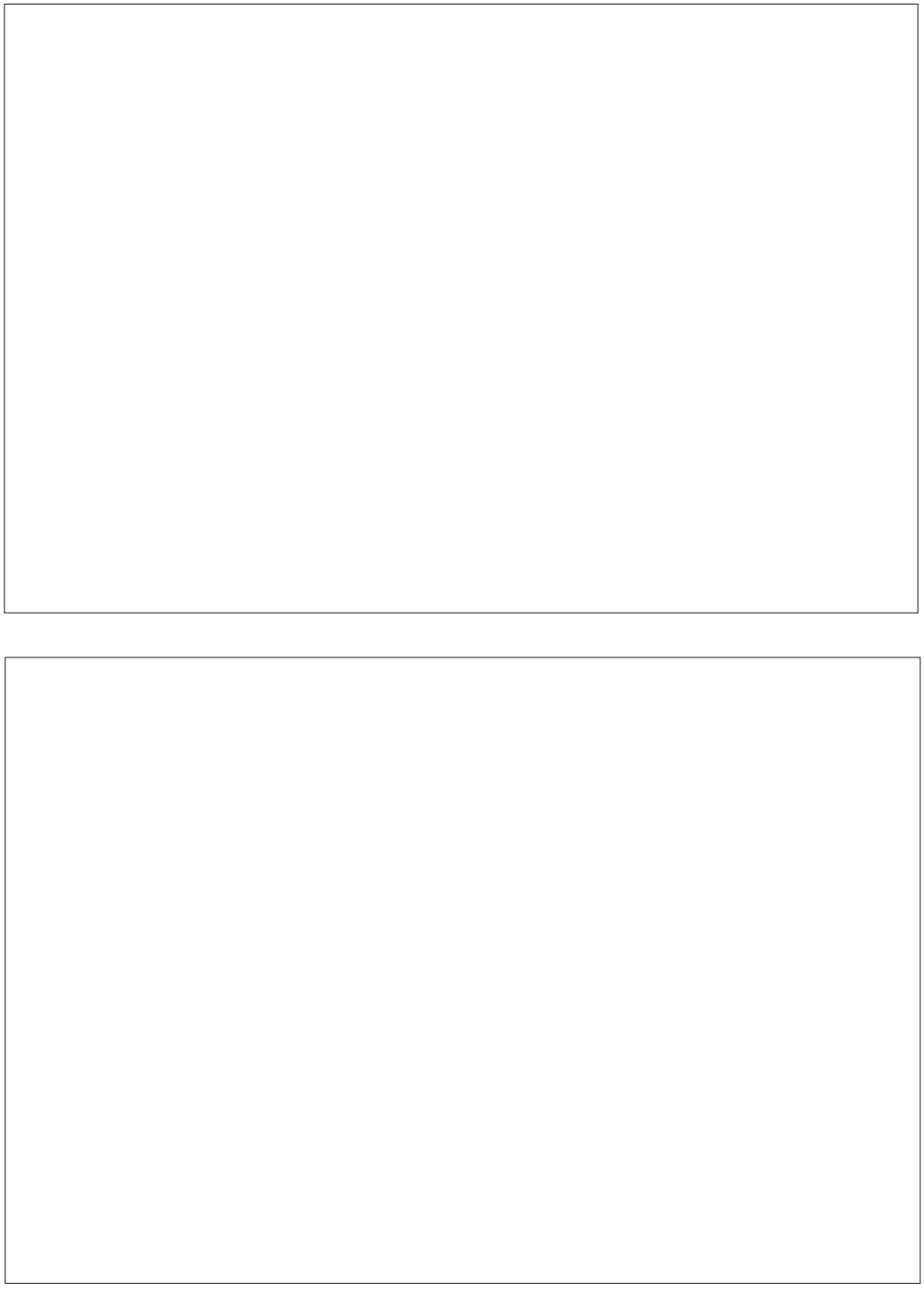

Figure 14.5 — Average flow RMSE at Colindeep Lane using as input FRONTIERS forecasts for (*a*) 13 frontal events; and (*b*) eight convective events (FOAG, 1993).

both the catchment and the precipitation are represented. Physics-based models are distributed models, as it is necessary to represent physical processes in a way which allows variation across a catchment, otherwise the model would be conceptual.

14.2.1 Lumped models

A lumping procedure which attempts to represent the relationship between the characteristics of the hydrograph and its physiographic factors may employ the unit hydrograph (UH) approach first proposed by Sherman (1932). The assumptions inherent in its use are as follows (Chow, 1951):

(*a*) The effective or excess rainfall (the amount of rain that finds its way into a river after rain has made up catchment deficits and surfaces and soil are saturated) has constant intensity within the effective duration and falls uniformly over the entire catchment;

(*b*) The duration of direct runoff is constant for a given excess rainfall duration regardless of the quantities involved;

(*c*) The ordinates of the unit hydrograph are directly proportional to the total amount of direct runoff.

This describes a linear system with certain properties as shown in Figure 14.1. The degree of linearity of a system can be quantified by the coherency, $\gamma(f)$. If a system is linear, $\gamma(f)$ is equal to unity, otherwise the values of coherence lie between 1 and 1 (Hino, 1970*a*) with light rainfall-runoff events being significantly more linear than heavy rainfall events (Hino, 1970*b*). Coherence is a function of the spectra and cross-spectra of rainfall and runoff.

An alternative approach is the use of transfer function (TF) models which are a form of UH model. Consider the following representation of river flow as an autoregressive (Markov) process:

$$Y_k = h_0U_k + h_1U_{k-1} + h_2U_{k-2} + ...+h_{k-1}u \ (k=1,2,...n) \quad (14.1)$$

This may be expressed in terms of previous rainfall and flow to provide an event-based rainfall/runoff model in the following form (see for example Cluckie and Owens, 1987);

$$yt = a_1y_{t-1} + \ldots a_2y_{t-2} + \ldots + a_py_{t-p} + b_1u_{t-1} + b_qu_{t-q} \quad (14.2)$$

Applying the *z*-transfer as defined in Gabel and Roberts (1980) to equation 14.2 we get:

$$y_k = H(z)u_k \ \ (k = 1,2, \ldots n) \quad (14.3)$$

It should be noted that the coefficients of the polynomial H(z) are equivalent to the UH ordinates.

14.2.2 Distributed models

The main criticism of the lumped models is that they require an assumption that the rainfall input is uniformly distributed over the catchment or, at least, that the spatial distribution is constant. This is an unrealistic assumption. Semi-distributed models consist of a system of interconnected cell units, each cell representing a definite portion, or area unit, of the catchment (see for example Diskin and Simpson, 1978). Figure 14.2 shows how sub-watersheds (sub-catchments) 8 and 11 of the Walnut Gulch (Arisona) Experimental Catchment is divided into model cells.

All cell units receive rainfall excess input which is variable with time, but assumed to be uniform across each area unit. Two types of cells are recognized, exterior or interior. Exterior cells without any channel inflow have only one input, namely the rainfall excess input. Interior cells are cells receiving channel inflow from upstream cells in addition to the rainfall excess input. As shown in Figure 14.2 the interconnections between the cells form a branching tree-like structure which approaches the form of the main drainage pattern of the catchment.

This modelling approach may be extended to formulations of many partial differential equations governing various physical processes and equations of continuity for surface and soil water flow. The SHE model (Abbott, *et al.,* 1986*a*, *b*) shown in Figure 14.3 is an example. The equations are applied to grids as small as 250 m × 250 m. Unfortunately experience has shown that, even with adequate calibration data in the form of flow records, these fully distributed models may still fail to provide consistent improvement in forecast accuracy. This is because rainfall inputs need to be provided with a spatial scale close to that of the model grid, and this can only be achieved using radar data (see for example, Anderl, *et al.,* 1976; Moore, 1987). However, Obled, *et al*. (1994) found that, for a rural medium-sized catchment (71 km^2), the sensitivity of a range of model formulations to the spatial variability of rainfall, although important, is not sufficiently organized in time and space to overcome the effects of smoothing and dampening caused by the model formulations. They concluded that this might not be the case for smaller urban catchments or over larger rural catchments.

14.3 FORECAST UPDATING

In real-time, flow forecasts can be improved by incorporating recent measurements of flow. The technique of incorporating these measurements to improve flow forecasts is known as "updating". Two forms of forecast updating may be considered, namely state updating and error prediction. In the former the model errors are used to adjust the amount of water in a storm (a state variable), which may be located in any part of the model. A variation of this approach is known as parameter updating in which one or more of the model parameters are varied in the light of recent model performance. The impact sought is to make the model predictions closer to the observed flows. In the latter an attempt is made to predict future model errors from present and past errors. The predicted error is added to the model forecast to obtain an updated forecast.

14.3.1 State updating

The term "state" is used to describe a variable of a model which mediates between inputs to the model and the model output (Szollosi-Nagy, 1976). In the case of rainfall-runoff models, the main input is usually rainfall and basin flow is the

model output. Typical state variables are the water contents of the soil, surface (channel) and groundwater stores. The flow rates out of the conceptual stores can also be regarded as state variables: examples are q_s, the flow out of the surface storage, and q_b, the flow out of the groundwater storage.

When an error, $\varepsilon = Q\text{-}q = Q\text{-}(q_s - q_b)$ occurs between the model prediction, q, and the observed value of basin runoff, Q, it would seem sensible to "attribute the blame" to misspecification of the state variables and attempt to "correct" the state values to achieve concordance between observed and model predicted flow. Misspecification may, for example, have arisen through errors in rainfall measurement which, as a result of the model water accounting procedure, are manifested through the values of the store water contents, or equivalently the flow rates out of the stores. A formal approach to "state correction" is provided by the Kalman filter algorithm (Jazwinski, 1970; Gelb, 1974; Moore and Weiss, 1980). This provides an optimal adjustment scheme for incorporating observations, through a set of linear operations, the linear dynamic systems subject to random variations which may not necessarily be Gaussian in form. For non-linear dynamic models, an extended form of Kalman filter based on a linearization approximation may be required which is no longer optimal in the adjustment it provides. The implication of this is that simpler, intuitive adjustment schemes can be devised. These provide potentially better adjustments than the more complex and formal extensions of the Kalman filter, which accommodates nonlinear dynamics through approximations. Such schemes which make physically-sensible adjustments are called "empirical state adjustment schemes".

It should be noted that all the above forms of adjustment utilize the same basic form of adjustment employed by the Kalman filter in which an updated state estimate is formed from the sum of the current state values, it is first related to a physical apportionment rule multiplied by a gain factor. This gain factor acts as a relaxation coefficient which is estimated through an off-line optimization using past flood event data. Unfortunately use of a Kalman filter can lead to instability induced by the complex impact of radar data measurement error characteristics.

A simple parameter updating approach developed for use with transfer function (TF) models such as that given in equation 14.3 has been described by Cluckie, *et al*. (1987) and by Cluckie and Owens (1987). A real-time correction factor, delta, scales the rainfall parameters of the model to match the model's steady-state gain with the event percentage runoff as follows:

$$y_t = a_1 y_{t-1} + a_2 y_{t-2} + \ldots + a_p y_{t-p} = \Delta b_1 u_{t-1} + \Delta b_2 u_{t-2} + \Delta b_q u_{t-q} \qquad (14.4)$$

The one-step-ahead forecast error is used to update delta. Owens (1986) used a method of updating delta in the following form:

$$\Delta_t = \mu\Delta_{t-1} + (1-\mu)\left(\frac{y_t - \left(a_1 y_{t-1} + a_2 y_{t-2} + \ldots + a_p y_{t-p}\right)}{b_1 u_{t-1} + \ldots + b_q u_{t-q}}\right) \qquad (14.5)$$

where $0 \le \mu \le 1$ is a smoothing factor, and $y_{t/t-1}$ is the forecast of y_t at time $t - 1$ using the value $\Delta_{0\text{-}1}$. Hence:

$$Y_t = (B(z)/A(z))\Delta_t U_t \qquad (14.6)$$

Since different types of error in the hydrograph cause differences in the adaptive correction factors, it is appropriate to use what Han (1991) refers to as a physically-realizable transfer function model in which the ratio B(Z)/A(Z) takes different values dependent upon volume, shape and timing errors in the hydrograph which are individually related to the error characteristics of the input rainfall data. While this can greatly improve model performance, it is only successful if the reasons for errors are known in real-time. Objective methods of tuning the model gain have yet to be developed and the use of expert systems or neural networks might be useful.

Other approaches to parameter updating are possible, but, as pointed out by Reed (1987), the range of possibilities is very large and a high degree of complexity may be needed to ensure reliability.

14.3.2 Auto-regressive moving average (ARMA) error prediction

As an alternative to empirical state updating, a distributed grid model may be provided with an auto-regressive moving average (ARMA) error prediction scheme, which exploits any direct serial correlation properties of a data series with the smoothing effects of an updated running mean through the series in order to forecast future errors. Predictions of the error are added to the deterministic model prediction to obtain the updated model forecast of flows. In contrast to the state adjustment scheme, which internally adjusts values within the model, the error prediction scheme is wholly external to the deterministic grid model operation. This method of updating is described further in what follows.

State correction techniques have been developed based on adjustment of the water content of conceptual storage elements in the belief that the main cause of the discrepancy between observed and modelled runoff will arise from errors and develop predictors of future errors based on this structure which can then be used to obtain improved flow forecasts. A feature of errors from a conceptual rainfall-runoff model is that there is a tendency for errors to persist so that sequences of positive errors (underestimation) or negative errors (overestimation) are common. This dependence structure in the error sequence may be exploited by developing error predictors which incorporate this structure and allow future errors to be predicted. Error prediction is now a well established technique for forecast updating in real-time (Box and Jenkins, 1970; Moore, 1982, 1985).

The two components of the ARMA model, namely the direct serial correlation properties of a data series, X_t, and the smoothing effects of an updated running mean through the series, X_t, are described by, for example, Shaw (1994).

Auto regression:

$$X_t = \alpha_1 X_{t-1} + \alpha_2 X_{t-2} + \alpha_p X_{t-p} + Z_t \qquad (14.7)$$

Moving average:

$$X_t = Z_t + \beta_1 Z_{t-1} + \beta_2 Z_{t-2} + \ldots \beta_q Z_{t-q} \qquad (14.8)$$

where Z_t are random numbers with zero mean and variance σ_2^2 (Chatfield, 1980). If the first-order terms of each component are combined, the series X_t, known as the Thomas-Fiering model (Maass, *et al.,* 1962), becomes:

$$X_t = \alpha_1 X_{t-1} + Z_t + \beta_1 + Z_{t-1} \; (-1 < \alpha_1 < 1) \text{ and } (-1 < \beta_1 < 1) \qquad (14.9)$$

Estimates of the parameters α_1 and β_1 can be obtained from the serial correlation coefficients r_1 and r_2 and lags 1 and 2, respectively:

$$r_1 = \frac{(1 - \alpha_1\beta_1)(\alpha_1 - \beta_1)}{1 + \beta_1^2 + 2\alpha_1\beta_1} \qquad (14.10)$$

$$r_2 = \alpha_1 r_1$$

The parameters of the ARMA model may be estimated by several different methods. Wang and Singh (1994) compare the least-squares, method of moments and maximum likelihood methods, using an auto-regressive (AR) model. They conclude that, provided the number of points representing the time-series is large enough, all three methods are approximately the same. An autocorrelation function approach is proposed which employs a minimization of the sum of squares of differences between the autocorrelation function calculated from the measured data series, and that from the data series generated by the model (or forecasts).

While this type of approach is increasingly being used with flow prediction models, it has not generally been used to provide updating of rainfall measurement forecasting procedures. One exception is the use of a Kalman filter approach as proposed by Cain and Smith (1977) and Collinge (1991). This technique is capable of recognizing gross errors in measurements of predictions. However, if measurement or forecast errors are small or absent, then simpler techniques are as good as those based on a Kalman filter approach (Anson and O'Connor, 1994). In practice, of course, measurements and forecast errors are present and Kalman filtering technique is relevant, although forecast efficiency is reduced, that is the least square matching between forecast and measured flows cannot be expected to be perfect.

14.4 REVIEW OF HYDROGRAPH FORECAST ACCURACY ATTAINED USING RESEARCH AND OPERATIONAL SYSTEMS

14.4.1 Impact of spatial, temporal and rainfall intensity resolution

The impact of radar and satellite data upon the accuracy of hydrograph forecasts will be dependent upon the spatial, temporal and intensity resolution of the data used. Kouwen and Garland (1989) found that a radar resolution of 10 km × 10 km over a 3 250 km^2 catchment was sufficient for modelling floods produced by either thunderstorms or frontal systems. However, Ogden and Julien (1994), investigating two catchments of size 32 km^2 and 121 km^2, found that the effect of radar data spatial resolution depended upon the importance of two processes, namely "storm smearing" and "watershed smearing".

Storm smearing occurs when the rainfall data length scale approaches or exceeds the rainfall correlation length (approximately 2.3 km for convective cells). This tends to decrease rain rates in high intensity regions and increase rain rates adjacent to low intensity regions thereby effectively reducing rainfall gradients. It is independent of basin size. Watershed smearing occurs when the radar grid size approaches the characteristics catchment size (square root of catchment area). In this case, the uncertainty of the location of rainfall within the catchment boundary is increased.

Hence, in convective rainfall in which large rainfall gradients are present, it is necessary to use a radar grid size of around 1 km × 1 km. For very small urban catchments (sewage systems) it may even be necessary to use a smaller grid size if watershed smearing is to be avoided. However, for large urban or rural catchments grid sizes of 2 km × 2 km or even 5 km × 5 km are quite adequate. Michaud and Sorooshian (1994) found that, for convective rainfall in an arid region, spatial averaging of rainfall over 4 km pixels led to consistent reductions in peak flow that, on average, represented 50 per cent of the observed flow.

The temporal variation of rainfall input to a hydrological model also has a significant effect on the predicted hydrograph. Ball (1994) noted that estimation of the time of concentration for a catchment is dependent on the temporal pattern of the rainfall access and may be 22 per cent longer or 19 per cent shorter than that predicted using a constant rate of rainfall excess. Hence, the time of concentration for a catchment must be determined taking into account the pattern of magnitude of the rainfall excess. However, the peak discharge was found to be independent on the pattern of rainfall excess. Hence we may conclude that if the temporal resolution of the rainfall data prevent a close reproduction of the actual rainfall variations, in time the resultant predicted hydrograph could be subject to significant timing errors. In practice, for convective rainfall, data must be available at intervals not greater than 5 minutes and even this could be too coarse in some cases, as illustrated by Figure 14.4.

Cluckie, *et al*. (1991) investigated the intensity resolution required of radar data. In this case, it was concluded that 8-bit (eight intensity levels) were adequate for most rural catchments and probably most urban catchments. The bulk of the process-describing information is concentrated at the low-frequency end of the spectra, and this portion of the signal is retained by flow forecasting models despite degradation of intensity resolution. Nevertheless, in convective rainfall a reduced intensity resolution may have the same effect as spatial resolution in causing storm smearing, that is reduce rainfall gradients.

14.4.2 Hydrograph accuracy from radar-based rainfall input

Early assessments of the impact of radar data input to flow forecasting (Anderl, *et al.,* 1976; Barge, *et al.,* 1979) were optimistic and hydrograph simulations were described showing considerable improvements over hydrographs derived using

raingauge data alone. However, others (Gorrie and Kouwen, 1977) noted that generally very little improvement was evident in convective rainfall. The effects of errors in radar measurements of precipitation were highlighted by Collier and Knowles (1986). Similar results were reported by Roberts (1987), who stressed the difficulty of using radar data which were not adjusted accurately in real time by whatever method.

Further problems are encountered when rainfall forecasts are input to hydrological models. Schultz (1987) investigated the impact of forecast hydrographs of variation in the forecast rainfall scenario used. A real-time adaptive model minimizing the sum of squares of deviations between the observed and forecast hydrograph was tested and found to be a promising approach. Likewise, Cluckie and Owens (1987), using the adaptive transfer function approach discussed in section 14.3.1, also reported encouraging results, although the occasional grossly incorrect forecast was noted and ascribed to a very large rainfall forecast error. More recently, adaptive distributed models have been developed, for example Chander and Fattorelli (1991), but these will require extensive real-time testing.

While these assessments provide indications of the potential of radar (and perhaps satellite) data and rainfall forecasts derived from them, it is necessary to provide long-term operational assessments of performance. The results, using an isolated event model (Haggett, *et al*., 1991), from an assessment of flood events in a small catchment in north London are shown in Figure 14.5. The variation of average root mean square hydrograph error is shown as a function of forecast lead time for both frontal and convective events (FOAG, 1993). There is a considerable difference between the two types of events, with convective events being much more poorly forecast. Improvements in performance for short lead times have been achieved using higher resolution forecast data — 2 km compared with the 5 km FRONTIERS forecast (Moore, *et al*., 1993) — but the basic difficulty of errors in input data, however caused, remains.

Error correcting procedures, as discussed in the previous section, are clearly essential for real-time operational systems. Moriyama and Hirano (1980) developed a rainfall-runoff model using the Kalman filter method. They found that considerable underestimates of surface rainfall made using radar could still provide hydrograph forecasts comparable with those derived using measurements from a very dense raingauge network. Further work using rainfall-runoff models in continuous operation is a high priority.

14.5 ADVANTAGES AND DISADVANTAGES OF REMOTELY-SENSED DATA

Lumped and, to a lesser extent, distributed models are used operationally to predict river flows. Raingauge measurements provide estimates of areal rainfall, although network density has a significant impact on the accuracy of the estimates. Satellite and radar data provide good spatial and temporal, precipitation measurement coverage from a single location. Radar data in particular have the capability of providing measurements over areas of 1 km^2 or less at intervals of 1 minute or less.

Unfortunately the data provided by radar and satellite systems require interpretation and comprehensive quality control before they can be used as input to models. Radar provides a direct measurement of precipitation, albeit in terms of the reflectivity of the hydrometeor. However satellite systems provide measurement of the brightness or temperature of the clouds which produce precipitation or the microwave properties of clouds (no active radar has yet been flown on a satellite) which may be interpreted in terms of precipitation. Microwave satellite systems also offer the prospect of providing data on catchment physical characteristics (Blyth, 1993).

The retrieval algorithms for both radar and satellite systems introduce uncertainties into the measurements of precipitation which may have a profound impact on flow forecasts produced using these data. Nevertheless, unless raingauge networks are very dense, the measurements provided by them also introduce significant sampling errors.

The advantages of data collection at a single location and spatial and temporal comprehensiveness of the measurements mean that the accuracy limitations of remotely-sensed data compared with measurements from a dense raingauge network are, in most circumstances, acceptable. This is not to say that work should not be undertaken to improve accuracy, but rather that present limitations of remotely-sensed data should be no bar to the development of hydrological models for use with remotely-sensed data. Indeed, the use of remotely-sensed data are the only practical way of modelling large remote catchments provided appropriate mathematical structures for the hydrological models are used (Schultz, 1993). Even for small catchments a blend of raingauge data with remotely-sensed data can provide enhanced measurements over either system alone.

14.6 SUMMARY AND CURRENT STATUS

Measuring and forecasting spatial and temporal variations of precipitation are fundamental elements of river flow forecasting. A range of hydrological model structures are available, some of which have been developed with the use of remotely-sensed data in mind. Whatever the type of input data available, it is essential that real-time error correction procedures are implemented. It is unrealistic to expect input data to provide continuously a completely accurate representation of catchment precipitation.

Remotely-sensed data offer certain advantages providing high resolution information from a single location. On the other hand, raingauge networks measure the actual rainfall, albeit at a point, and require little interpretation. Where possible, gauges and remotely-sensed data should be used together.

While digital radar and satellite data have been available for about 20 years, their use as input to hydrological models has progressed only slowly. Problems with data quality control and error handling have retarded progress. Nevertheless, there is now an appreciation of what is needed operationally and work is underway in several countries. It is scientifically healthy that different models are used.

Numerical weather prediction models have improved considerably over this same time period and they are now

capable of providing useful precipitation forecast information. It will be important to assess remotely-sensed data-based forecasts against these model-based forecasts in deciding what is best for hydrological forecasting. There is an increasing tendency for remotely-sensed data to be assimilated into models and for model output to be used with remotely-sensed data.

Numerous studies have shown that real-time flow forecasting using a range of input data provides accurate information for the flood hydrologist much of the time. However, on a number of occasions, including some extreme conditions, forecasts may be significantly in error. This may be due to the model formulation or calibration, or errors in the input data, but whatever the reason it is evident that there remains a need for continuing research and development. Concommitant with this is a need to assess continually model performance. This tends to be overlooked after model installation, with some notable exceptions, see for example Borrows, *et al*. (1992). Consequently, there are few if any long-term records with which to assess the impact of future changes, or indeed with which to compare procedures and models. This has recently been recognized by WMO (WMO, 1994*c*) and is recognized in the United States as an important element in the use of the data from the network of WSR-88D radars (Hudlow, *et al.,* 1991). Nevertheless, it is a matter of some urgency in many countries if assessments of the improvements or otherwise of systems using remotely-sensed or model data are to be obtained.

REFERENCES

Abbott, M. B., J. C. Bathurst, J. A. Cunge, P. E. O'Connell and J. Rasmussen, 1986*a*: An introduction to the European hydrological system — Système hydrologique européen, "SHE", 1: History and philosphy of a physically-based, distributed modelling system, *Journal of Hydrology*, 87, pp. 45–59.

Abbott, M. B., J. C. Bathurst, J. A. Cunge, P. E. O'Connell and J. Rasmussen, 1986*b*: Structure of a physically-based, distributed modelling system, *Journal of Hydrology*, 87, pp. 61–77.

Alaka, M. A., J. P. Charba and R. C. Elvander, 1977: *Thunderstorm Prediction for Use in Air Traffic Control*, Report No. FRA-RD-77-40, U.S. Department of Transportation, Federal Aviation Administration, Washington, D.C., 32 pp.

Albright, M. D., E. E. Decker, R. J. Reed and R. Dang, 1985: The diurnal variation of deep convection and inferred precipitation in the central tropical Pacific during January–February 1979, *Monthly Weather Review*, 113, pp. 1663–1680.

Anderberg, M. R., 1973: *Cluster Analysis for Applications*, Academic Press, London.

Anderl, B., W. Attmannspacher and G. A. Schultz, 1976: Accuracy of reservoir inflow forecasts based on radar rainfall measurements, *Water Resources Research*, 12, 2, pp. 217–223.

Andersson, T., 1991: An advective model for probability nowcasts of accumulated precipitation using radar, in *Hydrological Applications of Weather Radar* (I. D. Cluckie and C. G. Collier, eds.), Ellis Horwood Ltd, Chichester, pp. 325–330.

Andrieu, H. and J. D. Creutin, 1995: Identification of vertical profiles of radar reflectivity for hydrological applications using an inverse method. Part I: Formulation, *Journal of Applied Meteorology*, 34, pp. 225–239.

Andrieu, H., G. Delrieu and J. D. Creutin, 1995: Identification of vertical profiles of radar reflectivity for hydrological applications using an inverse method. Part II: Sensitivity analysis and case study, *Journal of Applied Meteorology*, 34, pp. 240–259.

Anson, M. and K. M. O'Connor, 1994: A reappraisal of the Kalman filtering techniques as applied in river flow forecasting, *Journal of Hydrology*, 161, pp. 197–226.

Arkin, P. A., 1979: The relationship between fractional coverage of high cloud and rainfall accumulations during GATE over the B-scale array, *Monthly Weather Review*, 107, pp. 1382–1387.

Arkin, P. A. and P. E. Ardanuy, 1989: Estimating climatic-scale precipitation from space: A review, *Journal of Climate*, 2, pp. 1229–1238.

Arkin, P. A and B. N. Meisner, 1987: The relationship between large-scale convective rainfall and cold cloud over the western hemisphere during 1982-84, *Monthly Weather Review*, 115, pp. 51–74.

Arking, A. and J. D. Childs, 1985: Retrieval of cloud cover parameters from multispectral satellite images, *Journal of Climate Applied Meteorology*, 24, pp. 322–333.

Atlas, D., 1964: Advances in radar meteorology, in *Advances in Geophysics*, 10, pp. 318–478, Academic Press, New York.

Atlas, D. and T. L. Bell, 1992: The relation of radar to cloud area-time integral and implcations for rain measurements from space, *Monthly Weather Review,* 120, pp. 1997–2008.

Atlas, D. and F. H. Ludlam, 1961: Multi-wavelength radar reflectivity of hailstorms, *Quarterly Journal of the Royal Meteorological Society*, 87, pp. 523–534.

Atlas, D. and O. Thiele, 1981: *Precipitation Measurements from Space*, Workshop reports, NASA, Goddard Space Flight Centre, Greenbelt, Maryland, October.

Atlas, D., D. Rosenfeld and D. A. Short, 1990: The estimation of convective rainfall by area integrals, Part I: The theoretical and empirical basis, *Journal of Geophysical Research*, 95, 3, pp. 2153–2160.

Atlas, D., C. W. Ulbrich and R. Meneghini,1982: *The Multiparameter Remote Measurement of Rainfall*, Technical Memorandum No. NASA TM 83971, Goddard Space Flight Center, NASA, Greenbelt, Maryland, 84 pp.

Auer, A. H., Jr., 1984: Hail recognition through the combined use of radar reflecitivity and cloud top temperature, *Monthly Weather Review.*

Auer, A. H., Jr. and J. D. Marwitz, 1972: Hail in the vicinity of organized updrafts, *Journal of Applied Meteorology*, 11, pp. 748–752.

Auer, A. H., Jr. and J. D. Marwitz, 1973: Reply to comments on "Hail in the vicinity of organized updrafts", *Journal of Applied Meteorology*, 12, 896 pp.

Auer, A. J., Jr., 1972: Distribution of graupel and hail with size, *Monthly Weather Review*, 100, pp. 325–328.

Austin, G. L. and A. Bellon, 1974: The use of digital weather radar records for short-term precipitation forecasting, *Quarterly Journal of the Royal Meteorological Society,* 100, pp. 658–664.

Austin, G. L. and A. Bellon, 1982: Very-short-range forecasting of precipitation by the objective extrapolation of radar and satellite data, in *Nowcasting*, Chapter 3.3 (K. A. Browning, ed.), Academic Press, London, pp. 177–190.

Austin, P. M., 1987: Relation between measured radar reflectivity and surface rainfall, *Monthly Weather Review*, 115, 5, pp. 1053–1070.

Bader, M. J. and W. T. Roach, 1977: Orographic rainfall in warm sectors of depressions, *Quarterly Journal of the Royal Meteorological Society*, 103, pp. 269-280.

Bader, M. J., C. G. Collier and F. F. Hill, 1983: Radar and raingauge observations of a severe thunderstorm near Manchester: 5/6 August 1981, *Meteorological Magazine*, 112, pp. 149–162.

Baer, F. and J. J. Tribbia, 1977: On complete filtering of gravity modes through non-linear initialization, *Monthly Weather Review,* 105, pp. 1536–1539.

Ball, G. H., 1965: *Data Analysis in the Social Sciences*, Proceedings of the Fall Joint Computer Conference, Spartan Books, Washington, D.C., pp. 533–560.

Ball, J. E., 1994: The influence of storm temporal patterns on catchment response, *Journal of Hydrology*, 158, pp. 285–303.

Barclay, P. A. and K. E. Wilk, 1970: Severe thunderstorm radar echo motion and related weather events hazardous to aviation operations, *ESSA, Technical Memorandum* No. ERLTM-NSSL 46, 63 pp.

Barge, B. L., R. G. Humphries, S. J. Mah and W. K. Kuhnke, 1979: Rainfall measurements by weather radar: Applications to hydrology, *Water Resources Research*, 15, 6, pp. 1380–1386.

Barrett, E. C., R. W. Herschy and J. B. Stewart, 1986: *The Columbus Project: Space Station User Requirements for Hydrology,* 28 February, Final Report to the Natural Environmental Research Council, Contract No. F60/96/15, 85 pp.

Bathurst, J. C., 1986*a*: Physically-based distributed modelling of an upland catchment using the Système hydrologique européen, *Journal of Hydrology*, 87, pp. 79–102.

Bathurst, J. C., 1986*b*: Sensitivity analysis of the Système hydrologique européen for an upland catchment, *Journal of Hydrology*, 87, pp. 103–123.

Battan, L. J., 1973: *Radar Observation of the Atmosphere*, University of Chicago Press, Chicago, 324 pp.

Beale, R. and T. Jackson, 1992: *Neural Computing: An Introduction*, Bristol, IOP Publishing.

Bell, R. S., 1978: The forecasting of orographically enhanced rainfall accumulations using 10-level model data, *Meteorological Magazine*, 107, pp. 113–124.

Bellon, A. and G. L. Austin, 1984: The accuracy of short-term rainfall forecasts, *Journal of Hydrology*, 70, pp. 35–49.

Bellon, A. and G. L. Austin, 1986: On the relative accuracy of satellite and raingauge rainfall measurements over middle latitudes during daylight hours, *Journal of Climate Applied Meteorology*, 25, pp. 1712–1724.

Bengtsson, L., 1985: Medium-range forecasting at the ECMWF, *Advanced Geophysics*, 28B, pp. 3-54.

Berri, G. J. and J. Paegle, 1990: Sensitivity of local predictions to inital conditions, *Journal of Applied Meteorology*, 29, pp. 256–267.

Beven, K., 1989: Changing ideas in hydrology — the case of physically-based models, *Journal of Hydrology*, 105, pp. 157–172.

Beven, K. J. and M. J. Kirkby, 1979: A physically-based variable contributing area model of basin hydrology, *Hydrological Science Bulletin*, 24, 13, pp. 43–69.

Bianco, A. and H. Huang, 1990: *Satellite and Radar Forecast Techniques for Short-term Prediction of Storm Motion Using the Remote Atmosphere Processing and Display (RAPID) System*, Geophysics Laboratory Technical Report, GL-TR-90-0179.

Blackmer, R. H., R. O. Duda and R. Reboh, 1973: *Application of Pattern Recognition to Digitised Weather Radar Data*, Final Report (Contract No. 1-36072), SRI Project No. 1287, Stanford Research Institute, Menlo Park, California, 89 pp.

Blanchard, D. C., 1953: Raindrop size distribution in Hawaiian rains, *Journal of Meteorology*, 10, pp. 457–473.

Blyth, K., 1993: The use of microwave remote sensing to improve spatial parametrisation of hydrologicl models, *Journal of Hydrology*, 152, pp. 103–129.

Bond, J. E., K. A. Browning and C. G. Collier, 1981: Estimate of surface gust speeds using radar observations of showers, *Meteorological Magazine*, 110, pp. 29–40.

Born, M. and E. Wolf, 1964: *Principles of Optics*, Second edition, McMillan, New York.

Borrows, P. F., R. J. Moore, C. M. Haggett, M. Crees, D. A. Jones, D. S. Hotchkiss and K. B. Black, 1992: *Development of a Weather Radar-based Rainfall Forecasting Technique for Real-time Operational Use*, in International Weather Radar Networking Final Seminar of the COST Project 73, (C. G. Collier, ed.), Kluwer Academic Publisher, pp. 243–249.

Bosart, L. F. and M. G. Landin, 1994: An assessment of thunderstorm probability forecasting skill, *Weather Forecasting*, 9, pp. 522–531.

Boucher, R. J., 1981: *Snowfall Rates Obtained from Radar Reflectivity Within a 50-km Range*, Technical Report No. AFGL-TR-81-0265 (Met. Div. Project 6670), US Air Force Geophysics Laboratory, 25 pp.

Bowen, B. A., 1989: *Cloud Classification Using Neural Computing Technology*, contractors report by Comp. Eng. Sens. Ltd., Ontario, Canada to Atmosphere Environment Service, Downsview, Ontario, Canada, 40 pp.

Box, G. E. P. and G. M Jenkins, 1970: *Time Series Analysis and Control*, Holden-Day, 553 pp.

Brice, C. R. and C. L. Fennema, 1970: Scene analysis using regions, *Artificial Intelligence*, 1, pp. 205–226.

Brown, R., P. D. Newcomb, J. Cheung-Lee and G. Ryall, 1994: Development and evaluation of the forecast step of the FRONTIERS short-term precipitation forecasting system, *Journal of Hydrology*, 158, pp. 79–105.

Brown, R., G. P. Sargent, P. D. Newcomb, J. Cheung-Lee and P. M. Brown, 1991: *Development of the FRONTIERS Precipitation Nowcasting System to Use Mesoscale Model Products*, Preprints of the twenty-fifth International Conference on Radar Meteorology, Paris, American Meteorological Society, pp. 79–85.

Browning, K. A., 1973: The structure of rainbands within a mid-latitude depression, *Quarterly Journal of the Royal Meteorological Society*, 99, 420, pp. 215–231.

Browning, K. A.,1978: Meteorological appliances of radar, *Rep. Prog. Phys.*, 41, pp. 761–806.

Browning, K. A., 1980: *Local Weather Forecasting*, Proceedings, Royal Society, London, Series A 371, pp. 179–211.

Browning, K. A., 1983: Air motion and precipitation growth in a major snowstorm, *Quarterly Journal of the Royal Meteorological Society*, 109, pp. 225–242.

Browning, K. A., 1990: Rain, rainclouds and climate, *Quarterly Journal of the Royal Meteorological Society*, 116, 495, pp. 1025–1051.

Browning, K. A. and C. G. Collier, 1989: Nowcasting of Precipitation Systems, *Review of Geophysics*, 27, 3, pp. 345–370.

Browning, K. A., F. F. Hill and C. W. Pardoe, 1974: Structure and mechanism of preciptation and the effect of orography in a wintertime warm sector, *Quarterly Journal of the Royal Meteorological Society*, 100, pp. 309–330.

Browning, K. A., M. E. Hardman, T. W. Harrold and C. W. Pardoe, 1993: The structure of rainbands within a mid-latitude depression, *Quarterly Journal of the Royal Meteorological Society*, 99, 420, pp. 215–231.

Browning, K. A., C. G. Collier, P. R. Larke, P. Menmuir, G. A. Monk and R. G. Owens, 1982: On the forecasting of frontal rain using a weather radar network, *Monthly Weather Review*, 110, pp. 534–552.

Bruen, M. and J. C. I Dooge, 1984: An effective and robust method for estimating unit hydrograph ordinates, *Journal of Hydrology*, 70, pp. 1–24.

Brussaard, G., 1976: *A Meteorological Model for Rain-induced Cross Polarization*, IEEE Trans., AP-24, pp. 5–11.

Brylev, G. B., V. M. Melnikov, N. F. Mikhailov, G. G. Schukin and I. A. Traakukin, 1995: *Current State of Radar Meteorology in Russia*, Proceedings, COST-75, International Seminar on Advanced Weather Radar Systems, September, CEC, Brussels.

Buckland, R. W., 1993: *Implications of Climate Variability for Food Security in the Southern African Development Community*, in ENSO/Famine Early Warning System Workshop, Budapest, October.

Bullock, C. S. and B. E. Heckman, 1986: *Forecast Office Operational Scenarios in the 1990s*, Preprints of the eleventh Conference on Weather Forecasting and Analysis, Kansas City, Missouri, 17–20 June 1986, American Meteorological Society, Boston, pp. 183–187.

Burgess, D. W. and P. S. Ray, 1986: Principles of radar. *Mesoscale Meteorology and Forecasting* (P. Ray, ed.), American Meteorological Society, Boston, Chapter 30*a*, pp. 85–117.

Burn, D. H. and D. B. Boorman, 1993: Estimation of hydrological parameters at ungauged catchments, *Journal of Hydrology*, 143, pp. 429–454.

Cain, D. E. and P. L. Smith, Jr., 1977: *A Sequential Analysis Strategy for Adjusting Radar Rainfall Estimates on the Basis of Raingauge Data in Real Time*, Proceedings of the Conference on Hydrometeorology, Toronto, pp. 280–285.

Calheiros, R. V. and I. I. Zawadzki, 1987: Reflectivity rain-rate relationships for radar hydrology in Brazil, *Journal of Applied Meteorology*, 26 pp. 118–132.

Campbell, S. D. and S. H. Olson, 1987: Recognizing low-altitude wind shear hazards from Doppler weather radar: An artificial intelligence approach, *Journal of Atmospheric and Oceanic Technology*, 4, 1, pp. 5–18.

Carbone, R. E., 1972: *Evaluation of a Dual Wavelength Hail Detector*, Proceedings of the fifteenth Conference on Radar Meteorology, American Meteorological Society, Boston, pp. 7–12.

Carbone, R. E., D. Atlas, P. J. Eccles, R. Fetter and E. Mueller, 1973: Dual wavelength radar hail detection, *Bulletin of the American Meteorological Society*, 54, pp. 921–924.

Carpenter, K. M., 1979: An experimental forecast using a non-hydrostatic mesoscale model, *Quarterly Journal of the Royal Meteorological Society*, 105, pp. 629–655.

Carpenter, K. M., 1982: Model forecasts for locally-forced mesoscale systems, in *Nowcasting* (K. A. Browning, ed.), Academic Press, London, pp. 223–234.

Chander, S. and S. Fattorelli, 1991: Adaptive grid-square-based geometrically distributed flood-forecasting model, Paper 38 in *Hydrological Applications of Weather Radar* (I. D. Cluckie and C. G. Collier, eds.), Ellis Horwood, Chichester, pp. 424–439.

Chandrasekar, V. and E. G. Gori, 1991: Multiple distrometer observations of rainfall, *Journal of Applied Meteorology*, 30, pp. 1514–1520.

Changnon, S. A., Jr., 1970: Hail streaks, *Journal of Atmospheric Science*, 27, 109 pp.

Chatfield, C., 1980: *The Analysis of Time Series: An Introduction*, Second edition, Chapman and Hall, London, 268 pp.

Chatfield, C., 1983: *Statistics for Technology*, Third edition, Chapman and Hall, London, 381 pp.

Cheng, M. and R. Brown, 1993: Estimation of area-average rainfall for frontal rain using the threshold method, *Quarterly Journal of the Royal Meteorological Society*, 119, pp. 825–844.

Cheng, M., R. Brown and C. G. Collier, 1993: Delineation of rain areas using Meteosat IR-VIS data in the region of the United Kingdom, *Journal of Applied Meteorology*, 32, pp. 884–898.

Cherry, S. M., 1978: *Dual Frequency Radars — Use for Attenuation Measurements and Solid-liquid Phase Determination*, Proceedings of the Radar Workshop, Graz, Austria, November.

Cherry, S. M. and J. W. F. Goddard, 1983: *URSI Symposium on Multiple Parameter Radar Measurement of Precipitation*, United Kingdom.

Chiu, L. S., 1988: *Rain Estimation from Satellite: Areal Rainfall-rain Area Relations*, Third Conference on Satellite Metorology and Ocean, Anaheim, California, American Meteorological Society, Boston, pp. 363–368.

Chiu, L. S. and B. Kedem, 1990: Estimating the exceedance probability of rain rate by logistic regression, *Journal of Geophysical Research*, 95, D3, pp. 2217–2227.

Chow, V. T., 1951: A general formula for hydrologic frequency analysis, *Trans. Am. Geophy. Union*, 32, pp. 231–237.

Ciccione, M. and V. Pircher, 1984: *Very-short-Time Forecasting of Rain from Single Radar Data*, Proceedings of the second International Symposium on Nowcasting, Norrköping, Sweden, 3-7 September, pp. 241–246.

Clark, C. O., 1943: Storage and the Unit Hydrograph, *Trans. ASCE*, 108, pp. 1333–1360.

Cluckie, I. D. and M. D. Owens, 1987: Real-time rainfall — runoff models and use of weather radar information, Chapter 12 in *Weather Radar and Flood Forecasting* (V. K. Collinge and C. Kirby, eds.), John Wiley and Sons, Chichester, pp. 191–190.

Cluckie, I. D., K. A. Tilford and G. W. Shepherd, 1991: Radar signal quantization and its influence on rainfall-runoff models, Chapter 39 in *Hydrological Applications of Weather Radar* (I. D. Cluckie and C. G. Collier, eds.), Ellis Horwood, Chichester, pp. 440–451.

Cluckie, I. D., P. F. Ede, M. D. Owens, A. C. Bailey and C. G. Collier, 1987: Some hydrological aspects of weather radar research in the United Kingdom, *Hydrological Sciences Journal*, 332, 3, pp. 329–346.

Collier, C. G., 1975: A representation of the effects of topography on surface rainfall within moving baroclinic disturbances, *Quarterly Journal of the Royal Meteorological Society*, 101, pp. 407–422.

Collier, C. G., 1977: The effect of model grid length and orographic rainfall efficiency on computed surface rainfall, *Quarterly Journal of the Royal Meteorological Society*, 103, pp. 247–253.

Collier, C. G., 1981: *Objective Rainfall Forecasting Using Data from the United Kingdom Weather Radar Network*, Proceedings IAMAP Symposium, Hamburg, 25–28 August, Special Publication No. ESA SP-165, pp. 201–206.

Collier, C. G., 1986*a*: Accuracy of rainfall estimates by radar, Part I: Calibration by telemetering raingauges, *Journal of Hydrology*, 83, pp. 207–223.

Collier, C. G., 1986*b*: Accuracy of rainfall estimates by radar, Part II: Comparison with raingauge network, *Journal of Hydrology*, 83, pp. 225–235.

Collier, C. G., 1989: *Applications of Weather Radar Systems: A Guide to Uses of Radar Data in Meteorology and Hydrology*, Ellis Horwood (Second edition published by Praxis Ltd., Chichester and John Wiley, 1996), 294 pp.

Collier, C. G., 1990: Assessing and forecasting extreme rainfall in the United Kingdom, *Weather*, 45, 4, pp. 103–112.

Collier, C. G., 1991: The combined use of weather radar and mesoscale numerical model data for short period rainfall forecasting, in *Hydrological Applications of Weather Radar* (I. D. Cluckie and C. G. Collier, eds.), Ellis Horwood, Chichester, pp. 331–348.

Collier, C. G. (ed.), 1995: *Proceedings of the COST-75 International Seminar on Advanced Weather Radar Systems*, September, Kluwer Academic Publishers Ltd., Dordocht or CEC, Brussels.

Collier, C. G. and J. M. Knowles, 1986: Accuracy of rainfall-estimates by radar, Part III: Application for short-term flood forecasting, *Journal of Hydrology*, 83, pp. 237–249.

Collier, C. G. and P. R. Larke, 1978: A case study of the measurement of snowfall by radar: An assessment of accuracy, *Quarterly Journal of the Royal Meteorological Society*, 104, pp. 615–621.

Collier, C. G., P. J. Hardaker and C. E. Pierce, 1995: *Radar and Satellite Identification of Deep Convection and Thunderstorms for Operational Flood Forecasting*, Proceedings of the COST-75 International Seminar on Advanced Weather Radar Systems (C. G. Collier, ed.), 20-23 September, Brussels, CEC Report EUR 16013EN, pp. 744–765.

Collier, C. G., P. R. Larke and B. R. May, 1983: A weather radar correction procedure for real-time estimation of surface rainfall, *Quarterly Journal of the Royal Meteorological Society*, 104, pp. 589–608.

Collier, C. G., G. Szejwach and J. Testud, 1990: *Rain Radar*, ESA SP-1119, Report of the Consultancy Group, 80 pp.

Collinge, V. K., 1991: Weather radar calibration in real time: Prospects for improvement, Chapter 2 in *Hydrological Applications of Weather Radar* (I. D. Cluckie and C. G. Collier, eds.), Ellis Horwood, Chichester, pp. 25–42.

Colquhoun, J. R., 1987: A decision tree method of forecasting thunderstorms, severe thunderstorms and tornadoes, *Weather Forecast*, 2, pp. 337–345.

Cooper, J. N. and R. H. Smiley, 1990: *An Object-oriented Toolbox for the Creation of Meteorological Workstations*, Preprints of the sixth International Conference on Interactive Information and Processing Systems for Meteorology, Ocean, and Hydrology, 5–9 February, Anaheim, California, American Meteorological Society, Boston, pp. 229–232.

Cox, D. R. and V. Isham, 1988: *A Simple Spatial-temporal Model of Rainfall*, Proceedings, Royal Society, London, Series A, 415, pp. 317–328.

Crane, R. K., 1976: *Rain Cell Detection and Tracking*, Preprints of the seventeenth Conference on Radar Meteorology, Seattle, Washington, American Meteorological Society, Boston, pp. 505–509.

Crane, R. K., 1990: Space-time structure of rain rate fields, *Journal of Geophysical Research*, 95, D3, pp. 2011–2020.

Crespi, M., M. Monai, A. D. Pesci and A. Trolese, 1995: *Improvements in Clutter Reduction and Precipitation Intensity Measurement for Monte Grande Radar*, Proceedings of the COST-75 International Seminar on Advanced Weather Radar Systems, September, CEC Brussels.

Crum, T. D. and R. L. Alberty, 1993: The WSR-88D and the WSR-88D Operational Support Facility, *Bulletin of the American Meteorological Society*, 74, 8, pp. 1669–1687.

Cullen, M. J. P., 1993: The unified forecast/climate model, *Meteorological Magazine*, 122, 1449, pp. 81–94.

Cullen, M. J. P. and R. J. Purser, 1984: An extended model of semi-geostrophic frontogenesis, *Journal of Atmospheric Sciences*, 41, pp. 1477–1497.

Curié, M. and D. Janc, 1993: Predictive capabilities of a one-dimensional convective cloud model with forced lifting and a new entrainment formulation, *Journal of Applied Meteorology*, 32, pp. 1733–1740.

Dalezois, N. R. and N. Kouwen, 1990: Radar signal interpretation in warm season rainstorms, *Nordic Hyd.*, 21, pp. 47–64.

Diskin, M. H. and E. S. Simpson, 1978: A quasi-linear, spatially distributed cell models for the surface runoff system, *Water Resources Bulletin*, 14, pp. 903-918.

Dixon, M. and G. Wiener, 1993: TITAN: Thunderstorm identification, tracking, analysis, and nowcasting — a radar-based methodology, *Journal of Atmospheric and Oceanic Technology*, 10, 6, pp. 785–797.

Donaldson, R. J., 1965: Methods for identifying severe thunderstorms by radar: A guide and bibliography, *Bulletin of the American Meteorological Society*, 46, pp. 174–193.

Doneaud, A. A., S. I. Niscov, D. L. Priegrutz and P. L. Smith, 1984: The area-time integral as an indicator for convective rain volumes, *Journal of Climate Applied Meteorology*, 23, pp. 555–561.

Doneaud, A. A., P. L. Smith, A. S. Dennis and S. Senggupta, 1981: A simple method for estimating convective rain volume over an area, *Water Resources Research*, 17, pp. 1676–1682.

Dooge, J. C. I. and M. Bruen, 1989: Unit hydrograph stability and linear algebra, *Journal of Hydrology*, 111, pp. 377–390.

Doswell, C. A. III 1986: Short-range forecasting, in *Mesoscale Meteorology* (P. Ray, ed.), American Meteorological Society, Boston, Chapter 29, pp. 689–719.

Doviak, R. J. and D. S. Zrnic, 1984: *Doppler Radar and Weather Observations*, Academic Press, New York, 458 pp.

Duda, R. O. and R. H. Blackmer, 1972: *Application of Pattern Recognition Techniques to Digitised Weather Radar*, Final Report covering the period 25 May 1971 to 31 March 1972, Contract No 1-36072, SRI Project No 1287, Stanford Research Institute, Menlo Park, California, 135 pp.

Duda, R. O. and P. E. Hart, 1973: *Pattern Classification and Scene Analysis*, John Wiley and Sons, New York.

Duncan, M. R., B. Austin, F. Fabry and G. L. Austin, 1993: The effect of gauge sampling density on the accuracy of streamflow prediction for rural catchments, *Journal of Hydrology*, 142, pp. 445–476.

Dunn, L. B. and J. D. Horel, 1994*a*: Prediction of Central Arizona convection, Part I: Evaluation of the NGM and

Eta model prediction forecasts, *Weather Forecasting*, 9, pp. 495–507.

Dunn, L. B. and J. D. Horel, 1994*b*: Prediction of Central Arizona convection, Part II: Further examination of the Eta model forecasts, *Weather Forecasting*, 9, pp. 508–521.

DWRHP, 1977: *Dee Weather Radar and Real-time Hydrological Forecasting Project*, Central Water Planning Unit, Reading, 172 pp.

Ebert, E., 1987: A pattern recognition technique for distinguising surface and cloud types in the polar regions, *Journal of Climate and Applied Meteorology*, 26, pp. 1412–1427.

Eccles, P. J. and D. Atlas, 1973: A dual-wavelength radar hail detector, *Journal of Applied Meteorology*, 12, pp. 847–856.

Elio, R. and J. de Haan, 1985: *Knowledge Representation in an Expert Storm Forecasting System*, Proceedings of the ninth Joint Conference on Artificial Intelligence, Los Altos, California, pp. 400–406.

Elio, R., J. de Haan and G. S. Strong, 1987: METEOR: An artificial intelligence system for convective storm forecasting, *Journal of Atmospheric and Oceanic Technology*, 4, 1, pp. 19–28.

Elvander, R. C., 1976: *An Evaluation of the Relative Performance of Three Weather Radar Echo Forecasting Techniques*, Preprints of the seventeenth Conference on Radar Meteorology, Seattle, Washington, American Meteorological Society, Boston, pp. 526–532.

Endlich, R. M., D. E. Wolf, D. J. Hall and A. E. Brain, 1971: Use of a pattern recognition technique for determining cloud motions from sequences of satellite photographs, *Journal of Applied Meteorology*, 10, pp. 105–117.

Fabry, F., G. L. Austin and D. Tees, 1992: The accuracy of rainfall estimates by radar as a function of range, *Quarterly Journal of the Royal Meteorological Society*, 118, pp. 435–453.

Fabry, F., A. Bellon, M. R. Duncan and G. L. Austin, 1994: High resolution rainfall measurements by radar for very small basins: The sampling problem reexamined, *Journal of Hydrology*, 161, pp. 415–428.

Farki, B., D. Dagorne, B. Guillot, P. LeBorgne and A. Marsouin, 1992: Classification of clouds over Africa with Meteosat 4, *Veille Climatique Satellitaire*, 43, pp. 54-77.

Filiberti, M. A., L. Eymard and B. Urban, 1994: Assimilation of satellite precipitable water in a meteorological forecast model, *Monthly Weather Review*, 122, pp. 486–506.

Folland, C. K. and A. Woodcock, 1986: Experimental monthly long-range forecasts for the United Kingdom, Part I: Description of the forecasting system, *Meteorological Magazine*, 115, pp. 301–318.

Folland, C. K., J. A. Owen, M. N. Ward and A. W. Colman, 1991: Prediction of seasonal rainfall in the Sahel rgion of Africa using empirical and dynamical methods, *Journal of Forecasting*, 10, pp. 21–56.

Foote, B. G. and C. A. Knight, 1979: Results of a randomized hail suppression experiment in northeast Colorado, Part I: *Journal of Applied Meteorology*, 18, pp. 1526–1537.

Foufoula-Georgiou, E. and P. Kumar, 1990: *Monitoring and Short-term Forecasting of Precipitation Fields using Fourier Domain Shape Analysis*, Conference of Operational Precipitation Estimation and Prediction, Anaheim, California.

Fritsch, J. M. and C. V. F. Chappell, 1980: Numerical prediction of convectively driven mesoscale pressure systems. Part I: Convective parametrisation, *Journal of Atmospheric Sciences*, 37, pp. 1722–1733.

Frontiers Operational Assessment Group (FOAG), 1993: *FRONTIERS Evaluation of Radar-Based Rainfall and River Flow Forecasts April 1992 to March 1993*, Meteorological Office/NRA Final Report of FOAG, Meteorological Office, 122 pp.

Gabel, R. A. and R. A. Roberts, 1980: *Signals and Linear Systems*, John Wiley and Sons, Inc.

Gal-Chen, T., 1978: A method for the initialisation of the anelastic equations: Implication for matching models with observation, *Monthly Weather Review*, 106, pp. 587–606.

Gelb, A (ed.), 1974: *Applied Optimal Estimation*, MIT Press, Cambridge, Massachussetts, 374 pp.

Georgakakos, K. P. and R. L. Bras, 1984*a*: A hydrologically useful station precipitation model, 1: Formulation, *Water Resources Research*, 20, 11, pp. 1585–1596.

Georgakakos, K. P. and R. L. Bras, 1984*b*: A hydrologically useful station precipitation model, 2: Applications, *Water Resources Research*, 20, 11, pp. 1597–1610.

Georgakakos, K. P. and M. D. Hudlow, 1984: Quantitative precipitation forecast techniques for use in hydrologic forecasting, *Bulletin of the American Meteorological Society*, 65, 11, pp. 1186–1200.

Georgakakos, K. P. and M. L. Kavvas, 1987: Precipitation analysis, modeling and prediction in hydrology, *Review of Geophysics*, 25, 2, pp. 163–178.

Georgakakos, K. P. and T. H. Lee, 1987: *Estimation of Mean Precipitation Fields Using Operationally Available Hydrometeorological Data and a Two-dimensional Precipitation Model*, IHR Report 315, Iowa Institute of Hydraulogical Research, University of Iowa, Iowa City, July, 80 pp.

Geotis, S. G., 1963: Some radar measurements of hailstorms, *Journal of Applied Meteorology,* 2, pp. 270–275.

Gill., A. E., 1982: *Atmosphere-Ocean Dynamics*, Academic Press.

Goddard, J. W. F. and S. M. Cherry, 1984: The ability of dual-polarization radar (co-polar linear) to predict rainfall rate and microwave attenuation, *Radio Science*, 19, 1, pp. 201–208.

Goddard, J. W. F., S. M. Cherry and V. N. Bringi, 1982: Comparisons of dual-polarization radar measurements of rain with ground-based distrometer measurements, *Journal of Applied Meteorology*, 21, 2, pp. 252–256.

Gokhale, N. R., 1975: *Hailstorms and Hailstone Growth*, State University of New York Press, Albany, 465 pp.

Golding, B. W., 1986: *Short-range Forecasting over the United Kingdom Using a Mesoscale Forecasting System*, Short and Medium-Range Weather Prediction, Collection of Papers, WMO/IUGG NWP Symposium, Tokyo, 4–8 August, pp. 563–572.

Golding, B. W., 1987: *Strategies for Using Mesoscale Data in an Operational Mesoscale Model*, Proceedings of the Symposium on Mesoscale Analysis and Forecasting, Vancouver, Canada, 17–19 August, ESA SP-282, pp. 569–578.

Golding, B. W., 1990: The Meteorological Office mesoscale model, *Meteorological Magazine*, 119, 1414, pp. 81–96.

Golding, B. W., 1995: Rainfall — Analysis and short-range prediction, Chapter 1 in *British Hydrological Society — Hydrological Uses of Weather Radar*, Occasional Paper No. 5, pp. 1–9.

Gorrie, J. E. and N. Kouwen, 1977: *Hydrological Applications of Calibrated Radar Precipitation Measurements*, Preprint of the Second Conference on Hydrometeorology, Toronto, Ontario, 25-27 October, American Meteorological Society, Boston, pp. 272-279.

Gray, D. M. and D. H. Male (eds.), 1981: *Handbook of Snow*, Pergamon Press, 776 pp.

Gray, W., 1991: *Vertical Profile Corrections based on EOF Analysis of Operational Data*, Preprints of the twenty-fifth International Conference on Radar Meteorology, 24-28 June, Paris, American Meteorological Society, Boston, pp. 821–823.

Gunn, K. and J. Marshall, 1958: The distribution with size of aggregate snowflakes, *Journal of Meteorology*, 15, pp. 452–461.

Haggett, C. M., G. F. Merrick and C. I. Richards, 1991: Quantitative use of radar for operational flood warning in the Thames area, Paper 53 in *Hydrological Applications of Weather Radar* (I. D. Cluckie and C. G. Collier, eds.), Ellis Horwood, Chichester, pp. 590–601.

Hall, D. K. and J. Martinec, 1985: *Remote Sensing of Ice and Snow*, Chapman and Hall, London, 189 pp.

Han, D., 1991: *Weather Radar Information Processing and Real-time Flood Forecasting*, Ph.D. thesis (unpublished), University of Salford.

Hand, W. H. and B. J. Conway, 1995: Nowcasting showers using an object oriented approach, in *Weather Forecasting*, 10, pp. 327–341.

Hanson, C. L., J. F. Zuzel and R. P. Morris, 1983: Winter precipitation catch by heated tipping-bucket gauges, *Trans. ASAE*, 26, 5, pp. 1479–1480.

Haralick, R. M., 1986: Statistical image texture analysis, in *Handbook of Pattern Recognition and Image Processing* (T. Young and K. Fu, eds.), Academic Press, New York, pp. 247–279.

Haralick, R. M. and G. L. Kelly, 1969: *Pattern Recognition with Measurement Space and Spatial Clustering for Multiple Images*, Proceedings IEEE, 57, pp. 654–665.

Hardaker, P. J. and A. H. Auer, 1994: The separation of rain and hail using single polarisation radar echoes and IR cloud-top temperatures, *Met. Apps.*, 1, pp. 201–204.

Hardaker, P. J., A. R. Holt and C. G. Collier, 1995: A melting layer model and its use in correcting for the bright band in single polarisation radar echoes, *Quarterly Journal of the Royal Meteorological Society*, 121, pp. 495–525.

Harries, J. E., 1994: *Earthwatch: The Climate from Space*, Ellis Horwood/John Wiley and Sons, Chichester, 216 pp.

Harrison, M. S. J., 1994*a*: Ensembles, higher-resolution models and future computing power — A personal view, *Weather*, 49, 12, pp. 398–406.

Harrison, M. S. J., 1994*b*: Monthly forecasting in the extra-tropics, *WMO Bulletin*, 43, 3, July, pp. 201–206.

Harrison, S. J. and K. Smith (eds.), 1989: *Weather Sensitivity and Services in Scotland*, Proceedings of the Symposium held at the University of Stirling, 4–5 February 1988, Scottish Academic Press, Edinburgh, 180 pp.

Harrold, T. W., 1974: Ground clutter observed in the Dee Weather Radar Project, *Meteorological Magazine*, 103, pp. 140–141.

Harrold, T. W. and P. G. Kitchingman, 1975: *Measurement of Surface Rainfall Using Radar When the Beam Intersects the Melting Layer*, Preprints of the sixteenth Radar Meteorology Conference, Houston, American Meteorological Society, Boston, pp. 473–478.

Harrold, T. W., E. J. English and C. A. Nicholass, 1974: The accuracy of radar-derived rainfall measurements in hilly terrain, *Quarterly Journal of the Royal Meteorological Society*, 100, pp. 331–350.

Heideman, K. F., H. Huang and F. H. Ruggiero, 1990: *Evaluation of a Nowcasting Technique Based on GOES IR Satellite Imagery*, Preprints of the fifth Conference on Satellite Meteorology and Ocean, London, American Meteorological Society, Boston, pp. 366–371.

Hendry, A. and Y. M. M. Antar, 1984: Precipitation particle identification with centimetre wavelength dual-polarisation radars, *Radio Science*, 19, 1, pp. 115–122.

Herschy, R. W., E. C. Barrett and J. N. Roozekrans, 1985: *Remote Sensing in Hydrology and Water Management*, Final Report, ESA Contract No. 5769/A84/D/JS(Sc), EARSeL, Strasbourg, 268 pp.

Herzegh, P. H. and J. W. Conway, 1986: *On the Morphology of Dual-polarization Radar Measurements: Distinguishing Meteorological Effects from Radar System Effects*, Preprints of the twenty-third Conference on Radar Meteorology, Volume 1: Snowmass, Colorado, American Meteorological Society, Boston, R55–R58.

Hill, F. F., 1984: The development of hailstorms along the south coast of England on 5 June 1983, *Meteorological Magazine*, 113, pp. 345–363.

Hill, F. F. and K. A. Browning, 1979: Persistence and orographic modulation of mesoscale precipitation areas in a potentially unstable warm sector, *Quarterly Journal of the Royal Meteorological Society*, 105, pp. 57–70.

Hill, F. F., K. W. Whyte and K. A. Browning, 1977: The contribution of a weather radar network for forecasting frontal precipitation: A case study, *Meteorological Magazine*, 106, pp. 68–89.

Hino, M., 1970*a*: Runoff forecasts by linear predictive filter, *ASCE Journal of Hydraulics*, 96, HY3, pp. 681–702.

Hino, M., 1970*b*: Runoff forecasting by variable transformation, *ASCE Journal of Hydraulics*, 96, HY4, pp. 871–878.

Holt, A. R., 1988: Extraction of differential propagation phase shift from data from S-band circularly polarised radars, *Electronics Letters*, 24, pp. 1241–1242.

Hoskins, B. J. and F. P. Bretherton, 1972: Atmospheric frontogenesis models, mathematical formulation and solution, *Journal of Atmospheric Sciences*, 27, pp. 11–37.

Houghton, J., 1991: *The Predictability of Weather and Climate*, The Bakerian Lecture 1991, Phil. Trans., Royal Society, London, Series A, 337, pp. 521–572.

Houze, R. A., 1981: Structure of atmospheric precipitation systems — A global survey, *Radio Science*, 16, 5, pp. 671–689.

Hudlow, M. D., J. A. Smith, M. L. Walton and R. C. Shedd, 1991: NEXRAD: New era in hydrometeorology in the USA, Paper 54 in *Hydrological Applications of Weather Radar* (I. D. Cluckie and C. G. Collier, eds.), Ellis Horwood, Chichester, pp. 602–612.

Hughes, C., I. C. Strangeways and A. M. Roberts, 1993: Field evaluation of two aerodynamic raingauges, *Weather*, 48, 3, pp. 66–71.

Jameson, A. R., 1975: *Dual Wavelength Doppler Radar Observations of a Hailstorm at Vertical Incidence*, Preprints of the sixteenth Radar Meteorological Conference, Houston, Texas, 22–24 April, American Meteorological Society, Boston, pp. 43–48.

Jameson, A. R., K. V. Beard and J. Bresch, 1981: *Complications in Deducing Rain Parameters from Polarization Measurements*, Preprints of the twentieth Conference on Radar Meteorology, 30 November–3 December, Boston, American Meteorological Society, Boston, pp. 586–589.

Jatila, E., 1973: Experimental study of the measurement of snowfall by radar, *Geophysica*, 12, 2, pp. 1–10.

Jazwinski, A. H., 1970: *Stochastic Processes and Filtering Theory*, Academic Press, 376 pp.

Jones, D. M. A., 1956: Raindrop size distribution in Hawaiian rains, *Journal of Meteorology*, 10, pp. 457–473.

Joss, J. and A. Waldvogel, 1967: Ein Spektrograph fur Niederschlag Stropfen mit automatischer Auswertung, *Pure App. Geophys*., 62, pp. 240–246.

Joss, J. and A. Waldvogel, 1990: *Precipitation Measurement and Hydrology: A Review*, presented at the Battan Memorial and Radar Conference, Chapter 29*a* (D. Atlas, ed.), American Meteorological Society, Boston, pp. 577–606.

Joss, J., K. Schram, J. C. Thams and A. Waldvogel, 1970: *On the Quantitative Determination of Precipitation by Radar*, Wissenschaftliche Mitteilung Nr. 63, Zurich, Eidenossische Kommission zum Studium der Hagelbildung und dert Hagelabwehr.

Kållberg, P. (ed.), 1989: *The HIRLAM Level 1 System*, Documentation Manual, (available from SHMI, Norrkoping, Sweden), 160 pp.

Karnieli, A. M., M. H Y. Diskin and L J. Lane, 1994: CELMOD5 — A semi-distributed cell model for conversion of rainfall into runoff in semi- and watersheds, *Journal of Hydrology*, 157, pp. 61–85.

Kavvas, M. L. and Z. Chen, 1989: *The Radar-based Short-term Prediction of the Time-space Evolution of Rain Fields*, Geophysics Laboratory, Hanson Air Force Base, Report, GL-TR-890103, 18 pp.

Kavvas, M. L. and K. R. Herd, 1985: A radar-based stochastic model for short-time increment rainfall, *Water Resources Research*, 21, 9, pp. 1437–1450.

Kedem, B., L. S. Chiu and Z. Karri, 1990: An analysis of the threshold method for measuring area-average rainfall, *Journal of Applied Meteorology*, 29, pp. 3–20.

Kitchen, M. and R. M. Blackall, 1992: Representativeness errors in comparisons between radar and gauge measurements of rainfall, *Journal of Hydrology*, 134, pp. 13–33.

Kitchen, M. and P. M. Jackson, 1993: Weather radar performance at long range — simulated and observed, *Journal of Applied Meteorology*, 32, 5, pp. 975–985.

Kitchen, M., R. Brown and A. G. Davies, 1994: Real-time correction of weather radar data for the effects of bright-band range and orographic growth in widespread precipitation, *Quarterly Journal of the Royal Meteorological Society*, 120, pp. 1231–1254.

Kittler, J., 1986: Feature selection and extraction, in *Handbook of Pattern Recognition and Image Processing* (T. Young and K. Fu, eds.), Academic Press, pp. 59–83.

Klazura, G. E. and D. A. Imy, 1993: A description of the initial set of analysis products available from the NEXRAD WSR-88D system, *Bulletin of the American Meteorological Society*, 74, 7, pp. 1293–1311.

Koistinen, J., 1991: *Operational Correction of Radar Rainfall Errors Due to the Vertical Reflectivity Profile*, Preprints of the twenty-fifth International Conference on Radar Meteorology, 24–28 June, Paris, American Meteorological Society, Boston, pp. 91–94.

Koiwai, Y. and T. Yoshida, 1987: *Application of Radar Meteorology in Japan*, Report, Japan Radio Company Ltd., Foundation of River and Basin Integrated Communication, Ministry of Construction, Tokyo, 21 pp.

Kopp, F. J. and H. D. Orville, 1994: The use of a two-dimensional, time-dependent cloud model to predict convective and stratiform clouds and precipitation, *Weather Forecasting*, 9, pp. 62–77.

Kouwen, N. and G. Garland, 1989: Resolution considerations in using radar rainfall data for flood forecasting, *Canadian Journal of Civil Engineering*, 16, pp. 279–289.

Krajewski, W. F and K. P. Georgakakos, 1985: Synthesis of radar rainfall data, *Water Resources Research*, 21, 5, pp. 764–768.

Krajewski, W. F., M. L. Morrisey, J. A. Smith and D. T. Rexroth, 1992: The accuracy of the area-threshold method: A model-based simulation study, *Journal of Applied Meteorology*, 31, pp. 1396–1406.

Krishnamurthi, T. N., H. S. Bedi and K. Ingles, 1993: Physical initialisation using SSM/I rain rates, *Tellus*, 45A, pp. 247–269.

Krishnamurthi, T. N., G. D. Rohaly and H. S. Bedi, 1994: On the importance of precipitation forecast skill from physical initialisation, *Tellus*, 46A, pp. 598–614.

Krstonovic, P. F. and V. P. Singh, 1992*a*: Evaluation of rainfall networks using entropy, I: Theoretical development, *Water Res. Man*., 6, pp. 279–293.

Krstonovic, P. F. and V. P. Singh, 1992*b*: Evaluation of rainfall network using entropy, II: Application, *Water Res. Man*., 6, pp. 295–314.

Laughlin, C. R., 1981: On the effect of temporal sampling on the observation of mean rainfall, in *Precipitation Measurements from Space*, D5-D66, Workshop Report (D. Atlas and O Thiele, eds.), NASA.

Lee, A. C. L., 1988: The influence of vertical air velocity on the remote microwave measurement of rain, *Journal of Atmospheric and Oceanic Technology*, 5, pp. 727–735.

Lee, B. D., R. D. Farley and M. R. Hyelmfelt, 1991: A numerical case study of convection initiation along colliding convergence boundaries in north-east Colorado, *Journal of Atmospheric Sciences*, 48, 21, pp. 2350–2366.

Lee, J., R. C. Weger, S. K. Sengupta and R. M. Welch, 1990: *A Neural Network Approach to Cloud Classification*, IEEE Trans on Geoscience and Remote Sensing, 28, 5, pp. 846–855.

Lee, T. H. and K. P. Georgakakos, 1990: A two-dimensional stochastic-dynamical quantitative precipitation forecasting model, *Journal of Geophysical Research*, 95, D3, pp. 2113–2126.

Leese, J. A., C. S. Novak and B. B. Clark, 1971: An automated technique for obtaining cloud motion from geosynchronous satellite data using cross-correlation, *Journal of Applied Meteorology*, 10, pp. 118–132.

Leith, C. E., 1980: Non-linear normal mode initialisation and quasi-geostrophic theory, *Journal of Atmospheric Sciences*, 37, pp. 958–968.

Lhermitte, R. M. and D. Atlas, 1961: *Precipitation Motion by Pulse Doppler*, Preprints of the ninth Weather Radar Conference, American Meteorological Society, Boston, pp. 218–223.

Lillesand, T. M. and R. W. Kiefer, 1987: *Remote Sensing and Image Interpretation*, John Wiley and Sons, New York.

Lilly, D. K., 1990: Numerical prediction of thunderstorms — Has its time come? *Quarterly Journal of the Royal Meteorological Society*, 116, pp. 779–798.

Lin, Y., P. S. Ray and K. W. Johnson, 1993: Initialisation of a modeled convective storm using Doppler radar-derived fields, *Monthly Weather Review*, 121, pp. 2757–2775.

Liu, J. and P. H. Herzegh, 1986: *Differential Reflectivity Signatures in Ice-phase Precipitation: Radar-aircraft Comparisons*, Preprints of the twenty-third Conference on Radar Meteorology, Volume 1, Snowmass, Colorado, American Meteorological Society, Boston, R59–R61.

Liu, Z. K. and J. Y. Xiao, 1991: Classification of remotely-sensed image data using artificial neural networks, *International Journal of Remote Sensing*, 12, 11, pp. 2433–2438.

Loague, K. M. and R. A. Freeze, 1985: A comparison of rainfall-runoff modelling techniques on small upland catchments, *Water Resources Research*, 21, pp. 229–240.

Lovejoy, S. and G. L. Austin, 1979: The delineation of rain areas from visible and IR satellite data for GATE and mid-latitudes, *Atmosphere-Ocean*, 17, pp. 77–92.

Lovejoy, S. and D. Schertzer, 1990: Multifractals, universality classes and satellite and radar measurements of cloud and rain fields, *Journal of Geophysical Research*, 95, D3, pp. 2021–2034.

Maass, A. M., M. M. Murfschmidt, R. Dorfman, H. A. Thomas, Jr, S. A. Marglin and G. M. Fair, 1962: *Design of Water-Resource Systems*, Harvard University Press, Cambridge, Massachussetts.

Marshall, J. S. and K. L. S. Gunn, 1952: Measurement of snow parameters by radar, *Journal of Meteorology*, 9, pp. 322–327.

Marshall, J. S. and W. Palmer, 1948: The distribution of raindrops with size, *Journal of Meteorology*, 5, pp. 165–166.

Mather, G. H., D. Treddenick and R. Parsons, 1976: An observed relationship between the height of the 45dBz contours in storm profiles and surface hail reports, *Journal of Applied Meteorology*, 15, pp. 1336–1340.

Maunder, W. J., 1986: *The Uncertainty Business*, Methuen and Company Ltd., London, 420 pp.

McArthur, R. C., J. R. Davis and D. Reynolds, 1987: Scenario-driven automatic pattern recognition in nowcasting, *Journal of Atmospheric and Oceanic Technology*, 4, pp. 29–35.

McCann, D. W., 1992: A neural network short-term forecast of significant thunderstorms, *Weather and Forecasting*, 7, pp. 525–534.

McCormick, G. C. and A. Hendry, 1972: *Results of Precipitation Backscatter Measurements at 1.8 cm with a Polarization Diversity Radar*, Preprints of the fifteenth Radar Meteorology Conference, American Meteorological Society, Boston, pp. 35–38.

McCormick, G. C. and A. Hendry, 1975: Principles for the radar determination of the polarisation properties of precipitation, *Radio Science*, 10, pp. 421–434.

McLeod, J. C., B. Q. de Lorenzis and J. M. Buillas, 1990: *Environment Canada's Experiences at SHOOTOUT '89*, Preprints of the sixth International Conference on International Information Processing Systems for Meteorology, Ocean and Hydrology, 5–9 February, Anaheim, California, American Meteorological Society, Boston, pp. 173–178.

Meneghini, R., J. Eckerman and D. Atlas, 1983: *Determination of Rain Rate from Space-borne Radar Using Measurements of Total Attenuation*, IEEE Trans. on Geoscience and Remote Sensing, GE-21, pp. 34–43.

Michaud, J. D. and S. Sorooshian, 1994: Effect of rainfall-sampling errors on simulations of desert flash floods, *Water Resources Research*, 30, 10, pp. 2765–2775.

Milton, S. F., 1990: Practical extended-range forecasting using dynamical models, *Meteorological Magazine*, 119, pp. 221–233.

Milton, S. F. and A. Van der Wal, 1994: *The Spin-up in Precipitation and Evaporation of Global and LAM Unified Model Forecasts, January 1992–May 1994*, Meteorological Office Forecasting Research Division, Technical Report No. 136, October (copy available at the National Meteorology Library, Bracknell).

Monk, G. A., K. A. Browning and P. R. Jonas, 1987: Forecasting applications of radar derived precipitation echo velocities in the vicinity of polar lows, *Tellus*, 39A, pp. 426–433.

Moore, R. J., 1982: Transfer functions, noise predictors, and the forecasting of flood events in real time, in *Statistical Analysis of Rainfall and Runoff* (V. P. Singh, ed.), Water Resources Publication, Colorado pp. 229–250.

Moore, R. J., 1985: The probability-distributed principle and run-off prediction at point and basin scales, *Hydrological Science Journal*, 30, 2, pp. 273–297.

Moore, R. J., 1987: Towards a more effective use of radar data for flood forecasting, Chapter 15 in *Weather Radar and Flood Forecasting* (V. K. Collinge and C. Kirby, eds.), John Wiley and Sons Ltd., pp. 223–238.

Moore, R. J. and G. Weiss, 1980: Real-time parameter estimation of a nonlinear catchment model using extended Kalman filters, in *Real-time Forecasting/Control of Water Resource System* (E. F. Wood, ed.), Pergamon Press, pp. 83–92.

Moore, R. J., R. M. Austin, D. S. Hotchkiss and K. B. Black, 1993: *Evaluation of FRONTIERS and Local Rainfall Forecasts for Use in Flood Forecasting Models*, Final Report, NRA R&D Project 298/1/T, Institute of Hydrology.

Moore, R. J., B. C. Watson, D. A. Jones and K. B. Black, 1991: Local recalibration of weather radar, Paper 6 in *Hydrological Applications of Weather Radar* (I. D. Cluckie and C. G. Collier, eds.), Ellis Horwood, Chichester, pp. 65–73.

Moriyama, T. and M. Hirano, 1980: Short-term forecasting for water level of flash flood by precipitation radar, *Journal of Hydrological Sciences and Hydraulics Engineering*, pp. 8–11.

Morrissey, M. L., 1994: The effect of data resolution on the area threshold method, *Journal of Applied Meteorology*, 33, pp. 1263–1270.

Moura, A. D., 1994: Prospects for seasonal-to-interannual climate prediction and applications for sustainable development, *WMO Bulletin*, 43, 3, July, pp. 207–215.

Mueller, E. A., 1977: Statistics of high radar reflectivity gradients, *Journal of Applied Meteorology*, 16, pp. 511-513.

Muench, H. S., 1976: Use of digital radar data in severe weather forecasting, *Bulletin of the American Meteorological Society*, 57, pp. 298–303.

Muench, H. S. and W. E. Lamkin, 1976: *The Use of Digital Radar in Short-range Forecasting*, Air Force Surveys in Geophysics No. 348, Technical Report No. AFGL-TR-76-0173, Meteorology Division Project 8628, US Air Force Geophysics Laboratory, Hanson Air Force Base, Massachussetts.

Murphy, A. H. and T. E. Sabin, 1986: Trends in the quality of National Weather Service forecasts, *Weather Forecasting*, 1, pp. 42–55.

Murphy, J. M. and T. N. Palmer, 1986: Experimental monthly long-range forecasts for the United Kingdom, Part II: A real time long-range forecast by an ensemble of numerical integrations, *Meteorological Magazine*, 115, pp. 337–349.

Newsome, D.H. (ed.), 1992: *Weather Radar Networking*, COST Project 73 Final Report of the Management Committee, Kluwer Academic Publishers for the CEC, 254 pp.

Niemczynowicz, J., 1987: Storm tracking using rain-gauge data, *Journal of Hydrology*, 93, pp. 135–152.

Norbury, J. R., 1974: A rapid-response raingauge for microwave attenuation studies, *J. Tech. Atmos.*, 8, pp. 245–251.

Norbury, J. R. and W. J. K. White, 1975: Intensity-time profiles for high-intensity rainfall, *Meteorological Magazine*, 104, pp. 221–227.

Obled, C., J. Wendling and K. Beven, 1994: The sensitivity of hydrological models to spatial rainfall patterns: An evaluation using observed data, *Journal of Hydrology*, 159, pp. 305–333.

Ogden, F. L. and P. Y. Julien, 1994: Runoff model sensitivity to radar rainfall resolution, *Journal of Hydrology*, 158, pp. 1-18.

Oki, R. and A. Sumi, 1994: Sampling simulation of TRMM rainfall estimation using radar AMeDAS composites, *Journal of Applied Meteorology*, 33, pp. 1597–1608.

Östlund, S. S., 1974: *Computer Software for Rainfall Analyses and Echo Tracking of Digitised Radar Data*, Technical Memorandum No. ERL-WMPO-15, Environment Research Laboratory, NOAA, Boulder, Colorado.

Owens, M. D., 1986: *Real-time Flow Forecasting Using Weather Radar*, Ph.D. thesis (unpublished), University of Birmingham.

Pankiewicz, G., 1995: Pattern recognition techniques for the identification of cloud and cloud systems, *Met. Apps.*, 2, pp. 257-271.

Parsons, D. B. and P. V. Hobbs, 1983: The mesoscale and microscale structure of cloud and precipitation in mid-latitude cyclones, XI: Comparison between observational and theoretical aspects of rainbands, *Journal of Atmospheric Sciences*, 40, pp. 2377–2397.

Peak, J. E. and P. M. Tag, 1994: Segmentation of satellite imagery using hiearchical thresholding and neural networks, *Journal of Applied Meteorology*, 33, pp. 605–616.

Peck, E. L., L. W. Larson and J. W. Wilson, 1973: Lake Ontario snowfall observational network for calibrating radar measurements in *Advanced Concepts and Technology in the Study of Snow and Ice Resources*, National Academy of Sciences, Washington D.C., pp. 412–421.

Pielke, R. A., 1981: Mesoscale dynamic modelling, *Advances in Geophysics*, 23, pp. 186–344.

Pollock, D. M. and J. W. Wilson, 1972: *Basin Precipitation — Land and Lake*, IFYGL Technical Plan, Volume 1, pp. 107–112.

Reed, D. W., 1987: *A Review of British Flood Forecasting Practice*, Report No. 90 Institute of Hydrology, Wallingford.

Roberts, G. K., 1987: The use of radar rainfall data in urban drainage models in Manchester, *Public Health Engineering*, 14, 6, pp. 61–64.

Roberts, W. F., W. R. Moninger, B. de Lorenzis, E. Ellison, J. Flueck, J. C. McLeod, C. Lusk, P. D. Lampru, R. Shaw, T. R. Stewart, J. Weaver, K. C. Yound and S. Zubruck, 1990: *SHOOTOUT 89: A Comparative Evaluation of AI Systems for Convective Storm Forecasting*, Preprints of the sixth International Conference on Information Processing Systems for Meteorology, Ocean and Hydrology, 5–9 February 1990, Anaheim, California, American Meteorological Society, Boston, pp. 167–172.

Rodda, J. C., 1997: Date, data everywhere, nor any drop to drink, NATO ASI Series, Vol. I46, *Land Surface Processes in Hydrology: Trials and Tribulations of Modelling and Measuring* (S. Sorooshian, H. V. Gupta and J. C. Rodda, eds.), Springer-Verlag, Berlin, pp. 3–18.

Rodriguez-Iturbe, I. and P. S. Eagleson, 1987: Mathematical models of rainstorm events in space and time, *Water Resources Research*, 23, 1, pp. 181–190.

Rosenfeld, D., E. Amitai and D. B. Wolf, 1995*a*: Classification of rain regimes by the three-dimensional properties of reflectivity fields, *Journal of Applied Meteorology*, 34, pp. 198–211.

Rosenfeld, D., E. Amitai and D. B. Wolf, 1995*b*: Improved accuracy of radar WPMM estimated rainfall upon application of objective classification criteria, *Journal of Applied Meteorology*, 34, pp. 212–223.

Rosenfeld, D., D. Atlas and D. A. Short, 1990: The estimation of convective rainfall by area integrals, Part II: The height-area threshold (Hart) method, *Journal of Geophysical Research*, 95, D3, pp. 2161–2176.

Rosenfeld, D., D. B. Wolff and D. Atlas, 1993: General probability-matched relations between radar reflectivity and rain base, *Journal of Applied Meteorology*, 32, pp. 50–72.

Rosenfeld, D., D. Atlas, D. B. Wolff and E. Amitai, 1992: Beamwidth effects on Z-R relations and area-integrated rainfall, *Journal of Applied Meteorology*, 31, pp. 454–464.

Rosenfeld, D., D. Atlas, D. B. Wolff and E. Amitai, 1994: The window probability matching method for rainfall measurements with radar, *Journal of Applied Meteorology*, 33, pp. 682–693.

Ruggiero, F. H., K. F. Heideman and J. Doherty, 1991: *An Evaluation of Three Techniques for Nowcasting Precipitation Fields Using Weather Radar*, Preprints of the twenty-fifth International Conference on Radar Meteorology, Paris, American Meteorological Society, Boston, pp. 83–86.

Rumelhart, D. E., G. E. Hinton and R. J. Williams, 1986: Learning representations by block-propagating errors, *Nature*, 323, pp. 533–536.

Sanderson, R. M., B. W. Golding and M. J. Bader, 1990: A heavy snowfall within a mesoscale convergence zone, *Meteorological Magazine*, 119, 1412, pp. 41–52.

Sauvageot, H., 1994: The probability density function of rain rate and the estimation of rainfall by area integrals, *Journal of Applied Meteorology*, 33, pp. 1255–1262.

Schmetz, J. and M. Nuret, 1987: Automatic tracking of high-level clouds in Meteosat infrared images with a radiance windowing technique, *ESA Journal*, 11, pp. 275–286.

Schultz, G. A., 1987: Flood forecasting based on rainfall radar measurements and stochastic rainfall forecasting in the Federal Republic of Germany, Chapter 13 in *Weather Radar and Flood Forecasting* (V. K. Collinge and C. Kirby, eds.), John Wiley and Sons Ltd., pp. 191–207.

Schultz, G. A., 1993: Hydrological modelling based on remote sensing information, *Advances in Space Research*, 13, 5, pp. 149–166.

Seddon, A. M., 1983: *The Application of Scene Analysis Techniques to Automatic Classification of Atmospheric Data from Multispectral Satellite Imagery*, Ph.D. thesis, University College, London.

Seddon, A. M. and G. E. Hunt, 1985: Segmentation of clouds using cluster analysis, *International Journal of Remote Sensing*, 6, 5, pp. 717–731.

Seed, A. W. and G. L. Austin, 1990*a*: Sampling errors for raingauge-derived mean areal daily and monthly rainfall, *Journal of Hydrology*, 118, pp. 163–173.

Seed, A. W. and G. L. Austin, 1990*b*: Variability of summer Florida rainfall and its significance for the estimation of rainfall by gauges, radar and satellite, *Journal of Geophysical Research*, 95, D3, pp. 2207–2215.

Sekhon, R. S. and R. C. Srivastava, 1970: Snow size spectra and radar reflectivity, *Journal of Atmospheric Sciences*, 27, pp. 229–367.

Seliga, T. A. and V. N. Bringi, 1976: Potential use of radar differential reflectivity measurements at orthogonal polarization for measuring precipitation, *Journal of Applied Meteorology*, 15, pp. 69–75.

Seliga, T. A., V. N. Bringi and H. H. Al-Khatib, 1981: A preliminary study of comparative measurements of rainfall rate using the differential reflectivity radar technique and a raingauge network, *Journal of Applied Meteorology*, 20, pp. 1360–1368.

Sevruk, B., 1986: Conversion of snowfall depths to water equivalents in the Swiss Alps, Proceedings of the Workshop on the Correction of Precipitation Measurements, 1–3 April 1985, Zurich, ETH, *Zurcher Geographische Schriften,* No. 23, pp. 81–88.

Shaw, E. M., 1994: *Hydrology in Practice*, Third edition, Chapman and Hall, 569 pp.

Shearman, R. J., 1977: The speed and direction of movement of storm rainfall patterns with reference to urban storm sewer design, *Hydrological Science Bulletin*, 22, pp. 421–431.

Shepard, D., 1968: *A Two-dimensional Interpolation Function for Irregularly Spaced Data*, Proceedings of the twenty-third ACM National Conference, Brandon/Systems Press, Princeton, New Jersey, pp. 517–524.

Sherman, L. K., 1932: Streamflow from rainfall by the unit graph method, *Engineering News Record*, 108, pp. 501–505.

Shukla, J., 1993: Dynamical predictability of monthly means, *Journal of Atmospheric Sciences*, 38, pp. 2547–2572.

Simpson, J., R. F. Adler and G. R. North, 1988: A proposed tropical rainfall measuring mission (TRMM) satellite, *Bulletin of the American Meteorological Society*, 69, pp. 278–295.

Sinclair, M. R., 1994: A diagnostic model for estimating orographic precipitation, *Journal of Applied Meteorology*, 33, pp. 1163–1175.

Smith, C. S., 1986: The reduction of errors caused by bright-bands in quantitative rainfall measurements made using radar, *Journal of Atmospheric and Oceanic Technology*, 3, pp. 129–141.

Smith, D. L., 1975: *The Applications of Manually-digitized Radar Data to Short-range Precipitation Forecasting*, Preprints of the sixteenth Conference on Radar Meteorology, Houston, American Meteorological Society, Boston, pp. 347–352.

Smith, E. A. and D. R. Phillips, 1971: *Automated Cloud Tracking Using Precisely Aligned Digital ATS Pictures*, Proceedings of the Conference on Two-dimensional Digital Signal Processing, Columbia, Massachussetts, pp. 10.201–10.22.26.

Smith, P. L., 1984: Equivalent radar reflectivity factors for snow and ice particles, *Journal of Climate Applied Meteorology*, 23, 8, pp. 1258–1260.

Snyder, F. F., 1938: Synthetic unit graphs, *Trans. AGH*, 19, pp. 447–454.

Sommeria, G., 1994: *Introduction to the Parametrisation of Physical Processes and Presentation of Boundary Layer Aspects*, ECMWF Seminar Proceedings, Ten Years of Medium-range Weather Forecasting, 4-8 September 1989, Volume II, pp. 1–37.

Srivastava, R. C. and A. R. Jameson, 1975: *Radar Detection of Hail*, Preprints, National Hail Research Experiment Symposium/Workshop on Hail, Volume 1, Estes Park, Colorado.

Srivastava, R. C. and A. R. Jameson, 1977: *Meteorological Monographs*, 16, 38, pp. 269–277.

Stewart, T. R., W. R. Moninger, J. Grassia, R. H. Brady and F. H. Merrem, 1989: Analysis of expert judgement in a hail forecasting experiment, *Weather Forecasting*, 4, pp. 24–34.

Strangeways, I. C., 1984: *Low Cost Hydrological Data Collection*, IAHS Symposium on Colleges in African Hydrology and Water Resources, Harare, pp. 229–233.

Strensrud, D. J. and Fritsch, J. M., 1994: Mesoscale corrective systems in weakly forced large-scale environments, Part III: Numerical simulations and inspection for operational forecasting, *Monthly Weather Review* 122, pp. 2084–2404.

Sulakvelidze, G. K., N. Sh. Bibilashvili and V. F. Lapcheva, 1967: *Formation of Precipitation and Modification of Hail Processes*, Israel Program for Scientific Translations, Jerusalem.

Sutton, G., 1989*a*: *Neural Networks*, Met. O 24, Internal Report No. 4 (copy available at the National Meteorology Library, Bracknell), unpublished.

Sutton, G. 1989*b*: *Learning by Back Propagation*, Met. O 24 Internal Report No. 9 (copy available at the National Meteorology Library, Bracknell), unpublished.

Szollosi-Nagy, A., 1976: *Introductory Remarks on the Space Modelling of Water Resource Systems*, International Institute for Applied Systems Analysis, RM-76-73, 81 pp.

Tapp, M. C. and White, P. W., 1976: A non-hydrostatic mesoscale model, *Quarterly Journal of the Royal Meteorological Society*, 102, pp. 277–296.

Tatehira, R., M. Hitsuma and Y. Makino, 1982: The mesoscale observational network in Japan, in *Nowcasting* (K. A. Browning, ed.), Academic Press, London, pp. 37–45.

Tatehira, R., H. Sato and Y. Makino, 1976: Short-term forecasting of digitised echo pattern, *Journal of Meteorological Research*, Japan Meteorological Agency, 28, pp. 61–70.

Theon, J. S., T. Matsuno, T. Sakata and N. Fuigono (eds.), 1992: *The Global Role of Tropical Rainfall*, A Deepak, 280 pp.

Tsonis, A. and G. L. Austin, 1981: Evaluation of extrapolation techniques for the short-term prediction of rain amounts, *Atmosphere-Ocean*, 19, pp. 54–65.

Turner, J. E., J. C. I. Dooge and T. Bree, 1989: Deriving the unit hydrograph by root selection, *Journal of Hydrology*, 110, pp. 137–152.

Ulaby, F. T., R. K. Moore and A. K. Fung, 1981: *Microwave Remote Sensing*, Volumes 1-3, Addison-Wesley, Reading, Massachussetts, 2162 pp.

US Army Corps of Engineers, 1956: *Snow Hydrology*, North Pacific Division, Portland, Oregon, pp. 67.

Waelbroeck, H., R. Lopez-Pena, T. Morales and F. Zertuche, 1994: Prediction of tropical rainfall by local phase space reconstruction, *Journal of Atmospheric Sciences*, 51, 22, pp. 3360–3364.

Waldvogel, A., B. Federer and P. Grimm, 1979: Criteria for the detection of hail cells, *Journal of Applied Meteorology*, 18, 12, pp. 1521–1525.

Waldvogel, A., W. Schmid and B. Federer, 1978*a*: The kinetic energy of hailfalls, Part I: Hailstone spectra, *Journal of Applied Meteorology*, 17, pp. 1680–1693.

Waldvogel, A., B. Federer, W. Schmid and J. Mezeix, 1978*b*: The kinetic energy of hailfalls, Part II: Radar and hailpads, *Journal of Applied Meteorology*, 17, pp. 1680–1693.

Walton, M. L. and E. R. Johnson, 1986: *An Improved Precipitation Projection Procedure for the NEXRAD Flash-flood Potential System*, Preprints of the twenty-third Conference on Radar Meteorology, Volume 3: Snowmass, Colorado, American Meteorological Society, Boston, JP62–65.

Wang, G-T and V. P. Singh, 1994: An autocorrelation function method for estimation of parameters of autogressive models, *Water Res. Man.*, 8, pp. 33–56.

Ward, M. N. and C. K. Folland, 1991: Prediction of seasonel rainfall in the north Nordeste of Brazil using eigenvectors of sea-surface temperature, *International Journal of Climatology*, 11, pp. 711–743.

Ward, M. N., C. K. Folland, K. M. Maskell, A. W. Colman, D. P. Powell and K. B. Lane, 1983: Experimental seasonal forecasting of tropical rainfall at the UK Meteorological Office, in *Prediction of Interannual Climate Variations* (J. Shukla, ed.), NATO ASI Series, Volume 16, Springer-Verlag, pp. 197–216.

Waterman, D. A., 1986: *A Guide to Expert Systems*, Addison Wesley, 419 pp.

Weisner, C. J., 1970: *Hydrometeorology*, Chapman and Hall Ltd, 232 pp.

Wickerts, S., 1982: *Fine-scale Structures in Time and Space of Rainfall Rate*, National Defence Research Institute, FOA Report C 20448-E2, Stockholm, March, 79 pp.

Wiggert, V., S. S. Östlund, G. L. Lockett and J. V. Stewart, 1976: *Computer Software for the Assessment of Growth Histories of Weather Radar Echoes*, NOAA Technical Memorandum No. EDRL WM PO-35, Weather Modification Program Office, NOAA, Boulder, Colorado, 86 pp.

Wilk, K. E. and K. C. Gray, 1970: *Processing and Analysis Techniques Used with the NSSL Weather Radar System*, Preprint of the fourteenth Conference on Radar Meteorology, American Meteorological Society, Boston, pp. 369–374.

Willmott, C. J., C. M. Rowe and W. D. Philpot, 1985: Small-scale climate maps: A sensitivity analysis of some common assumptions associated with grid-point interpolation and contouring, *The American Cartographer*, 12, 1, pp. 5–16.

Wilson, J. W., 1966: *Movement and Predictability of Radar Echoes*, Report, US Weather Bureau Contract CWB-11093, The Travellers Weather Research Center, Hartford, Connecticut.

Wilson, J. W., 1978: *Observation of Radome Transmission Losses at 50m Wavelengths*, Preprints of the eighteenth Conference on Radar Meteorology, American Meteorological Society, Boston, pp. 288–291.

Wilson, J. W. and E. A. Brandes, 1979: Radar measurement of rainfall — A summary, *Bulletin of the American Meteorological Society*, 60, pp. 1048–1052.

Winston, P. H., 1984: *Artificial Intelligence*, Addison Wesley, 524 pp.

Wolf, D. E., D. J. Hall and R. M. Endlich, 1977: Experiments in automatic cloud tracking using SMS-GOES data, *Journal of Applied Meteorology*, 16, pp. 1219–1230.

World Meteorological Organization, 1982: *Methods of Correction for Systematic Error in Point Precipitation Measurement for Operations Use* (B. Sevruk), Operational Hydrology Report No. 21, WMO-No. 589, Geneva.

World Meteorological Organization, 1983: V*ery Short-range Forecasting: Observations, Methods and Systems* (S. Bodin), World Weather Watch Planning Report No. 38, WMO-No. 621, Geneva.

World Meteorological Organization, 1986*a*: *A Simple Numerical Model of the Loss of Rainfall Due to Wind from a Conically-shaped Collector and a Suggested New Collector Shape* (C. K. Folland), Proceedings of the Workshop on the Correction of Precipitation Measurements, Zurich, 1–3 April 1995, Instruments and Observing Methods Report No. 25, WMO/TD-No. 104, pp. 233–238, Geneva.

World Meteorological Organization, 1986*b*: *Report of the Workshop on Global Large-scale Precipitation Data Sets for the World Climate Research Programme*, ICSU/WMO/WCRP WCP-111, WMO/TD-No. 94, Geneva.

World Meteorological Organization, 1988*a*: *Application of Satellite Data for Estimation of Precipitation* (R. Kuittinen), Technical Report to the Commission for Hydrology No. 26, WMO/TD-No. 300, Geneva.

World Meteorological Organization, 1988*b*: *Concept of the Global Energy and Water Cycle Experiment (GEWEX): Report of the JSC Study Group on GEWEX*, WCRP-5, WMO/TD-No. 215, Geneva.

World Meteorological Organization, 1989: *Canadian Participation in the WMO Solid Precipitation Measurements Intercomparison: Preliminary Results* (B. E. Goodison and J. R. Metcalfe), Proceedings of the International Workshop on Precipitation Measurements, St. Moritz, Switzerland, 3–7 December 1989, Instruments and Observing Methods Report No. 48, WMO/TD-No. 328, pp. 121–125, Geneva.

World Meteorological Organization, 1990: *Global Precipitation Climatology Project — Implementation and Data Management Plan*, WMO/TD-No. 367, Geneva.

World Meteorological Organization, 1994: *Guide to Hydrological Practices*, Fifth edition, WMO-No. 168, Geneva.

World Meteorological Organization, 1995*a*: *Management Overview of Flood Forecasting Systems (MOFFS): Version 3*, Technical Reports in Hydrology and Water Resources No. 51, WMO/TD-No. 715, Geneva.

World Meteorological Organization, 1995*b*: *Numerical Weather Prediction Progress Report for 1994*, NWP Report Series No. 21, WMO/TD-No. 708, Geneva.

World Meteorological Organization, 1995*c*: *Report of the Tenth Session of the CAS/JSC Working Group on Numerical Experimentation*, Tallahassee, Florida, 7-11 November 1994, CAS/JSC/WGNE Report No. 10, WMO/TD-No. 678, Geneva.

Wright, B. J. and B. W. Golding, 1990: *The Impact of Radar and Satellite Imagery in a Mesoscale NWP System, Weather Radar Networking*, Seminar on COST Project 73 (C. G. Collier and M. Chapuis, eds.), Kluwer Academic Publishers, pp. 378–390.

Yamada, T., T. Oki, E. Nakakita and M. Shüba, 1993: Rainfall mechanism and prediction, Paper 2, *Journal of Hydroscience Hydraulic Engineering*, Special Issue, Res. Practice Hydraulic Eng. in Japan, No. 51–3, Hydrology, pp. 27–82.

Yoshino, F. and D. Kozeki, 1985: *Study on Short-term Forecasting of Rainfall Using Radar Raingauge*, Report, Hydrology Division, Public Works Research Institute, Ministry of Construction, Japan, 19 pp.

Zawadzki, I. I., 1973: Statistical properties of precipitation patterns, *Journal of Applied Meteorology*, 12, pp. 459–472.

Zawadzki, I. I., 1975: On radar-rainguage comparison, *Journal of Applied Meteorology*, 14, pp. 1430–1436.

Zawadzki, I. I., 1984: *Factors Affecting the Precision of Radar Measurements of Rain*, Preprint of the twenty-second Conference on Radar Meteorology, Zurich, Switzerland, American Meteorological Society, Boston, pp. 251–256.

Zawadzki, I. I., J. Morneau and R. Laprise, 1994: Predictability of precipitation patterns: An operational approach, *Journal of Applied Meteorology*, 3, pp. 1562–1571.

Zhang, D-L, J. S. Kain, J. M. Fritsch and K. Gao,1994: Comments on parametrisation of convective precipitation in mesoscale numerical models: A critical review, *Monthly Weather Review*, 122, pp. 2222–2231.

Zhaobo, S., 1994: Empirical-statistical techniques in seasonal forecasting, *WMO Bulletin*, 43, 3, July, pp. 216–220.

Zipser, E. J., 1983: *Nowcasting and Very-short-range Forecasting in the National STORM Program: Scientific*

and Technological Bases and Major Objectives, University Corporation for Atmospheric Research, Boulder, Colorado, pp. 6.1–6.30.

Zittel, W. D., 1976: *Computer Applications and Techniques for Storm Tracking and Warning*, Preprints of the seventeenth Conference on Radar Meteorology, Seattle, Washington, American Meteorological Society, Boston, pp. 514–521.

Zubrick, S. M. and C. E. Riese, 1985: *An Expert System to Aid in Severe Thunderstorm Forecasting*, Preprints of the fourteenth Conference on Severe Local Storms, American Meteorological Society, Boston, pp. 117–122.

Zucherberg, F. L., 1976: *An Application of the Binomial Distribution to Radar Observations for Short-range Precipitation Forecasting*, Preprints of the sixth Conference on Weather Forecasting and Analysis, Albany, New York, American Meteorological Society, Boston, pp. 228–231.

OPERATIONAL HYDROLOGY REPORTS

WMO No.	Report No.		
332	No. 1	—	Manual for estimation of probable maximum precipitation (Second edition)
337	No. 2	—	Automatic collection and transmission of hydrological observations*
341	No. 3	—	Benefit and cost analysis of hydrological forecasts. A state-of-the-art report
356	No. 4	—	Applications of hydrology to water resources management*
419	No. 5	—	Meteorological and hydrological data required in planning the development of water resources*
425	No. 6	—	Hydrological forecasting practices*
429	No. 7	—	Intercomparison of conceptual models used in operational hydrological forecasting
433	No. 8	—	Hydrological network design and information transfer
461	No. 9	—	Casebook of examples of organization and operation of Hydrological Services
464	No. 10	—	Statistical information on activities in operational hydrology*
476	No. 11	—	Hydrological application of atmospheric vapour-flux analyses*
513	No. 12	—	Applications of remote sensing to hydrology
519	No. 13	—	Manual on stream gauging — Volume 1: Field work — Volume 2: Computation of discharge
559	No. 14	—	Hydrological data transmission
560	No. 15	—	Selection of distribution types for extremes of precipitation
561	No. 16	—	Measurement of river sediments
576	No. 17	—	Case studies of national hydrological data banks (planning, development and organization)
577	No. 18	—	Flash flood forecasting
580	No. 19	—	Concepts and techniques in hydrological network design
587	No. 20	—	Long-range water-supply forecasting
589	No. 21	—	Methods of correction for systematic error in point precipitation measurement for operational use
635	No. 22	—	Casebook on operational assessment of areal evaporation
646	No. 23	—	Intercomparison of models of snowmelt runoff
650	No. 24	—	Level and discharge measurements under difficult conditions
655	No. 25	—	Tropical hydrology
658	No. 26	—	Methods of measurement and estimation of discharges at hydraulic structures
680	No. 27	—	Manual on water-quality monitoring
683	No. 28	—	Hydrological information referral service — INFOHYDRO Manual
686	No. 29	—	Manual on operational methods for the measurement of sediment transport
704	No. 30	—	Hydrological aspects of combined effects of storm surges and heavy rainfall on river flow
705	No. 31	—	Management of groundwater observation programmes
717	No. 32	—	Cost-benefit assessment techniques and user requirements for hydrological data
718	No. 33	—	Statistical distributions for flood frequency analysis
740	No. 34	—	Hydrological models for water-resources system design and operation
749	No. 35	—	Snow cover measurements and areal assessment of precipitation and soil moisture
773	No. 36	—	Remote sensing for hydrology — Progress and prospects
754	No. 37	—	Hydrological aspects of accidental pollution of water bodies
779	No. 38	—	Simulated real-time intercomparison of hydrological models
804	No. 39	—	Applications of remote sensing by satellite, radar and other methods to hydrology
803	No. 40	—	Land surface processes in large-scale hydrology
806	No. 41	—	An overview of selected techniques for analysing surface-water data networks
813	No. 42	—	Meteorological systems for hydrological purposes
884	No. 43	—	Current operational applications of remote sensing in hydrology
885	No. 44	—	Areal modelling in hydrology using remote sensing data and geographical information system
886	No. 45	—	Contaminants in rivers and streams — Prediction of travel time and longitudinal dispersion

* Out of print